FILM COOLING IN LAMINAR, TRANSITIONAL AND TURBULENT HYPERSONIC BOUNDARY LAYERS

BY

James Arthur Hunter B. Eng.

November 1969

This thesis is submitted for the Doctor of Philosophy at the University of London in the Faculty of Engineering and also for the Diploma of Imperial College.

SUMMARY

This thesis describes an experimental study of film cooling in laminar and turbulent hypersonic boundary layers.

Schlieren photographs and heat transfer measurements were obtained over a flat plate model in a zero pressure gradient Mach 8.2 uniform flow.

A laminar boundary layer was tangentially injected with air such that $0.0276 \leqslant m \leqslant 0.0685$ for matched pressure conditions. It was found that the larger the coolant mass flow rate the greater was the cooling effectiveness close to the slot. However, the larger the injection rate the less was the transition Reynolds number which resulted in higher heat transfer than that without coolant flow. A mathematical model depicting the flow field as two parallel streams which do not mix was tested and found to be a useful approximation in prediction of the heat flux prior to transitional effects becoming dominant.

Vortex generators were used to generate a turbulent boundary layer on the flat plate used above but with a different nose and coolant feed system. Air, Freon, and helium were injected at matched pressure conditions for various flow rates such that $0.0131 \leqslant m \leqslant 0.0556$. The coolant was laminar on injection but transition was evident when helium and air were used as coolants. Turbulent mixing rapidly destroyed the coolant layer with a resulting mixture of the two streams existing over the rest of the model.

Air and Freon injection at similar mass flow rates showed the superiority of Freon at reducing the isothermal wall heat flux. Comparing the heat transfer distributions for helium and air, at similar mass injection rates, demonstrated that air was a better isothermal wall coolant. For design considerations requiring a constant wall temperature a heavy gas with a low thermal conductivity will reduce wall heat transfer. If design criteria demands a low adiabatic wall temperature distribution then a light gas with a high specific heat would be most beneficial.

The turbulent boundary layer semi-empirical theory for the prediction of film cooling effectiveness was extended to include the flow situation of a turbulent hypersonic mainstream and a laminar subsonic secondary stream. Variation of temperature over the boundary layer was not considered negligible. The method developed accounts for the displacement of measured data from the low speed theories which were developed for two turbulent streams mixing.

An appendix to this thesis explains the design and calibration of the heat transfer measuring equipment which utilized platinum thin film thermometers.

ACKNOWLEDGEMENTS

The Author wishes to convey his appreciation to Mr. J. L. Stollery for the interest, guidance and constant moral support given throughout all phases of this work.

Mr. B. J. Belcher and the electronics staff provided valuable assistance during the construction phase of the heat transfer equipment.

Members of the Department Workshop, who constructed the model and provided ready advise during the experimental phases, require a special acknowledgement of appreciation.

The support of the Ministry of Technology is gratefully acknowledged. Dr. J.K. Harvey provided useful discussions and advice during the absence of Mr. J.L. Stollery.

Finally, the author is very greatly indebted to his wife, Margaret, for her tolerance, understanding and the typing of this thesis.

INDEX

LIST OF FIGURES

PAGE

PAGE

LIST OF TABLES

NOTATION

A $= \frac{2kL}{\dot{m}_c s' Cp_t}$

A' Voltage rise with gauge pulsed in air.

A^+ Voltage rise with gauge pulsed in water

A^* Analogue calibration factor

B $= Z^{\frac{1}{2}} e^{-z} \int_0^Z Z_1^{-\frac{1}{2}} e^{z'} \, dz_1$

C Capacitance

C' Constant used in laminar film cooling calculation

C_f Coefficient of friction

Cp Specific heat capacity at constant pressure

$D(\phi)$ Dawsons integral of ϕ

D_1 $= Cp_c / Cp_\infty - 1$

D_2 $= W_\infty / W_c - 1$

D_3 $= \rho_\infty u_\infty \delta \int_0^1 \frac{u/u_\infty}{h/h_\infty} \, dz$

E Voltage representative of temperature

E_o Standing voltage over resistance gauge

F Change in gauge temperature from initial value

G Universal gas constant

$\bar{G}$ Amplifier gain

H Coefficient of heat transfer

I Current

J Joules constant

K' Constant (see text)

$\bar{K}$ Thermal diffusivity

L Span of slot

M Mach number

P Pressure

P_1 Pressure of working gas in barrel of the gun tunnel

P_4 Pressure of driver gas in the gun tunnel

P_p Plenum chamber pressure

Pr Prandtl number $(= \frac{\mu C_P}{k})$

R Resistance or gas constant

R' Constant used to determine rate of jet spread

R_o Gauge resistance at reference state

Re_x Reynolds number based on x

Re_c Slot Reynolds number

St Stanton number

T Temperature

T* Eckert's reference temperature

V Voltage

V_A Analogue output voltage

V_{out} Output voltage

W Molecular weight

$\bar{X}_T = \frac{x}{m s} \quad (Re_c \frac{\mu_c}{\mu_\infty})^{-\frac{1}{4}}$

$\bar{X}_L = (\frac{x}{m s})^{\frac{1}{2}} \quad (Re_c \frac{\mu_c}{\mu_\infty})^{-\frac{1}{2}}$

$Z = y/\delta$

Z_1	Dummy integration variable
c	Heat capacity
d	Splitter plate trailing edge thickness
f	A function
f'	Reynold's analogy factor
g	Acceleration due to gravity
h	Enthalpy
k	Thermal conductivity
l	Thickness
m	$= \frac{\rho_c u_c}{\rho_\infty u_\infty}$ mass velocity parameter
$\dot{m}$	Mass flow rate
m_f	Mass fraction
$\dot{q}$	Wall heat transfer rate
$\dot{q}_i$	Heat input to coolant layer
r	Recovery factor or resistivity
s	Slot height or Laplace transform variable
s'	Height of coolant layer after expansion
t	Time
t_1	Time after pulse voltage applied to gauge
u	Velocity in the x direction
x	Streamwise Cartesian co-ordinate normal to slot
x_o	Distance from slot to leading edge of model
x_1	Distance from slot to start of hypothetical layer

x' Distance from slot to first effect of heat flux at the wall

x'' Distance from slot to start of wall effect on velocity profile

y Cartesian co-ordinate normal to wall

y' Cartesian co-ordinate normal to wall starting from top of slot.

z_1 Dummy variable

α Temperature co-efficient of resistance

$\alpha' = \frac{u_c + u_\infty}{2\, u_\infty}$ used in velocity profile calculation

$\beta = \sqrt{\rho c k}$ material thermal characteristics

γ Ratio of specific heats

δ Height of boundary layer

δ^* Displacement thickness

$\eta' = \frac{h_{aw} - h_{o\infty}}{h_{oc} - h_{o\infty}}$

η'' Film cooling effectiveness $= \frac{T_{aw} - T_{o\infty}}{T_{oc} - T_{o\infty}}$

λ $\frac{u_\infty - u_c}{u_\infty + u_c}$ used in velocity profile calculation

μ Viscosity

$\xi = \sigma \frac{y'}{x}$ used in velocity profile calculation

ρ Density

σ Rate of jet spread parameter

σ^* Incompressible jet spread parameter (= 12)

τ Skin friction

ψ Dummy time variable

Δ	Change of property
Θ	Momentum thickness

SUFFICES

aw	Adiabatic wall
bl	boundary layer
c	Coolant
e	Entrained into the layer
g	Pyrex glass
inc	Incompressible
ι	Hypothetical layer
o	Stagnation
pc	End of potential core
r	Recovery
ref	Reference state
w	Wall or water
∞	Mainstream

SUPERSCRIPTS

*	Condition evaluated using Eckerts reference temperature T*

1. INTRODUCTION AND REVIEW OF LITERATURE

Film cooling is a method of providing thermal relief to surfaces exposed to high temperatures by injection of a coolant gas through slots. Gas turbines, ramjet engines, rocket motors, afterburners, and nuclear reactors are some examples where film cooling has application. Aerodynamic heating of hypersonic vehicles could be reduced by this technique.

Without some form of protection excessive heating may not only reduce the strength of the materials used but could also cause distortion of shapes which may adverseley affect the flow pattern. Regenerative backside cooling may be insufficient to prevent the exposed surface from melting or ablating under severe heat loads. Ceramic insulation coatings are limited in lifetime as the abrasive resistance qualities are usually poor. Development of materials with strength properties at high temperatures seems to be limited.

Injection of a coolant fluid into the boundary layer is a well established means of thermal protection. A liquid layer on the surface would evaporate rapidly but would provide adequate reduction of heat transfer. Injection of fluid through holes at discrete locations is a promising means of local heat transfer control. By increasing the number of holes so that a porous wall exists will allow a gas or liquid to be forced through the walls. This technique, known as sweat or transpiration cooling, would have its application on stagnation points but may cause some structural weakening. Even though this method provides adequate protection at the injection station, most of the coolant gas mixes with the outside stream and is swept away providing little protection in the downstream region.

Film cooling separates the hot gas and the wall by a film of gaseous coolant which is injected through slots. Since this film will gradually be destroyed by turbulent mixing, it must be renewed at some distance downstream through additional slots. The distance between injection stations will depend upon the quantity, heat capacity, and the rate of mixing.

Eckert (1954) states that film cooling with air, provides better thermal protection close to the injection station than transpiration cooling but transpiration cooling provides a better cooling effectiveness for a given mass flow over a larger area.

Film cooling can be examined with laminar, transitional, or turbulent mainstream flows which could be subsonic or supersonic. Then there is the possibility of a laminar, transitional or turbulent coolant film at any Mach number. The case of supersonic coolant flow could have its static pressure matched or underexpanded after injection. Foreign gases could also be used as coolants.

Blowing over the surface is a means of reducing skin friction and heat transfer or could be used to energize the fluid near the wall in order to delay boundary layer separation. An investigator interested in fuel injection by this method would be more interested in the mixing process while one interested in thermal protection is primarily interested in the effect on the surface.

It has been suggested that film cooling of a ramjet intake of a hypersonic aircraft by using the fuel would not only assist in thermal protection but would provide the engine with a preheated and premixed propellant. Film cooling could have future application in reduction of

extremely high local heat transfer rates produced by a shock wave striking a surface. Re-attachment of separated shear layers results in high heat transfer. The benefits of film cooling, where design considerations require these conditions to exist, are likely to be considerable.

The purpose of this present work is to provide new experimental data for laminar coolants injected into laminar and turbulent hypersonic boundary layers. Also the usefulness of the semi empirical correlations based on the boundary layer model have been extended to cover these flow fields.

1.1 Laminar Film Cooling

Past investigations of laminar boundary layers with laminar tangential coolant injection have been mainly experimental. Eckert et al (1963) supplies a comprehensive review of literature available up to 1963 while Schetz and Gilreath (1967) provide further useful references for supersonic mainstream flows.

Hatch and Papell (1959) derived a simple model based on no mixing of the two streams and applied two empirical modifications in an attempt to account for turbulent mixing destroying the coolant film. Richards (1967) modified the no mixing model and had considerable success in predicting the heat transfer distribution on a flat plate with four gas coolants. Libby and Schetz (1963) used an integral method related to the heat conduction equation to solve the momentum and energy equation which provided a solution of the velocity and temperature fields. Their theoretical study was not compared with measured data.

Stagnation point injection was investigated by Dannenburg (1962), who used helium and a hemispherical model, as well as by Redeker and Miller (1966) who successfully applied the discrete layer concept. Roland et al (1966) investigated the use of film cooling in nozzle throats.

Application of the discrete layer concept is normally useful for distances of about one hundred slot heights downstream of the injection station but all the investigators mentioned above noticed a tendency for early transition. This could partially be explained by the shear layer resulting from the velocity difference between the two streams causing turbulent mixing. Also if the coolant static pressure is not matched with the mainstream static pressure there would be coolant layer expansion on injection which would be a disturbing influence on the laminar flow field. Transition results in a wall heat flux which is greater than the no injection laminar heat flux which is disadvantageous far downstream. Powers and Albacete (1966) noticed that the transition Reynolds number increased with a heavy gas injection. Richards (1967) confirmed this fact.

Albacete and Glowacki (1966) conducted a theoretical study of foreign gas injection into a supersonic boundary layer. They used real gas arguments for Mach numbers up to 3 to show that heavier gases, at low $T_w/T_{o\infty}$, were more effective than light gases at reducing heat transfer.

1.2 Turbulent Film Cooling

In the film cooling flow configuration there exists the mixing of two streams moving in the same direction.

This phenomena of free turbulent shear flow has produced a vast amount of literature on the mixing process. Azzouz and Pratt (1968) have compiled a fairly comprehensive literature review and quote 92 references of which 10 are other literature surveys containing several hundred further references. The case of an incompressible jet issuing into quiescent air has had considerable success in theoretical prediction but if either or both streams are compressible, are of different species, have significant initial turbulence levels, or have chemical reactions occurring then the problem is much more complicated. Experimental data on mixing between streams of different velocity, composition, and temperature have shown that mass and heat diffuse more rapidly than momentum but no satisfactory explanation of this phenomena is available.

Density differences have been found to be an important parameter in the determination of mixing rates between two streams. The effects of compressibility complicate the mixing process further. Some authors have attempted to solve compressible flow mixing problems using incompressible solutions modified by a correction factor or mathematical transformation but these approaches cannot represent the actual physical process.

The mixing process depends not only on the density ratio ρ_c/ρ_∞ but also on the velocity ratio u_c/u_∞ in some manner. The parameter governing mixing could be a momentum ratio $\rho_c u_c^2 / \rho_\infty u_\infty^2$ or a mass flux ratio $\rho_c u_c / \rho_\infty u_\infty$ but no conclusive evidence is available.

Zakkay and Fox (1966) extended low speed work to Mach numbers of 4 and 12 in a turbulent wake with and without base injection. They concluded that the models used, that were successful at low Mach numbers, were inadequate to explain the mixing phenomena at these velocities.

In the analysis of turbulent flow problems the fluctuations of properties should be considered along with the mean distributions but this necessitates a knowledge of the turbulent fluctuations which is indeed a complex problem. Little experimental data on the supersonic turbulence structure exists.

The inclusion of a wall as a boundary on a side of one of the moving streams will result in a wall boundary layer. Interaction between a free turbulent shear flow and a boundary layer will further complicate the mixing process.

Analysis of turbulent flows, because of their complexity, depend upon empirical results obtained from experiments. Application of experimental flow empirical relations to flow situations which are different, may not result in accurate predictions. No general solution has been successful over a wide range of experimental conditions.

Azzouz and Pratt (1968) state that the effect of increasing the turbulence level initially present in the stream has the effect of reducing the rate of mixing significantly. Two photographic studies were quoted in their literature survey. The first was by Ragsdale and

Edwards (1965) who injected a Bromine jet into a subsonic air stream and found the effect of a honeycomb section upstream of the injection station, which increased the turbulence level in the mainstream, had the effect of reducing the rate of mixing significantly. However, the second study by Hawkins (1967) using a hydrogen jet issuing into a supersonic airstream, was unaffected by the initial turbulence level.

Non-uniformity of density in free turbulent shear flow is known to strongly affect turbulent mixing but theoretical and experimental understanding of its influence is not refined. Work on this phenomena is presently under investigation (Roshko (1969)).

Townsend (1966) considered the mixing phenomena of jets of various species, and velocities issuing into ambient fluids. Photographs demonstrated the slow jet spreading of a carbon dioxide jet issuing into air and the considerably faster mixing of a hydrogen jet into air. El Ehwany (1965) noticed this more rapid mixing for his helium wall jet and free jet models in an external stream while a heavier gas did not mix as readily. Experiments in low Mach number combined flow fields have shown that a fast moving heavy gas will delay mixing more than a slow moving light gas.

Selection of a suitable relation for compressible mixing rates must be an approximation as incompressible mixing of two streams of different densities is still unresolved.

It is not surprising that past investigators, examining compressible turbulent flow fields consisting of different species, densities and velocities, have used simple mathematical models in an attempt to analyse the wall jet film cooling phenomena. The work presented here continues with these simple models.

The flow field for a turbulent boundary layer with secondary tangential gas injection where the velocity of the coolant is less than that of the mainstream, can be divided into two main regions. Near the slot where initial mixing of the two streams begins, the wall temperature remains essentially that of the coolant gas stagnation temperature. Turbulent mixing is not severe enough to cause the hot gas of the mainstream boundary layer to be felt at the wall through the layer of coolant until some distance downstream. This "potential core" region will have a limited length as turbulent mixing destroys the coolant layer. Further downstream the hot gases have had sufficient time to reach the wall which increases wall temperature. Progressing further from the slot the effect of the coolant absorbing heat from the boundary layer rapidly becomes less significant until there is no effect of coolant injection remaining. This second region has been called the boundary layer like region as fully developed turbulent velocity profiles are formed.

Subsonic flow of the primary and coolant streams have been theoretically and experimentally investigated using a boundary layer mathematical model to calculate the adiabatic wall temperature, T_{aw}. Wieghart (1946) assumed similarity for the velocity and temperature profiles which resulted in an asymptotic solution of the turbulent boundary layer equations.

Further development of this basic model by Tribus and Klien (1953), Hartnell et al (1961), Seban and Back (1962), Kutateladze and Leont'ev (1963), Librizzi and Cresci (1964), and Stollery and El-Ehwany (1965) resulted in similar expressions for the film cooling effectiveness, differing only in the constant K'. For air injected into air :

$$\eta' = K'(\bar{X}_T)^{-.8}$$

where η' is the film cooling effectiveness and :

$$\bar{X}_T = \frac{x}{ms}\left(Re_c \frac{\mu_c}{\mu_\infty}\right)^{-\frac{1}{4}}$$

where $\bar{X}_T$ is a non dimensional distance downstream of the injection station. These studies required that the two streams mix completely at each downstream station and that velocity profiles are similar. The results are strictly asymptotic solutions which show good agreement with experiments for large values of $\bar{X}_T$.

Experimental investigations by Chin et al (1958), Papell and Trout (1969), Seban (1960), Nishiwaki et al (1961) also confirm the region which this model has its application. More recent investigations by Burns (1967), Pia (1968) and Burns and Stollery (1968) have shown the effect of velocity and density ratios as well as the slot lip thickness on the effectiveness, η' . In general as the density ratio ρ_c/ρ_∞ increases, η' increases and as the velocity ratio u_c/u_∞ increases up to unity there is an increase in η' . By tapering the splitter plate down to a sharp trailing edge it has been noted that η' increases. This is to be expected as the small wake generated behind this plate will have less destabilizing effect on the flow field.

The vortex sheet produced by the velocity difference between the mainstream and coolant may cause transition in a laminar coolant to enhance mixing.

Although a boundary layer exists on the coolant side of the splitter plate, it would be small compared to the mainstream boundary layer for two reasons. First, the free stream boundary layer has developed over a long distance upstream of the slot while the coolant came directly from a plenum chamber near the slot. Also the Mach number of the coolant is much lower (subsonic) than the mainstream and the boundary layer growth should be less.

A boundary layer on the wall will grow in the coolant potential core region according to whether laminar or turbulent conditions exist. This effect of the wall presence, manifests itself by modifying the no wall velocity profile of two mixing streams. However, further downstream the velocity profiles will rapidly approach those of a fully developed turbulent boundary layer as the initial velocity decrement is smoothed out.

Experimental investigations of tangential injection into a supersonic mainstream to determine a means of maximizing thermal relief have been conducted by Chin et al (1966), Gilreath and Schelz (1966), Goldstein (1966), and Richards (1967). Murkerjie and Martin (1966) considered secondary air tangentially injected into a supersonic axisymmetric diffuser as a means of thermal protection and made measurements of the base pressure variation. Schetz and Favin (1966) investigated the combustion process of hydrogen tangentially injected into a supersonic air stream.

Goldstein et al (1968) conducted an experimental and analytical investigation of the two dimensional normal air injection into a supersonic turbulent boundary layer. Use of a reference state to account for the property variations across the combined flow field allowed results to be compared with incompressible boundary layer model theories.

Seban (1960) stated that the upstream boundary layer thickness had little effect on the low speed film cooling effectiveness. Burns and Stollery (1969) agree the effect is small but suggest that it could become important if ρ_c/ρ_∞ is low.

2. FILM COOLING THEORIES

2.1 Laminar Discrete Layer Theory

Richards (1967) modified the model proposed by Hatch and Papell (1959) and was quite successful in predicting the wall heat transfer on an isothermal flat plate. The assumptions used were :

1. The coolant exists as a discrete layer.

2. The velocity across the layer remains constant at the injection velocity for all stations downstream.

3. The temperature distribution through the coolant layer is linear at a given downstream location.

4. The heat transferred to the coolant layer is the same as that to a flat plate whose wall temperature is equal to the initial total temperature of the coolant.

5. The coolant travels a distance x' from the slot before heat diffuses through the layer.

A heat balance on an element of coolant and the assumption of a Blasius skin friction relation to determine the heat input resulted in the differential equation :

$$\frac{dq}{dx} + Aq = Aq_i \qquad 2.1.$$

where $A = \frac{2kL}{\dot{m}_c s' Cp}$ and where k is the coolant thermal conductivity, L the slot width, $\dot{m}_c$ the coolant mass flow, s' the height of the coolant layer, Cp the specific heat at constant pressure and x the distance downstream of the slot.

By defining $Z = A(x + x_o)$, where x_o is the distance of the slot downstream of the model nose, the differential equation is solved to give :

$$q(x) = q_i(x)\, Z^{\frac{1}{2}} e^{-Z} \int_0^Z Z_1^{-\frac{1}{2}}\, e^{Z_1}\, dZ_1 + C' e^{-Z} \qquad 2.2.$$

Richards expanded e^{Z_1} as a power series and completed the integration to give :

$$q(x) = e^{-Z}\left[2q_i\, Z\left(1 + \frac{Z}{3} + \frac{Z}{10} + \frac{Z}{42} + \ldots\right) + C'\right] \qquad 2.3.$$

Equation 2.2. can be modified by using $Z_1 = y_1^2$ to give :

$$q(x) = q_i\, Z^{\frac{1}{2}}\, 2e^{-Z} \int_0^{\sqrt{Z}} e^{y_1^2}\, dy_1 + C' e^{-Z} \qquad 2.4.$$

Here the term $e^{-Z}\int_0^{\sqrt{Z}} e^{y_1^2}\, dy_1$ is Dawson's Integral which

is tabulated by Abramowitz (1964) p. 319. Hence using $D(\sqrt{Z})$ to represent Dawson's Integral for $\sqrt{Z}$ gives :

$$q(x) = 2q_i Z^{\frac{1}{2}} D(\sqrt{Z}) + C'e^{-Z} \qquad 2.5.$$

The numerical evaluation of the function B defined by :

$$B = Z^{\frac{1}{2}}e^{-Z} \int_0^Z Z_1^{-\frac{1}{2}} e^{Z_1} dZ_1 \qquad 2.6.$$

was computed on an IBM 7094 and the results plotted in figure 1. Equation 2.2. reduces to :

$$q(x) = q_i B + C'e^{-Z} \qquad 2.7.$$

Assuming the heat input :

$$q_i(x) = B'(x + x_o)^{-\frac{1}{2}} \qquad 2.8.$$

where B' is a constant depending on the mainstream conditions. The final heat flux distribution would be :

$$q(x) = B\,B'\,(A/Z)^{\frac{1}{2}} + C'e^{-Z} \qquad 2.9.$$

The constant C' can be calculated using the boundary condition of $q = 0$ when $x = x'$, the distance from the slot to the first effects of heat diffusion felt at the wall.

2.2 The Boundary Layer Model

Stollery and El-Ehwany (1965) described the use of a mathematical model for the determination of film cooling

effectiveness in low speed turbulent flows. The assumptions used were :

(i) The flow is boundary-layer-like and its thickness grows as a normal boundary layer

i.e. $\delta = K_1 \times (Re_x)^{-N}$

(ii) The pressure is constant throughout the flow field

(iii) The temperature and velocity boundary layers have the same thickness (i.e. Pr = 1)

(iv) The velocity profiles are similar at each station downstream of the slot

(v) The temperature variation of specific heat is negligible and mixing is such that Cp = f (x) only.

A total enthalpy balance over the layer on an adiabatic wall gives :

$$\dot{m}_l h_{aw} = \dot{m}_c h_{oc} + \dot{m}_e h_{o\infty} \qquad 2.10.$$

where the coolant mass flow rate per unit width is :

$$\dot{m}_c = \rho_c u_c s \qquad 2.11.$$

and the total mass flow in the layer is :

$$\dot{m}_l = \int_0^{\delta} \rho u \, dy \qquad 2.12.$$

The mass entrained into the layer is :

$$\dot{m}_e = \dot{m}_L - \dot{m}_c \qquad 2.13.$$

Substitution into 2.10. yields :

$$\eta' = \frac{h_{aw} - h_{o\infty}}{h_{oc} - h_{o\infty}} = \frac{\dot{m}_c}{\dot{m}_L} \qquad 2.14.$$

where η' is the adiabatic wall effectiveness depending on enthalpy.

The similar velocity profiles of assumption (iv) obeyed a power law relation such that :

$$\frac{\rho u}{\rho_\infty u_\infty} = \left(\frac{y}{\delta}\right)^n \qquad 2.15.$$

On substitution of 2.15. into 2.12. and 2.14. yields :

$$\eta' = \frac{n+1}{K_1} \left(\frac{x}{m\ s}\right)^{N-1} \left(Re_c \frac{\mu_c}{\mu_\infty}\right)^N \qquad 2.16.$$

where the injection parameter $m = \frac{\rho_c u_c}{\rho_\infty u_\infty}$ and the slot Reynolds number $Re_c = \frac{\rho_c u_c s}{\mu_c}$

This asymptotic solution assumes complete mixing of the two streams at each downstream station.

For foreign gas injection the specific heat of this ideal gas mixture can be given by :

$$Cp(x) = m_{fc}\ Cp_c + m_{f\infty}\ Cp_\infty \qquad 2.17.$$

where m_{fc} and $m_{f\infty}$ are the mass fraction of the coolant and mainstream gases. Substitution of 2.17. into 2.14. gives :

$$\eta' = \frac{1}{1 + \frac{Cp_c}{Cp_\infty} \frac{T_{oc} - T_{aw}}{T_{aw} - T_{o\infty}}} = \frac{\dot{m}_c}{\dot{m}_L} \qquad 2.18.$$

Equation 2.16. is general for any mass velocity power relation and any rate of layer growth which conforms to that specified in assumption (i). For turbulent film cooling Stollery and El-Ehwany used n = 1/7, N = 1/5, and K_1 = 0.37 to give :

$$\eta' = 3.09 \ (\bar{X}_T)^{-4/5} \qquad 2.19.$$

where :

$$\bar{X}_T = \frac{x}{ms} \ (Re_c \frac{\mu_c}{\mu_\infty})^{-\frac{1}{4}} \qquad 2.20.$$

2.3 Turbulent Film Cooling Correlations.

Other low speed effectiveness theories include :

Tribus and Klien (1953)

$$\eta' = 5.77 \ (Pr)^{2/3} (\frac{x}{ms})^{-.8} \ Re_c^{.2} \ \frac{Cp_c}{Cp_\infty} \qquad 2.21.$$

Kuateladz and Leont'ev (1963)

$$\eta' = 3.1 \left[4.16 + \frac{x}{m\ s} Re_c^{-.2}\right]^{-.8} \qquad 2.22.$$

Librizzi and Cresci (1964)

$$\eta' = 3.0 \left[3 + \left(\frac{x}{m\ s}\right)^{.8} Re_c^{-.2}\right]^{-1} \qquad 2.23.$$

Goldstein (1966)

$$\eta' = 162 \left(\frac{x}{m\ s}\right)^{-1.2} \quad \text{for } m > 0.12$$
$$\eta' = 550 \left(\frac{x}{s}\right)^{-.2} m^{.8} \quad \text{for } m \leqslant 0.12 \qquad 2.24.$$

Goldstein et al (1968) suggests that the variation of fluid properties over the mixing region can be estimated using Eckerts reference temperature over an adiabatic wall for supersonic mainstream flows. A reference density is suggested which would enable high speed film cooling measurements to be compared with low speed theories. The suggested correlation parameter with effectiveness based on enthalpy was :

$$\frac{x}{m\ s} (Re_c \frac{\mu_c}{\mu_\infty})^{-\frac{1}{4}} \frac{\rho^*}{\rho_\infty} \qquad 2.25.$$

where ρ^* was calculated at the reference temperature

$$T^* = T_\infty + 0.72 (T_r - T_\infty) \qquad 2.26.$$

Assuming molecular diffusion and turbulence generated in the flow field is sufficient to cause adequate mixing to enable the boundary layer to be applicable to the laminar film cooling case, then the calculations of Van Driest (1952) would be useful. The Mach 8.2 adiabatic wall ρu profile for a laminar boundary layer was found to give n = 4 and K_1 was found to be 16 while N = ½. Now equation 2.16. becomes :

$$\eta' = 0.313\ (\bar{X}_L)^{-1} \qquad 2.27.$$

where :

$$\bar{X}_L = \left(\frac{x}{m\ s}\right)^{\frac{1}{2}} \left(Re_c \frac{\mu_c}{\mu_\infty}\right)^{-\frac{1}{2}}$$

3. EXTENSION OF THE BOUNDARY LAYER MODEL

3.1 Introduction

The boundary layer model is an asymptotic theory which has been found valuable for determination of film cooling effectiveness far downstream of the injection station. Film cooling would probably find its application with the slot located very close to regions of peak heat loads. An examination of the flow close to the slot and possible extension of the boundary layer model to include these regions would be useful.

The aim of this analysis is to extend the boundary layer model application to regions close to the slot in high speed mainstream flows.

3.2 Mass Flow in the Mixing Layer

Assuming that the mass velocity profiles do not obey a power law relation but that the velocity profiles close to

the slot are similar, equation 2.12. upon substitution of $Z = y/\delta$ becomes :

$$\dot{m}_L = \rho_\infty u_\infty \delta \int_0^1 \frac{u}{u_\infty} \frac{\rho}{\rho_\infty} \, dz \qquad 3.1.$$

Using the perfect gas assumption $P = \rho RT$ and the definition of enthalpy $h = CpT$ in a constant pressure flow field gives :

$$\dot{m} = \rho_\infty u_\infty \delta \int_0^1 \frac{u/u_\infty}{h/h_\infty} \frac{Cp/Cp_\infty}{R/R_\infty} \, dz \qquad 3.2.$$

Both the specific heat Cp and the gas constant R in equation 3.2. can vary over the layer.

The restriction of perfect mixing of the two streams in the mixing region is certainly realistic in turbulent flow but with laminar flow this may not be representative of actual conditions.

In any perfect gas mixture the specific heat is the sum of the mass fractions, m_f, of the component parts :

$$Cp(x) = m_{fc} \, Cp_c + (1 - m_{fc}) \, Cp_\infty \qquad 3.3.$$

Similarly for the gas constant R :

$$R(x) = m_{fc} \, R_c + (1 - m_{fc}) \, R_\infty \qquad 3.4.$$

Here $m_{fc} = \frac{\dot{m}_c}{\dot{m}_L}$ and $R = \bar{G}/W$ where $\bar{G}$ is the universal gas constant and W the molecular weight of the gas. Substitution of these relationships into 3.3. and 3.4. yields :

$$\frac{Cp}{Cp_\infty} = \frac{\dot{m}_c}{\dot{m}_L}\left(\frac{Cp_c}{Cp_\infty} - 1\right) + 1$$

$$\frac{R}{R_\infty} = \frac{\dot{m}_c}{\dot{m}_L}\left(\frac{W_\infty}{W_c} - 1\right) + 1 \qquad 3.5.$$

which can be combined with equation 3.2.

It would be useful if the enthalpy variation over the mixing layer could be expressed as a function of the velocity profile. For unit Prandtl number the turbulent energy equation with the Crocco assumption of dh/dx = 0 reduces to :

$$h = - u^2/2 + C_1 u + C_2 \qquad 3.6.$$

The relationship of 3.6. also applied to the laminar boundary layer momentum and energy equations. This special equation relating enthalpy and velocity means that the laminar energy equation is automatically satisfied when the laminar momentum equation is satisfied.

Rotta (1964) states that the first term on the right hand side of 3.6. is often multiplied by the recovery factor, r, to compensate for the fact that Pr may differ from unity.

The constants C_1 and C_2 are determined by the boundary conditions :

$$h = h_w \text{ at } u = 0$$
$$h = h_\infty \text{ at } u = u_\infty \qquad 3.7.$$

If the recovery factor is representative of the local recovery factor then the adiabatic wall enthalpy, h_{aw}, is defined as :

$$h_{aw} = h_\infty + r \frac{u_\infty^2}{2} \qquad 3.8.$$

Solving for the constants C_1 and C_2, using equation 3.8. and some manipulation with equation 3.6 yields :

$$\frac{h}{h_\infty} = \frac{h_w}{h_\infty}\left(1 - \frac{u}{u_\infty}\right) + \frac{h_{aw}}{h_\infty}\left(1 - \frac{u}{u_\infty}\right)\left(\frac{u}{u_\infty}\right) + \left(\frac{u}{u_\infty}\right)^2 \qquad 3.9.$$

Substitution of 3.9. and 3.5. into 3.2. gives :

$$\dot{m}_L = \rho_\infty u_\infty \delta \frac{\frac{\dot{m}_c}{\dot{m}_L}\left(\frac{Cp_c}{Cp_\infty} - 1\right) + 1}{\frac{\dot{m}_c}{\dot{m}_L}\left(\frac{W_\infty}{W_c} - 1\right) + 1} \int_0^1 \frac{\frac{u}{u_\infty}}{\frac{h}{h_\infty}\left(1 - \frac{u}{u_\infty}\right) + \frac{h_w}{h_\infty}\left(1 - \frac{u}{u_\infty}\right)\left(\frac{u}{u_\infty}\right) + \left(\frac{u}{u_\infty}\right)^2} dz \qquad 3.10.$$

Equation 3.10. reduces to a simple quadratic which is solved by standard methods :

$$\dot{m}_L^2 + \dot{m}_L\left(\dot{m}_c D_2 - D_3\right) - \dot{m}_c D_1 D_3 = 0 \qquad 3.11.$$

where

$$D_1 = Cp_c/Cp_\infty - 1$$

$$D_2 = W_\infty/W_c - 1$$

$$D_3 = \rho_\infty u_\infty \delta \int_0^1 \frac{u/u_\infty}{h/h_\infty} dz$$

3.3 Velocity Profiles

Between the mainstream and the injected coolant is a free jet boundary. The two streams, each at a constant velocity, will mix together and smooth out the velocity discontinuity. Gortler (1960) solved the equations of motion for the incompressible case by assuming the velocity variation obeyed a power series which resulted in a set of differential equations which could be solved numerically. The series converged very rapidly and the first two terms of this exact solution provided a velocity distribution in terms of the error function. The result of the calculation was :

$$u = \frac{u_\infty + u_c}{2} \left[1 + \frac{u_\infty - u_c}{u_\infty + u_c} \operatorname{erf} \xi \right] \qquad 3.12.$$

where :

$$\xi = \sigma \frac{y'}{x} \qquad 3.13.$$

and σ is known as the jet spreading parameter which must be calculated from experiment. The variable y' is the vertical distance parameter from the meeting of the two streams while the error function used here is :

$$\operatorname{erf} \xi = \frac{2}{\sqrt{\pi}} \int_0^{\xi} e^{-t^2} \, dt$$

The problem of a compressible turbulent jet issuing into quiescent air was examined by Maydew and Reed (1963).

They arrived at the following conclusions :

1. The mixing region spreads linearly with distance from the nozzle exit.

2. The nondimensionalized velocity profiles are similar at all axial stations at all Mach numbers.

3. Gortler's error function theoretical velocity distribution for incompressible flow agreed with the measured results.

4. The effect of varying static pressure had negligible effect on velocity profiles and the jet spreading parameter.

5. The spreading rate of the mixing region decreases with Mach number (i.e.σ increases).

This spreading of the mixing region of a jet into quiescent air has been the subject of investigation for some considerable time. Some of the many investigators include Tollmien (1945), Gooderum et at (1950), Bershader and Pia (1950), Pia (1957), Vasiliu (1962), Korst and Tripp (1957) and Channapragada (1963). Korst and Tripp (1957) suggested the spread parameter had the functional form :

$$\sigma = 12 + 2.76\ M_\infty$$

while Channapragada (1963) suggested :

$$\frac{\sigma}{\sigma^*} = \left[R' \frac{\rho_\infty + \rho_c}{\rho_\infty} \right]^{-1} \qquad 3.14.$$

where σ^* is the incompressible jet spread parameter, usually equal to 12, and R' is a constant which equals 0.25 for Mach 8.2 flow.

With a turbulent mainstream and a laminar coolant, the flow field close to the slot in this study will approximate to that of a compressible turbulent jet spreading into a quiescent (laminar) fluid and equation 3.12. is applicable.

Turbulent mixing of the two streams implies that the hot mainstream gases will be present to the edge of the mixing zone and will not be felt at the wall until this edge meets the surface. This will occur when $y' = -s$ and $x = x_{pc}$ where x_{pc} is the distance from the slot to the end of the potential core. Substitution of these conditions into equation 3.13 gives :

$$\xi_{pc} = \sigma \left(\frac{-s}{x_{pc}} \right) \qquad 3.15.$$

The velocity variation over the mixing region (equation 3.12.) at the end of the potential core can be written as :

$$u = \tfrac{1}{2} \left[u_\infty (1 + \operatorname{erf} \xi_{pc}) + u_c (1 - \operatorname{erf} \xi_{pc}) \right] \qquad 3.16.$$

When $\operatorname{erf} \xi_{pc} = -1$ then $u = u_c$ which implies that no high speed mainstream fluid has penetrated the coolant layer to cause a velocity change. However $\operatorname{erf} \xi_{pc} -1$ occurs when $\xi_{pc} = -\infty$ which is impractical for the definition of the jet boundary edge. Assuming the lower edge of the jet exists where $\xi_{pc} = -2$ then $\operatorname{erf} \xi_{pc} = -.995$. Substitution into 3.15.yields:

$$x_{pc} = \frac{\sigma s}{2} \qquad 3.17.$$

A knowledge of the rate of jet spread (equation 3.14.) and the slot height permits an estimation of the potential core length.

A wall boundary layer will grow from the slot to modify the error function profile close to the surface. As the distance from the slot increases the modification will grow in height until the combined velocity field will resemble that of a normal turbulent boundary layer. Experimental measurements of velocity profiles in low speed film cooling flows have been made by Harnett et al (1961), Seban and Back (1962), Goldstein et al (1965), Escudier (1955), Pia and Whitelaw (1967), and Burns and Stollery (1969). For $u_c/u_\infty \leq 1$ and thin lip geometry, the general shape of the profile, after about 15 slot heights downstream, seems to obey the error function suggested in the outer region. Closer to the wall the velocity profile resembles the 1/7 power law.

In this study for turbulent mainstream flow, the error function velocity profile of equation 3.12 . is used with a 1/7 power law wall boundary layer profile patched on close to the wall. The rate of growth of this patch was assumed to be dependant on the coolant conditions to the end of the potential core and upon the mainstream conditions further downstream. The laminar mainstream flow film cooling velocity profile assumed a linear velocity profile patch in a similar manner to the turbulent case.

Figure 2b demonstrates how the assumed turbulent velocity profile smooths out and becomes fuller from the end of the potential core to 125 slot heights downstream. Included in Figure 2a are some of the definitions of important

parameters used in the boundary layer model.

3.4 Growth of the Layer

The boundary layer model assumption (i) of section 2.2. states that the hypothetical layer grows as a hypersonic boundary layer.

Shapiro (1954) page 1093 considered the growth of turbulent boundary layers at high Mach numbers. For a Mach 8.2 turbulent flow :

$$\delta/\theta = 46.165 \qquad 3.18.$$

where δ is the height of the layer and θ the momentum thickness. The calculation technique assumed a 1/7 power law velocity profile but Shapiro adds "the value of δ/θ is insensitive to the exact shape of the velocity profile".

The momentum equation for a constant mainstream Mach number reduces to :

$$\frac{\tau_w}{\rho_\infty u_\infty^2} = \frac{d\theta}{dx} = \tfrac{1}{2} C_f \qquad 3.19.$$

Hayes and Probsein (1959) suggest the use of Eckert's (1955) reference temperature to relate the incompressible skin friction coefficient to the compressible case. The empirical method has been found to be useful for calculations up to $M_\infty = 8.2$. The suggested relation was :

$$\frac{C_f}{C_{f_{inc}}} = \left(\frac{\mu^*}{\mu_\infty}\right)^{.2} \left(\frac{\rho^*}{\rho_\infty}\right)^{.8} \qquad 3.20.$$

where μ^* and ρ^* are calculated at the reference temperature :

$$T^* = .5\ (T_\infty + T_w) + .22\ (T_r - T_\infty) \qquad 3.21.$$

The Blasius formula for calculation of the turbulent incompressible skin friction coefficient has been accepted as an accurate representation :

$$\tfrac{1}{2}\ C_{f_{inc}} = .0286\ Re_x^{-.2} \qquad 3.22.$$

Combining 3.19, 3.20, 3.22.and integrating yields :

$$\delta = K_L\ x^{4/5} \qquad 3.23.$$

where K_L for this study became 0.1515 for x in inches.

3.5 Adiabatic Wall Temperature Estimation

The specific heat of the mixture is related to the mass flow in the layer by equation 3.3. The mass flow in the layer is related to the adiabatic wall enthalpy by equation 3.10. Also the adiabatic wall temperature is related to the film cooling effectiveness and mass flow in the layer by equation 2.18. These equations are presented here again and re-numbered for clarity :

$$Cp = \frac{\dot{m}_c}{\dot{m}_L}\ (Cp_c - Cp_\infty) + Cp_\infty \qquad (i)$$

$$\dot{m}_L = \rho_\infty u_\infty \delta\ \frac{\frac{\dot{m}_s}{\dot{m}_c}\left(\frac{Cp_c}{Cp_\infty} - 1\right) + 1}{\frac{\dot{m}_s}{\dot{m}_c}\left(\frac{W_\infty}{W_c} - 1\right) + 1} \int_0^1 \frac{u/u_\infty}{\frac{h_w}{h_\infty}\left(1 - \frac{u}{u_\infty}\right) + \frac{h_{aw}}{h_\infty}\left(1 - \frac{u}{u_\infty}\right)\left(\frac{u}{u_\infty}\right) + \left(\frac{u}{u_\infty}\right)^2}\ dz \qquad (ii)$$

$$\eta' = \frac{\dot{m}_c}{\dot{m}_t}$$

$$\eta'' = \frac{T_{aw} - T_{o\infty}}{T_{oc} - T_{o\infty}} = \frac{Cp_c/Cp_\infty \ \eta'}{1 + (Cp_c/Cp_\infty - 1)\ \eta'} \qquad \text{(iii)}$$

These three equations have three unknowns $\dot{m}_t$, T_{aw}, and Cp. The calculation method assumes a T_{aw} and estimates a C_p to obtain $\dot{m}_t$ from (ii). A new value of Cp was found from (i). Recalculation continued until there was convergence on a particular value of Cp. A value of $\dot{m}_t$ results which was used to calculate a new T_{aw} from (iii). The new T_{aw} was used to find another value of Cp by the first interation and hence a third value of T_{aw}. The convergence of T_{aw} required about five runs through the double interation prior to the assumed and calculated T_{aw} agreeing to within one degree. Simultaneous solution of the three equations enabled the calculation of heat transfer directly from equation 3.26. and 3.27.

From the slot to the end of the potential core there is no mainstream gas penetration to the wall and the film cooling effectiveness is unity, ($T_{aw} = T_{oc}$). Equation 3.23. is used to determine the origin of the hypothetical layer.

3.6 Heat Transfer Calculation

Rotta (1964) used Colburn's modification to Reynolds analogy which should account for the fact that Pr ≠ 1.

$$St = \frac{C_f}{2Pr^{2/3}} \qquad 3.24.$$

where St is the stanton number.

Assuming the combined flow field viscosity obeys a power law relationship similar to pure air flow then :

$$\frac{\mu}{\mu_\infty} = \left[\frac{T^*}{T_\infty}\right]^{.75} \qquad 3.25.$$

Combining 3.25. with 3.20. and 3.22. yields :

$$\tfrac{1}{2} C_f = .0286 \left(.28 + \frac{T_w}{2T_\infty} + .22 \frac{T_{aw}}{T_\infty}\right)^{-.65} Re_x^{-1/5} \qquad 3.26.$$

Using the definition of Stanton number and Reynolds analogy the heat transfer to the wall becomes :

$$q = \rho_\infty u_\infty Cp \frac{C_f}{2Pr^{2/3}} (T_{aw} - T_w) \qquad 3.27.$$

Calculation of the skin friction coefficient from 3.26. enables the heat transfer rate to follow directly from 3.27. for a known adiabatic wall temperature.

Figure 3 demonstrates the calculated variation of specific heat for helium, air, and Freon injection for similar mass flow rates into a Mach 8.2 air mainstream flow.

3.7 Application of the Boundary Layer Model Extension.

The relaxation of the power law dependence upon the mass velocity profile equation 2.15. has the effect of changing equation 2.16. to :

$$\eta' = \frac{1}{K_1 \int_0^1 \frac{\rho u}{\rho_\infty u_\infty} dz} \left[\frac{x}{m\ s}\right]^{N-1} \left[Re_c \frac{\mu_c}{\mu_\infty}\right]^N \qquad 3.28.$$

Defining a parameter K' such that :

$$K' = \frac{1}{K_1 \int_0^1 \frac{\rho u}{\rho_\infty u_\infty} dz} \qquad 3.29.$$

it is clear that the variation of the mass velocity profile by other than the power law dependence will have the effect of increasing K'.

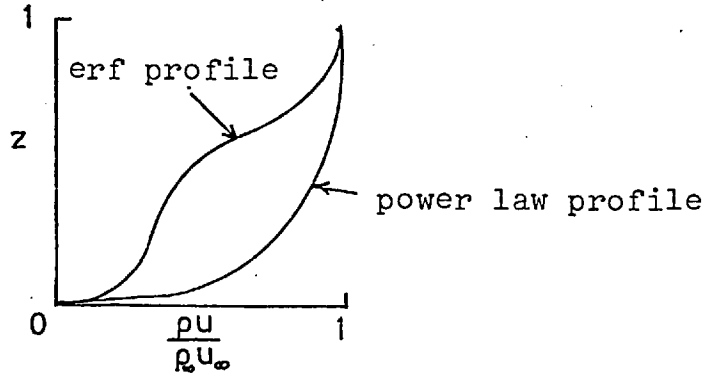

In the actual film cooling flow field, as measured by several low speed investigations, pitot profiles tended to follow the general error function approximation close to the slot. High speed film cooling flows would have a marked variation of density in regions of high du/dz which would have an effect on the constant K'. Goldstein (1968) et al noticed this shift in data due to an increased K' with supersonic external flow and produced a reference density factor to account for this phenomena. The method presented here should prove to be useful in such cases.

The boundary layer extension should be valid for turbulent mainstream boundary layers but some doubt exists as to its application of laminar film cooling.

A laminar mainstream boundary layer with coolant injection has a free jet boundary between the two streams which will cause a certain degree of mixing between them. Even if molecular motion is the only mixing mechanism the velocity discontinuity will be smoothed. The shear layer between the two streams is likely to cause rotational flow and a further smoothing of the velocity profile.

In this study sufficient mixing between two laminar streams is assumed to exist to test the boundary layer model application.

4. DESCRIPTION OF APPARATUS

4.1 The Gun Tunnel

The measurements were made using the older of the two hypersonic gun tunnels in the Aeronautics Department of Imperial College. Stollery et al (1960)and Needham (1960) describe this facility and its capabilities. Essentially it is a blown-down tunnel utilizing an aluminium piston to separate the driver gas from the working gas. A shock wave preceeds the piston down the length of the barrel compressing and heating the working gas. Multiple shock reflections off the barrel end, further compress and heat the working gas prior to passing it through the convergent divergent nozzle which accelerates the gas to the required Mach number. By varying the ratio of the barrel pressure to the driver pressure the unit Reynolds number $\frac{\rho_\infty u_\infty}{\mu_\infty}$ of the mainstream flow could be changed.

All measurements were conducted using a Mach 8.2 contoured nozzle which provided uniform flow conditions over the length

of the model. The running time of the tunnel was of the order of 40 milliseconds which allowed a surface temperature rise of about $2^{o}K$.

4.2 Flat Plate Models

A 12 inch long by 5 inch wide mild steel flat plate was pedestal mounted at zero incidence ½ inch below the nozzle centre line. Opatowski (1964) calibrated the Mach 8.2 contoured nozzle and observed that nozzle contour discontinuities tended to focus on the centre line. Once the model was mounted in this position and the blockage difficulties solved, no adjustments were made to the relative position of the model, nozzle exit place, and diffusers.

A pyrex plate 3 inches wide and 12 inches long, with 72 platinum thin film resistance thermometers, was flush mounted along the centre of flat plate model. Two nose attachments (figure 4) which contain the coolant plenum chambers were used. Nose attachment A was added for the laminar film cooling tests while turbulent film cooling tests were conducted using nose B. Both nose extensions had lip thicknesses of 0.005 inches and were adjustable to allow the slot height to be varied.

A 0.005 inch steel shim 5 inches long and 0.25 inches wide was perforated at 0.125 inch intervals to produce uniform delta shaped elements. When these were bent to the upright position they presented a swept delta shape inclined at about 30 degrees to the flow direction. The top of these vortex generators was 0.060 inches above the flat plate surface. This strip was attached with Araldite 0.125 inches from the leading

edge of nose B. Richards (1967) studied this method of generating a turbulent boundary layer in a hypersonic flow. For the test conditions and vortex generators used, Richards demonstrated that the 6 inch distance between generators and slot should provide completely turbulent flow at the slot.

Vertical side plates were added to confine the high pressures beneath the model from affecting the flow on the upper surface. Small side plates extending vertically upwards on each side of the slot proved to make no significant difference in the two dimensionallity of the coolant flow and thus were not used.

Table 1 lists further dimensions for both model nose extensions.

4.3 Coolant Feed System

A Brooks 1307 fullview flowmeter was connected to a high pressure gas cylinder for the cases of foreign gas injection or left open to the atmosphere when air was used as the coolant. The flow rate was controlled by a 1/8 inch diameter needle valve. Control of coolant flow time was obtained by inserting a solenoid valve between the flowmeter and the model. By opening this valve approximately one second prior to initiating mainstream flow, a steady coolant mass flow rate was achieved and the tunnel static pressure was not raised to an unacceptable level.

A feed tube from the solenoid valve was passed through a sealed hole in the working section and attached to a T tube enabling two rubber tubes to be connected to the model.

Nose A provided a plenum chamber 0.25 inches deep and 2.5 inches long. The coolant was turned through 180° prior to injection 0.895 inches from the leading edge. Nose extension B was designed to give better two dimensionallity on injection than that provided by A. The two coolant feed tubes were connected to a primary settling chamber attached to the underside of the flat plate. Five copper tubes carried the coolant from the primary chamber to the main plenum chamber 3.5 inches ahead of the slot. This larger chamber provided an area ratio of about 8:1 with the slot exit area. The $\frac{1}{8}$ inch splitter plate was supported on three sides by the body of the nose as well as by 3 circular columns equally spaced across the width and midway along its length. By tapering the splitter plate 1 inch back from the slot minimum area was obtained at the slot exit.

4.4 Heat Transfer Measurement

Appendix A of this thesis described the use of platinum thin film resistance thermometers to measure heat transfer rates directly. Briefly the resistance change of the thin film gauges caused by a temperature increase in the pyrex backing material, resulted in an out-of-balance voltage to appear across a Wheatstone bridge. This signal was amplified and passed into an analogue circuit which solved the thermal diffusion equation producing a voltage proportional to the heat transfer rate as a function of time. Land Polaroid cameras equipped with a high speed film (3000 ASA equivalent) were mounted on three Tektronix 502 oscilloscopes to record the voltages.

Preparation of these gauges is fully explained in Appendix A.

The time base of the oscilloscopes was triggered by a flip-flop circuit activated by a Schmidt trigger which was itself triggered by a microphone. The noise of the bursting diaphragms started the chain of events.

4.5 Pitot Pressures

A Hilger 382 micromanometer with a 0 - 5 inches of water head was calibrated with an inclined mercury manometer. The model was inserted in the working section with a rack of 5 pitot tubes, of 0.040 inches inside diameter, mounted across the model such that the pitot tubes were as close to the exit plane of the slot as was possible. After reducing the pressure in the tunnel working section to some predetermined value, the solenoid valve was opened and recordings made of mass flow rate, pitot pressure, and tunnel static pressure. In this way the calibration of the flow meter, and two dimensionallity of the coolant flow was determined.

4.6 Schlieren System

Flow visualization was obtained using a conventional single pass schlieren system. The concave spherical mirrors were arranged to give an amplification factor of 0.8. Either Ilford fast blue sensitive plates (type XK) or a normal polaroid camera could be used to record the resulting image.

The spark source utilized a 1μf electrolytic capacitor charged up to 12 kilovolts which discharged over a gap of 1.2 inches in an argon atmosphere of approximately 10 psi gauge pressure. The trigger mechanism consisted of an induction coil

which initiated the discharge of a smaller capacitor. This discharge ionizes the argon near one of the electrodes attached to the large condenser with the resulting ionization of the atmosphere between the 1.2 inch gap. The main capacitors discharged, producing a brilliant short duration light flash. The first stage of this trigger system, the induction coil, was itself triggered by a time delay unit connected to the microphone system described in section 4.4. By suitable settings on the time delay unit, the spark was initiated once steady flow conditions were achieved over the model.

The knife edge was set parallel to the flow for all cases studied.

5. MAIN PARAMETER DETERMINATION

5.1 Coolant Conditions

The pitot pressure measurements described in section 4.5 provided the coolant stagnation pressure, P_{oc}, while the coolant stagnation temperature, T_{oc}, was equal to room temperature. Knowledge of these two parameters enabled calibration of the flowmeter. Figure 5 demonstrates the two dimensionallity for both nose extensions while figure 6 compares the flowmeter calibration curve with the calculated values.

Assuming the coolant will expand from the stagnation conditions obeying the isentopic adiabatic perfect gas laws then :

$$\frac{T_c}{T_{oc}} = \left(1 + \frac{\gamma-1}{2} M_c^2\right)^{-1} \qquad 5.1.$$

$$\frac{P_c}{P_{oc}} = \left(1 + \frac{\gamma - 1}{2} M_c^2\right)^{-\frac{\gamma}{\gamma - 1}} \qquad 5.2.$$

The mass flow of the coolant at the slot is :

$$\dot{m}_c = \rho_c u_c \, sL \qquad 5.3.$$

which when combined with the equation of state $\rho_c = \frac{P_c}{RT_c}$, the definition of Mach number $M_c = \frac{u_c}{\sqrt{\gamma RT_c}}$, equation 5.1, and 5.2. yields :

$$\dot{m}_c = \sqrt{\frac{\gamma}{R\,T_{oc}}} \; Mc \; sL \; P_{oc} \left(1 + \frac{\gamma - 1}{2} M_c^2\right)^{-\frac{\gamma+1}{2(\gamma-1)}} \qquad 5.4.$$

For a choked slot $M_c = 1$ and equation 5.4 becomes :

$$\dot{m}_c = \sqrt{\frac{\gamma}{R\,T_{oc}}} \; sL \; P_{oc} \left(\frac{2}{\gamma+1}\right)^{\frac{\gamma+1}{2(\gamma-1)}} \qquad 5.5.$$

Hence a relation between coolant stagnation pressure and mass flow rate.

With underchoked flow the coolant static pressure equals the mainstream static pressure which on combining 5.4 and 5.2 gives a relationship between coolant Mach number and mass flow rate:

$$M_c \left(1 + \frac{\gamma - 1}{2} M_c^2\right)^{\frac{1}{2}} = \sqrt{\frac{RT_{oc}}{\gamma}} \; \frac{\dot{m}_c}{P_\infty \, sL} \qquad 5.6.$$

If the Mach number of the coolant is equal to one (the slot is choked) the coolant is assumed to expand

isentropically to a supersonic flow according to equation 5.2 :

$$M_c = \left\{ \frac{2}{\gamma - 1} \left[\left(\frac{P_{oc}}{P_\infty} \right)^{\frac{\gamma - 1}{\gamma}} - 1 \right] \right\}^{\frac{1}{2}} \qquad 5.7.$$

The height to which an underexpanded no mixing coolant would expand, s', can be estimated by assuming isentropic expansion to the Mach number provided by equation 5.7. The equation is that used in nozzle design to calculate area ratios :

$$\frac{s'}{s} = \frac{\left(1 + \frac{\gamma - 1}{2} M_c^2\right)^{\frac{\gamma + 1}{2(\gamma - 1)}}}{M_c \left(\frac{\gamma + 1}{2}\right)^{\frac{\gamma + 1}{2(\gamma - 1)}}} \qquad 5.8.$$

Coolant viscosity was determined using the following relationships for T_c in degrees Rankine :

Air $\quad \mu = 2.27 \dfrac{T_c^{3/2}}{T_c + 198.6} \times 10^{-8}$ lb sec/ft^2

Freon $\quad \mu = 759.3 \left(\dfrac{T_c}{460}\right)^{.650} \times 10^{-8}$ lb sec/ft^2

Helium $\quad \mu = 1533 \left(\dfrac{T_c}{672}\right)^{.662} \times 10^{-8}$ lb sec/ft^2

The thermal conductivity k for air and helium were obtained from Hilsenrath et al (1955) while k for Freon was obtained from the British Oxygan handbook.

The Freon gas used is known as Freon - 12, dichlorodifluoromethane, $C\,Cl_2F_2$, with the trade name Arcton - 12.

5.2 Mainstream Conditions

Needham (1963) measured the stagnation temperatures and pressures in the Imperial College gun tunnel for a variety of drive pressure to barrel pressure ratios. By assuming an adiabatic isentropic perfect gas expansion from the stagnation conditions to the required Mach number the mainstream flow conditions were calculated. Appendix C contains a Fortran IV programme which calculates these conditions for drive pressures ranging from 500 psig to 2,500 psig in steps of 100 psi and barrel pressures from 0 psig to 100 psig in steps of 5 psig.

5.3 Film Cooling Effectiveness

Film cooling effectiveness based on temperature as used by past investigators is defined as :

$$\eta'' = \frac{T_{aw}(x) - T_{o\infty}}{T_{oc} - T_{o\infty}} \qquad 5.9.$$

Seban has shown that the heat transfer coefficient, H, without coolant injection can be represented by :

$$H = \frac{q_{\dot{m}_c=0}}{(T_w - T_{aw})_{\dot{m}_c=0}} \qquad 5.10.$$

He further states that H maintains its value with the presence of a coolant film. Hence for a constant wall temperature and an adiabatic wall temperature for no injection equal to the

mainstream stagnation temperature :

$$T_{aw} = \frac{q}{q_{\dot{m}=0}} \quad (T_{o\infty} - T_w) + T_w \qquad 5.11.$$

Film cooling effectiveness based on enthalpy is defined as :

$$\eta' = \frac{h_{aw} - h_{o\infty}}{h_{oc} - h_{o\infty}} \qquad 5.12.$$

For $Cp = f(x)$ only, equation 5.12. becomes :

$$\eta' = \left[1 + \frac{Cp_c}{Cp_\infty} \left(\frac{T_{oc} - T_{aw}}{T_{aw} - T_{o\infty}} \right) \right]^{-1} \qquad 5.13.$$

which can be rearranged to give an effectiveness based on temperature :

$$\eta'' = \frac{Cp_c/Cp_\infty \, \eta'}{1 + (Cp_c/Cp_\infty - 1)\eta'} = \frac{T_{aw} - T_{o\infty}}{T_{oc} - T_{o\infty}} \qquad 5.14.$$

6. RESULTS AND DISCUSSION

6.1 Preliminary Tests

To determine the laminar flat plate transition Reynolds number, nose extension A was attached to the model with the slot height reduced to zero. The stagnation temperature and unit Reynolds number were held constant at $1040^{\circ}K$ and 1.72×10^5 per inch respectively in a Mach 8.2

external flow. Heat transfer measurements were made along the length of the model and compared with the predicted distribution using the reference temperature method proposed by Eckert (1955). He stated that incompressible relations for calculation of skin friction and heat transfer would be valid for compressible flows if the fluid properties were evaluated at a reference temperature T* where :

$$T^* = .5\ (T_w + T_\infty) + .22\ (T_r - T_\infty)$$

Figure 7f demonstrates that transition had not occured and the transition Reynolds number was estimated to be in excess of 2.22×10^6 beyond the end of the plate. Schlieren photographs supported this conclusion.

As extensive study of transition in this hypersonic tunnel, conducted by Richards (1967), support the argument of laminar flow to the end of the plate for the test conditions used here.

Nose extension B, with the vortex generators, was attached to the flat plate with the slot height reduced to zero. A heat transfer distribution was measured for constant stagnation temperature and unit Reynolds number of $685^{\circ}K$ and 6.102×10^5 per inch in a Mach 8.2 external flow. The schlieren photographs of figure 14 clearly show the turbulent nature of the boundary layer while the heat transfer distribution, on the same figure, falls off in a manner similar to the Van Driest theoretical prediction. Measured heat flux values are not in agreement with the theory because of the difficulty in estimating the location of the turbulent boundary layer virtual origin. In this case the virtual

origin was assumed to be located at the vortex generator strip. The theoretical line being lower than the measured values is an indication that the virtual origin was located between the vortex generator strip and the slot.

6.2 Laminar Film Cooling

6.2.1. Schlieren Photographs

Schlieren photographs are presented in figure 8 for five air coolant injection rates to demonstrate the effect of unmatched pressures on the flow field.

Photograph 8a, for an injection rate of $\dot{m}_c$ = 0.078 lb/min, shows a shock wave starting near the slot (dark line) which is followed by an expansion fan (white region). This flow pattern is representative of an underexpanded coolant diagramatically represented below :

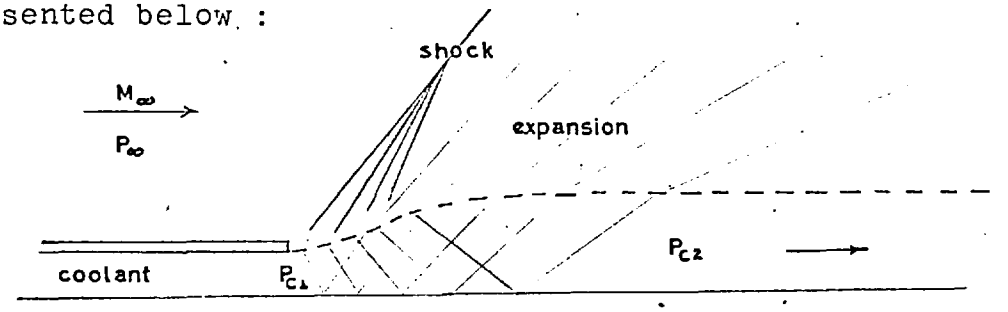

The coolant static pressure at the injection station P_{c1} is greater than the mainstream static pressure, P_∞, so the coolant layer expands until the pressures are equal ($P_{c2} = P_\infty$). This pattern will result when the slot is choked.

Decreasing the mass injection rate reduces the intensity of the slot shock until it seems to disappear at just matched pressure conditions (figure 8c).

The complicated flow pattern which results under just matched pressure conditions as shown in figure 8c, could be explained by considering slot geometry. In actual fact the trailing edge injection lip has a finite thickness and for $P_\infty = P_{c1} = P_{c2}$, there would be a mainstream flow expansion around the upper corner. A small wake and flow recirculation would probably result which would itself increase the turbulence level behind this lip. The expansion fan would be followed immediately by a recompression to turn the flow parallel to the coolant flow direction. A further expansion behind the weak shock would result if the coolant was induced to separate from the surface. This "separation bubble" has been photographed by Visich and Libby (1960) (fig. 13 of NASA TN D - 247) who used $M_\infty = 3.95$ and $M_c = .5$ with $u_c/u_\infty = .12$. The schlieren photographs presented in the above report support the arguments mentioned above. Also more recently, Burns, investigating film cooling at low speeds at Imperial College, noticed this separation bubble and has made some excellent schlieren photographs of this phenomena. In the schlieren photographs presented here, no sign of a separation bubble was visible. By reducing the thickness of this lip the resulting expansion and recompression shock would be made weaker but would always be present.

Schlieren photographs of figure 8 all show the laminar boundary layer developing from the model leading edge. At the slot the boundary layer separates to become a free shear layer which interacts with the coolant film. This shear layer can be seen to extend to the end of the plate but seems to be growing in height with increasing distance downstream. Comparing figure 8a with figure 8e it seems that the shear layer boundaries become less well defined with decreasing injection rate.

Far downstream the original schlieren plates showed some density variations that could be the development of turbulent eddies but this alone is insufficient evidence of transition. Chapman et al (1958)studied transition in a laminar shear layer over a rear facing step and found that stability increased with Mach number. The nature of the shear layer in this study is unknown due to lack of information obtained.

6.2.2. Heat Transfer Distribution and Previous Laminar Theory Correlations.

Heat transfer distributions were measured for five air coolant mass injection rates through a fixed slot height of 0.083 inches. Table 2 is a summary of some of the important flow parameters while Table 3 lists the results of the heat transfer measurements.

Figures 7a to 7e are plots of the measured results which are compared with the no injection distribution. Richards discrete layer theory (see section 2.1) prediction is included on each graph. Figure 7a with an injection rate of $\dot{m}_c$ = 0.072 lb/min shows signs of early transition at about 4 inches from the slot. As the coolant mass injection rate is reduced (figures 7b to 7d) the effects of transition are delayed and the discrete layer theory provides a better prediction of the heat transfer distribution. Consider equation 2.7 repeated below :

$$q(x) = q_i B + C' e^{-z}$$

When $z>1$, B is larger than unity (see figure 1). For increasing z the negative second term on the right hand side, becomes smaller and at some value of z the equation would predict a value of $q(x)$ greater than $q_i(x)$. Calculation for the cases considered in this study showed the limit of $z<2.5$ was necessary to prevent a calculated heat transfer from exceeding the no injection heat input.

In the real flow situation a wall boundary layer will result which will invalidate the no mixing model assumption of a constant velocity across the coolant layer. To accommodate the same coolant mass s' would increase. As heat is added the density of the coolant would decrease which would also increase s' in a constant pressure flow field. A smaller actual B would be the result of the larger s', hence a real heat transfer distribution smaller than that predicted by the equation. Decreasing the injection rate reduces the coolant velocity such that a larger quantity of heat would be absorbed by a given mass of coolant in a given time and the reduced density effect is likely to be noticeable on the measured heat flux. Figure 7e is an example of a larger predicted heat flux than the measured value.

A mean line through the measured values was drawn and superimposed onto one graph in figure 7f. As $\dot{m}_c$ was increased the heat transfer close to the slot was reduced but the destabalizing effect of higher injection rates caused early transition and high heat transfer rates.

The discrete layer correlation parameter suggested by Richards was :

$$\frac{2k\bar{L}x}{\dot{m}_c s\bar{C}p} \quad (1 + \frac{x_o}{x'})^{\frac{1}{2}}$$

where x' is the distance from the slot to first heating effects at the wall. In these tests a nominal value of x' = 0.5 inches was used. Results of calculations demonstrated that the predicted q distribution was insensitive to the choice of x'.

Prior to the effects of transition becoming dominant, the near choked coolant cases correlated well (figure 9). The lowest injection rate examined ($\dot{m}_c$ = 0.029 lb/min) showed a wide departure from the other data. Disagreement in the correlation for the lowest injection rate was expected since the predicted q distribution was poor.

Lucas and Galladay (1967) used a modified Hatch and Papell (1959) function in an attempt to correlate laminar film cooling data. They suggested the correlation parameter:

$$\frac{H\ Lx}{\dot{m}_c Cp} \quad (\frac{su}{\bar{K}})^{\frac{1}{8}} \quad f\ (\frac{u}{u_c})$$

where, for $u_\infty/u_c > 1$, $f\ (\frac{u_\infty}{u_c}) = 1 + \tan^{-1}\ (u_\infty/u_c - 1)$, H_∞ is the heat transfer coefficient and was estimated using Eckerts (1955) reference temperature. The coolant thermal diffusivity, $\bar{K}$, was calculated with Cp = .24 Btu/lb^{o}R and the thermal conductivity, k, was taken to be that of air at the injection static temperature. The use of this correlation

group plotted against film cooling effectiveness, η'', is seen in figure 10. The resulting scatter indicates that the empirical correlation parameter is not useful for all laminar film cooling flows. Since this particular parameter consists of functions not based on theory, it was felt that a further empirical modification could be included here. By multiplying by $M_c^{\frac{1}{2}}$ the scatter of the data is shown to be reduced considerably in figure 11. There is no theoretical justification for this modification and its inclusion is on a pure utilitarian basis.

6.2.3. Boundary Layer Model

Applicability of the boundary layer model to the laminar film cooling case is doubtful as stated in section 3.7. Assuming that sufficient mixing will result, equation 2.27 will apply.

Figure 12 is a plot of film cooling effectiveness against $\bar{X}_L$. Use of the power law velocity profile is shown to provide a poor prediction. However, the more complex analysis of equation 3.28 seems to be more representative of the measured values. Again the low coolant injection rate of $\dot{m}_c = 0.029$ lb/min deviates the most from the predicted values. Using the boundary layer model adiabatic wall temperature prediction and Reynolds analogy to obtain a heat transfer distribution resulted in poor predictions as seen in figures 7a to 7e.

A marginal improvement in correlation resulted when the starting length, X_1, of the layer was included as shown in figure 13.

These results indicated that the boundary layer model for the laminar film cooling flow field is not a useful method for prediction purposes. Since the schlieren photographs indicated that the two laminar streams did not mix together, it was not surprising that the complete mixing boundary layer model correlations were unsuccessful.

6.3 Turbulent Film Cooling

6.3.1 Schlieren Photographs

Helium, air, and Freon were injected into a turbulent Mach 8.2 boundary layer through a slot 0.080 inches high. Three mass flow rates were used for each gas such that the coolant static pressure matched the mainstream static pressure.

Figure 14 includes two schlieren photographs of the no injection flow pattern. The first, for the slot height reduced to zero, clearly shows the turbulent nature of the boundary layer. The wide nose shock is due to the large vortex generators 6 inches ahead of the slot. The weak shock emanating from the slot is caused by the slight discontinuity between the nose and the main body. In the other photograph the slot height was increased to 0.080 inches and plugged with plasticine so no recirculation of fluid would occur into the plenum chamber. Here the boundary layer separates over the rear facing step and re-attaches about two slot heights downstream. The strong re-attachment shock is clearly visable. A considerable disturbance to the flow can be seen as dark areas above and below this shock.

Helium injection for $\dot{m}_c$ = 0.02925 lb/min as shown in figure 15 presents a similar flow pattern to that of the no injection rear facing step. Just after the slot is a light region where the helium probably exists as a single species but the mixing process rapidly destroyed the coolant film. A recompression shock similar to the reattachment shock of figure 14 was noticed to become less well defined as the helium injection rate was increased (figures 16 and 17).

Air injection schlieren photographs for the three mass injection rates are shown in figures 18 to 20. Again the outside boundary layer is seen to be turbulent but now a distinct shear layer is seen between the two streams. This layer represents a boundary between the coolant and the hot mainstream but becomes less well defined and eventually disappears. Further downstream the mixing region close to the surface has a distinct turbulent nature. For all three cases a weak recompression wave can be seen downstream of the slot (as with the no injection case) but the disturbance above this shock is not as intense as with the helium. This weakening of the recompression wave is probably due to the fact that much more coolant mass was available to fill in the area behind the slot. Comparing the highest helium injection rate photograph ($\dot{m}_c$ = .0515 lb/min. figure 17) with the lowest air injection rate ($\dot{m}_c$ = .0655 lb/min figure 18) the two seem very similar with the only exception being the shear layer between the streams.

For Freon injection (figures 21 to 23) the shear layer between the two streams is very clear and seems to extend much further downstream than for the air injections at similar

injection rates. Again the shear layer becomes less well defined downstream of the slot and the turbulent nature of the flow is seen. Figure 23 has a series of expansion fans imbedded in the coolant film. Injection was not tangential but at a slight angle and the coolant turned around the corner causing the expansion fan.

The Freon injection photographs show shear layers that were much longer than either the air or helium cases which indicates Freon was not mixing as readily.

6.3.2. Heat Transfer Distributions

Important flow parameters for the nine coolant injections are listed in Table 4 while Table 5 contains the results of the heat transfer measurements.

The first point of comparison between the three gases is the length of the potential cores in figure 24. Helium provided a very small potential core while the air and Freon injection cases had potential cores of considerable length. No marked difference was noted between the lengths of the potential cores for air and Freon injection.

Similar injection parameters of $m = 0.0231$ for helium and $m = 0.0294$ for air showed air to provide better heat relief on the isothermal surface. Comparison of the air coolant $m = 0.0543$ and Freon coolant $m = 0.0556$ shows Freon to be the better isothermal wall coolant.

This result seems the exact opposite to what one would expect as helium has the highest heat absorbing qualities while Freon the least. Wall heat transfer is governed by the

relation :

$$q = k_w \left.\frac{\partial T}{\partial y}\right|_w \qquad 6.1.$$

where k_w is the thermal conductivity which varies inversley with the square of the molecular diameter of the molecules present at the wall. Wall temperature gradients on an isothermal surface are known to be very large in hypervelocity flows and are directly related to velocity gradients. Comparing the thermal conductivity of the three gases, helium is found to have the largest while Freon has the lowest. Mixtures of foreign coolant and mainstream air would have a wall thermal conductivity which is dependant on the wall concentration and the species of coolant. Helium injection would provide a relatively large k_w, Freon injection a relatively small k_w, while for air injection, k_w would be unaltered except for the normal temperature dependance. Table 4 shows that the helium injection velocities are on order of magnitude larger than Freon injection velocities. This would produce large wall velocity gradients and hence large temperature gradients as well as large temperatures which will increase k_w for helium injection. Air has a thermal conductivity between helium and Freon while the air injection velocities are also between the two extremes. It seemed that the isothermal wall heat transfer rate is more dependant on the thermal conductivity of the mixture and the wall velocity gradients than upon the mixture specific heat.

The general shape of the velocity profiles at the end

of the potential core would be similar to the diagram below.

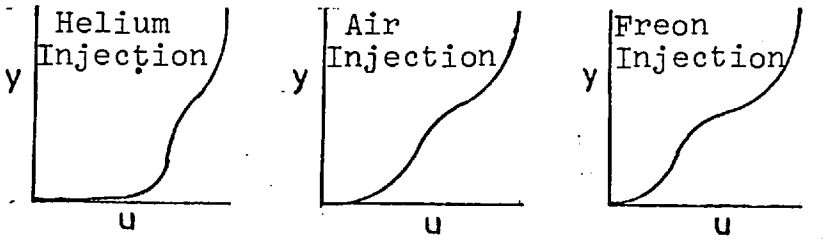

Turbulent mixing of the two streams would probably smooth the velocity profiles such that there will be two regions of high shear. The first will be in the region of the initial meeting of the two streams and the second close to the wall. Helium injection because of the high velocity would result in higher temperature gradients close to the wall than would the slower moving air and Freon coolants. Also the slower moving coolants would have more of the shear at regions removed from the wall such that the heat produced must pass through more coolant to reach the surface.

On an adiabatic wall $\frac{\partial T}{\partial y} = 0$ and the greater heat absorbing ability of helium would show its superiority over heavier gases at reducing T_{aw}.

For both the helium and Freon injection cases an increase in the coolant mass was accompanied by a decrease in heat transfer. However, by doubling the amount of air injection no significant thermal relief was measured. Examination of the air slot Reynolds numbers indicates that for m = 0.0294 Re_c = 254 and for m = 0.0543 Re_c = 516. Transition of the laminar coolant film probably occured closer to the slot in the latter case. Early transition would enhance mixing of the two streams and remove coolant from regions of high shear. An

increased mixing rate would also tend to smooth the velocity profile towards 1/7th power law normally associated with fully developed turbulent flow. When this occurs the regions of highest shear are located near the wall, reducing the blocking effect of the coolant film.

The almost non existant potential core with helium injection indicated that transition occured within a few slot heights of the injection station. Freon injection provided no indications of laminar coolant layer transition.

6.3.3 Previous Theory Correlations

The experimental values for air η'' in this study are compared with the prediction of four low speed theories in figure 25. The agreement of the low speed theories with the measured data is due primarily to the use of the ρ^*/ρ_∞ factor, suggested by Goldstein (1968), being applied to the data in calculation of $\bar{X}_T$. Neglecting the reference density ratio would result in shifting the data points to the right by a factor of 10.5 in this case. Goldstein observed this shift in his supersonic data and accounted for it by considering density variation due to aerodynamic heating to be significant over the mixing region. The shifting of the data to values of $\bar{X}_T$ larger than low speed predictions indicates that film cooling with compressible flow is more efficient than with incompressible flow. Past investigators of compressible mixing (section 3.3) have found that compressibility has the effect of delaying mixing (i.e. increasing the rate of jet spread parameter ϕ). Delaying of mixing results in better thermal blockage effects of the coolant film. This fact

seems to imply that less coolant is necessary in high speed flows to achieve a required thermal relief than that indicated by low speed experiments. The benefit of film cooling in flow fields where this method is likely to find application is most encouraging.

Figure 26 demonstrates how the low speed theory of Tribus and Klein (1953) for all three gas species coolants agree with the reference density modified data. Considerable scatter is evident in the data which is probably due to coolant transition. The coolants all had low slot Reynolds numbers which implied laminar flow on injection. However, the coolant feed system had several flow situations which would probably increase the turbulence level in the coolant. The final plenum chamber 8:1 area reduction prior to injection helped to reduce this problem.

6.3.4. Patankar - Spalding Solution

Patankar and Spalding (1967) developed a finite difference method of solving the two dimensional boundary layer equations. Calculations of many boundary layer flows have been very successful when realistic relations for important parameters and boundary conditions are applied. Cole et al (1967) adapted the calculation procedure to a film cooling model.

The computations employed a version of Prandtl's mixing length theory to describe the effective viscosity relating local shear stress and velocity gradient:

$$\mu_{eff} = \rho \ell^2 \left| \frac{\partial u}{\partial y} \right|$$

where μ_{eff} is the effective viscosity, ρ the density, ℓ the mixing length, and $\partial u/\partial y$ the velocity gradient normal to the surface. The above definition was applied at distances removed from the wall and was defined using accepted dependances on distance from the wall. Van Driest's modification to the effective viscosity formula was used very close to the wall where viscous effects are important. Initially the effective Prandtl and Schmidt numbers were assumed constant but modifications by Pia and Whitelaw (1967) included variation of the effective Schmidt number in the boundary layer.

Conservation of mass, momentum, and energy equations for steady boundary layer flow, were expressed in terms of non-linear, simultaneous, parabolic differential equations and were solved exactly using a finite difference marching integration scheme.

The calculation starts as a free mixing layer(between two square velocity profile streams) from the lip of the slot which spreads into both the turbulent mainstream and turbulent coolant due to mixing. The lower edge of the free mixing layer reaches a smooth impermeable adiabatic wall at the end of the potential core region. Boundary conditions were changed at this point and calculations continued. Modifications on this model were made such that a wall temperature variation with distance downstream could be used as a lower boundary condition and wall kinetic heating was not zero.

Constant specific heats and the ideal gas law $P/\rho T$ = CONSTANT which was dependant upon mainstream and coolant gas

species were concepts assumed to apply for the computations. Viscosity variation was dependant upon a component viscosity procedure and viscosity temperature variation was assumed to obey a 0.7 power law.

The results of these calculations for heat transfer are plotted in figures 15 to 23. For the air and Freon injection cases the predictions were not successful due to the fact that the actual flow comprised of a turbulent mainstream and a laminar coolant at the slot. It is of interest to note that the calculated heat transfer distribution asymptotes to the no injection measured heat transfer. With hydrogen injection the calculations were somewhat more successful except for the determination of the end of the potential core. Low speed experiments compared with the calculations also showed that prediction of the end of the potential core was poor. Excellent agreement with the lowest hydrogen injection rate considered in this study (figure 15) demonstrates the usefulness of the finite difference method when the actual flow approximates to the calculation boundary conditions.

Further developments on the programme to increase its flexibility and account for initial velocity profile shapes at the slot were being processed at the time of writing. Finite difference solutions of the film cooling problem could prove to be very beneficial for design purposes.

6.3.5. Boundary Layer Model Extension

The simple boundary layer model of section 2.2 for a Mach 8.2 mainstream and a 1/7 power law representing the mass

velocity ratio reduces equation 2.16 to :

$$\eta' = 3.28\ (\bar{X}_T)^{-.8} \qquad 6.2.$$

where :

$$\bar{X}_T = \frac{x}{m\ s}\ (Re_c \frac{\mu c}{\mu_\infty})^{-\frac{1}{4}}$$

Figure 27 is a plot of the film cooling effectiveness based on temperature against the parameter $\bar{X}_T$. The data points are seen to be displaced to the right by an order of magnitude from the prediction of equation 6.2 but the - 0.8 power law seems to relate the two parameters. Lack of agreement is due primarily to the selection of the ρu profile in the mixing region.

Using the more complex method of section 3 to obtain the constant relating η'' to $\bar{X}_T$, figure 27 demonstrates that the predictions commence from $\eta'' = 1$ near the falling off of the data. The extended boundary layer model assumes that the rate of mixing remains constant for increasing distance downstream which results in the predicted values falling off more rapidly than the data. Near the end of the potential core the mathematical flow representation is probably close to reality but the wall boundary layer will change the velocity profiles such that they are not similar with increasing x and the rate of mixing will not be constant.

The boundary layer model proposed by Stollery and El-Ehwany assumed similar velocity profiles in the mixing

region. Applying this assumption such that the profiles at the end of the potential core are similar to all those further downstream provides a means of calculating a value of the constant, K', which is applicable over the whole flow field.

The calculations were conducted in two different manners. The first, termed the "delayed mixing model", assumes a turbulent stream expanding into a laminar fluid with σ determined from equation 3.14. Air and Freon injection of this study are well represented by the approximation. Figure 28 demonstrates the success of the method. The helium coolant became transitional very soon after injection and the laminar coolant assumption is not valid. By extrapolating the heat transfer data back to q = 0 at the wall, the distance x_{pc} was obtained and was utilized to obtain a value of σ from equation 3.17. The much smaller value of σ was responsible for rapidly smoothing of the velocity discontinuity as would occur with the mixing of two turbulent streams. The results of this "Complete mixing model" are shown to fit the helium data in figure 28. Table 6 lists the results of calculations.

The proposed delayed mixing model method of calculating K' accounts for the shift in data noticed by Goldstein and this study. It seems that property variations due to aerodynamic heating over the boundary layer must be considered.

Calculated heat transfer distributions for the delayed mixing model are plotted for all cases (figures 15 to 23)

and demonstrate reasonable agreement with the measurements close to the slot for air and Freon injection. Helium injection demonstrated wide departures from the calculated heat transfer distribution. Transition of the helium coolant a few slot heights downstream and the skin friction calculation method could account for the discrepancy.

Use of the complete mixing model requires some method of estimating x_{pc} other than the turbulent jet expansion into a laminar fluid approximation suggested in section 3.3. Calculations demonstrated that the method was insensitive to small changes in an estimated x_{pc}.

Richards (1968) measured heat transfer distribution for film cooling of a turbulent Mach 8.2 boundary layer. His results are compared with the predicted heat transfer of the delayed mixing model in figure 29. The reasonable agreement is encouraging.

7. CONCLUSIONS

7.1 Laminar Film Cooling

An experimental investigation of tangential injection of air into a laminar Mach 8.2 flat plate boundary layer was conducted using heat transfer measurements and schlieren photography.

For choked and near choked coolant injection, an increase in slot Reynolds numbers was found to decrease the transition Reynolds number. The discrete layer theory

proposed by Richards (1967) was found to be adequate in predicting the wall heat transfer distribution prior to transitional effects or effects of increasing s' becoming dominant.

A further empirical modification to the Lucas and Golladay (1967) empirical correlation parameter was found to correlate all cases investigated while the discrete layer correlation was useful only for the choked and near choked slot injections.

Mixing of the coolant and mainstream gases was insufficient for the proposed boundary layer model to be useful for the laminar film cooling flow.

7.2 Turbulent Film Cooling

The results of measured heat transfer distribution for laminar helium, air, and Freon tangentially injected into a turbulent hypersonic isothermal flat plate boundary layer indicated that the heavier gases reduced the no injection heat transfer more effectively than the lighter gases. On an isothermal surface the temperature gradients into the boundary layer and the thermal conductivity of the coolants determine the wall heat flux.

For design purposes requiring a constant low temperature wall the heavier gases (injected tangentially such that the coolant remains laminar for a maximum distance) would provide more reduction in heat transfer than light gases. Light gases, with a high specific heat, would be more beneficial for situations requiring a low adiabatic wall temperature distribution.

Use of the ρ^*/ρ_∞ reference state factor as proposed by Goldstein et al (1966) was found useful in correlating the present compressible film cooling data with the incompressible prediction of Tribus and Klien (1953).

Extension of the boundary layer model to cases of hypersonic turbulent boundary layers tangentially injected with laminar coolants while accounting for property variations over a compressible Mach 8.2 flow field was found useful in prediction of the displacement of the measured data from the low speed theories. The displacement of the data suggests that film cooling is more efficient in compressible than incompressible flows. Further investigations of this flow situation with a wide range of Mach numbers, density, and temperature ratios are necessary to test the validity of the method.

Maximum thermal relief using film cooling in turbulent flow can be achieved by using a maximum quantity of laminar slow moving, high heat capacity coolant that resists mixing with the mainstream and is injected through a large slot with a small lip thickness.

7.3 Suggestions for further work.

1. Experimental investigations to determine the effect of velocity, density, species, and initial turbulence level on the wall heat transfer for the turbulent hypersonic film cooling flow fields. Mixtures of air-helium, air-Freon, etc., could be used as coolants and vortex generators or a grid

system inside the plenum chamber are possible means of achieving these flows. A further check on the delayed mixing theory proposed here as well as the reference density method of Goldstein would be interesting.

2. Experimental measurements of concentration profiles using techniques developed at FFA by Stalker.

3. Effect of the wall on the mixing process in turbulent hypersonic film cooling could be theoretically modified to improve the delayed mixing model prediction.

4. A theoretical analysis similar to that of Albacete (1966) to determine the effect of light, medium, and heavy gas injection for varying temperature and specific heat ratios in the turbulent high Mach number film cooling flows.

5. The Spalding finite difference calculation method shows some promise and further developments could prove useful.

REFERENCES

Abramowitz M. Stegun I.A.	1964	"Handbook of Mathematical Functions with Formulae, Graphs and Mathematical Tables". National Bureau of Standards, Applied Mathematics Series 55.
Albacete L.M. Glowacki W.J.	1966	"Skin Friction and Heat Transfer Characteristics of the Compressible Laminar Boundary Layer with Injection of a Light, Medium, and Heavy Gas". NOLTR 66 - 215 Aerodynamics Report 277.
American Institute of Physics Handbook	1963	McGraw Hill
Ames Research Staff	1953	"Equations, Tables and Charts for Comparable Flow". NACA 1135.
Anon		"Data of Arcton Refrigerants". Imperial Chemical Industries, London
Azzouz D. Pratt N.H.	1968	"Supersonic Turbulent Mixing - Literature Survey and Assessment of the State-of-the-art" Dept. of Aeronautics and Astronautics University of Southampton A.A.S.U. Report 281.
Bayley F.J. Turner A.B.	1968	"Bibliography of Heat Transfer Instrumentation". ARC R and M 3512.
Bershader D. Pai S.I.	1950	"On Turbulent Mixing in Two Dimensional Supersonic Flow." Journal of Applied Physics Vol.21 No.6
Bogdan L.	1964	"High Temperature Thin Film Resistance Thermometers for Heat Transfer Measurement". NASA CR 26
Bogdan L.	1964	"Measurement of Radiative Heat Transfer with Thin Film Thermometers". NASA CR 27.

Brokaw R.S.	1961	"Alignment Charts for Transport Properties, Viscosity, Thermal Conductivity and Diffusion Coefficients for Non-Polar Gases and Gas Mixtures at Low Density". NASA TR - R 81.
Burns W.K. Stollery J.L.	1967	"Isothermal Mixing of a Wall Jet of Foreign Gas with an Air Mainstream". I.C. Dept. of Aeronautics Internal Report EHT/TN/5.
Burns W.K. Stollery J.L.	1968	"Film Cooling: the influence of foreign gas injection and slot geometry on impervious wall effectiveness". I.C. Dept. of Aeronautics EHT/TN/12, see also Int. J. Heat Mass Transfer Vol. 12 pp 935 - 951
Carslaw H.S. Jaeger J.C.	1948	"Conduction of heat in solids". Oxford University Press. Oxford.
Channapragada	1963	"Compressible jet spread parameter for mixing zone analysis". AIAA 1 p 2188.
Chapman D.R. Kvehn P.M. Larson H.K.	1958	"Investigation of separated flows in supersonic streams with emphasis on the effect of transition". NACA 1356.
Chin J.H. Skirvin S.C. Hayes L.E. Silver A.H.	1958	"Adiabatic wall temperature downstream of a single tangential slot". ASME Paper 58-A-107.
Chin J.H. Skirvin S.C. Hayes L.E. Burgraff F.	1961	"Film cooling with multiple slots and louvres". Journal of Heat Transfer, Trans ASME Series C 83 pp 281-292
Clarke J.F. McChesney M.	1964	"The dynamics of real gases". London Butterworths.
Clauser F.H.	1956	"Turbulent Boundary Layers". Advances in applied mechanics Vol. IV Acad Press New York pp 2 - 51.

Colburn A.P.	1933	As used by Rotta (1964) p.8.
Cole E.H. Spalding D.B. Stollery J.L.	1968	"The influence of kinetic heating and molecular weight differences on heat transfer and adiabatic wall effectiveness in film cooling systems". Imperial College, Dept. of Mech. Eng. Report EHT/TN/11.
Cole E.H. Spalding D.B. Stollery J.L.	1967	"Film cooling effectiveness calculated by a finite difference procedure". I.C. Dept. of Mech. Eng. Report EHT/TN/3.
Cooper E.G.	1961	"Mullard reference manual of transistor circuits". Wightman and Company.
Dannenberg R.E.	1962	"Helium film cooling on a hemisphere at Mach 10". NASA D.1550.
Deissler R.G. Loeffer A.L.	1958	"Analysis of turbulent flow and heat transfer on a flat plate at high Mach numbers with variable fluid properties". NACA TN 4262.
Eckert E.R.G. Livingood N.B.	1954	"Comparison of effectiveness of convection, transpiration, and film cooling methods with air as coolant" NACA 1182.
Eckert E.R.G.	1955	"Engineering relations for skin friction and heat transfer to surfaces in high velocity flow". J.Ae.Sc.Vol.22 p.585.
Eckert E.R.G.	1963	"Heat transfer: A Review of current literature". International Journal Heat Mass Transfer Vol. 6. p. 772.
El-Ehwany	1965	Ph.D. Thesis University of London.

Escudier M.P. Nicoll W.B. Spalding D.B. Whitelaw J.H.	1967	"Decay of a velocity maximum in a turbulent boundary layer". Aeronautical Quarterly Vol. XVIII part 2. p. 121.
Ferri	1964	"Review of problems in application of supersonic combustion". J.R. Aero. Soc. Vol. 68 p. 575.
Fishenden M. Saunders O.A.	1950	"An introduction to heat transfer". Oxford University Press, Oxford.
Gartshore I.S. Newman B.G.	1969	"The turbulent wall jet in an arbitary pressure gradient". The Aeronautical Quarterly Vol. XX Part 1.
Gilreath H.E. Schetz J.A.	1966	"A study of tangential slot injection in supersonic flow". Proceedings, Aeronautical Eng. Conference, University of Maryland.
Ginoux J.J.	1962	"Effect of gas injection in separated supersonic flows". VKI - TCEA TN 7.
Gortler H.	1951	As described in Schliching pp 598 - 600.
Goldstein R.J. Shavitt G. Chen T.S.	1965	"Film cooling effectiveness with injection through a porous section" Journal of Heat Transfer Trans ASME C Vol 87 No.3 pp 353 - 361.
Goldstein R.J. Eckert Tsou F.K. Haji - Sheikh A.	1966	"Film cooling with air and helium injection through a rearward facing slot into a supersonic air flow". AIAA Vol. 4 No.6 p. 981.
Goldstein R.J. Basil R.B. Eckert E.R.G.	1966	"Film cooling with helium injection into an incompressible air flow" Int.J. Heat Mass Transfer Vol.9 pp 1341 - 1350.
Goldstein R.J. Eckert E.R.G. Wilson D.J.	1968	"Film cooling with normal injection into a supersonic flow". Journal of Engineering for Industry ASME TRANS November 1968 pp 584 - 588.

Gooderum P.B. Wood G.P. Brevoort M.J.	1950	"Investivation with an interferometer of the turbulent mixing of a free supersonic jet". NACA 963.
Hall J.G. Hertzberg A.		"Recent advances in transient surface temperature thermometry" Jet Propulsion Vol. 28, No.11.
Handbook of Chemistry and Physics - 46th edition	1966	"Chemical Rubber Company Publishing Firm".
Hartnett J.P. Birkebak R.C. Eckert E.R.G.	1961	"Velocity distribution, temperature distribution, effectiveness and heat transfer for air injected through a tangential slot into a turbulant boundary layer". Journal of Heat Transfer Trans. ASME series C 83 293-306.
Hatch J.E. Papell S.S.	1959	"Use of a theoretical flow model to correlate data for film cooling or heating an adiabatic wall by tangential injection of gases of different fluid properties". NASA TN D-130.
Hawkins R.	1967	As used in Azzouz and Pratt (1968) p. 41.
Hayes W.D. Probstein R.F.	1959	"Hypersonic flow theory". Academic Press
Hilsenrath J. et al	1955	"Tables of thermal properties of gases". National Bureau of Standards Circular 564.
Hodgman C.D.	1962	"C.R.C. Standard Mathematical Tables". Chemical Rubber Publishing Co.
Holden M.H.	1963	"Heat transfer in separation flow" Ph.D. Thesis University of London.

Holder D.W. North R.J.	1963	"Schlieren Methods" National Physical Laboratory - Notes on Applied Science No.31.
Korst H.H. Tripp W.	1957	"The pressure on a blunt trailing edge separating two supersonic 2-D air streams of different Mach numbers and stagnation pressure but identical stagnation temperatures". 5th Midwestern Conference on Fluid Mechanics U. of Mich. Press p.187.
Krylov V.I.	1962	"Approximate calculation of integrals". The MacMillan Company.
Kurzrock J.W.	1963	"Selection of surface thermometers for measuring heat flux". Cornell Aero. Lab. CAL - 124.
Kutataladze S.S. Leont'en A.I.	1963	"Film cooling with a turbulent gaseous boundary layer". Thermal Physics of High Temperatures Vol. 1 pp 281.
Lewis H.F.	1966	"A film cooling experiment on a convergent divergent nozzle". AEDC - TR - 66 - 78.
Libby P.A. Schetz J.A.	1963	"Approximate analysis of the slot injection of a gas in laminar flow" AIAA Vol. 1. p.1056.
Librizzi J. Cresci R.J.	1964	"Transpiration cooling of a turbulent boundary layer in an axisymmetrical nozzle". AIAA J.2 pp. 617 - 624.
Lin C.C.	1953	"On the stability of the laminar mixing region between two parallel streams in a gas". NACA TN 2887.
Lin C.C.	1959	"Turbulent flows and heat transfer". High speed Aerodynamics and jet propulsion Vol. V. Oxford University Press.

Lucas J.G. Golladay R.L.	1967	"Gaseous film cooling of a rocket motor with injection near the throat". NASA TN D 3836.
Maydew R.C. Reed J.F.	1963	"Turbulent mixing of axisymmetric compressible jets with quiescent air". ARC 24 941. See also AIAA Journal Vol. 1. 1963 p. 1443.
Mukerjee T. Martin B.W.	1968	"Film cooling by air injection through a backward facing annular tangential slot in a supersonic axisymmetric parallel diffuser". I.C. Dept. Mech. Eng. SF/TN/13.
Myer R.F.	1960	"A heat flow meter for use with thin film surface thermometers". NRCC Report LR 279.
Myer R.F.	1963	"Further comments on analogue networks to obtain heat flux from surface temperature measurements". NRCC Report LR 375.
McCracken D.D. Dorn W.S.	1964	"Numerical methods and fortran programming". John Wiley & Sons Inc.
Needham D.A.	1963	"Progress report on the Imperial College Hypersonic Gun Tunnel". Imperial College Report No.118.
Nishiwaki N. Hirata M. Tsuchida A.	1961	"Heat transfer on a surface covered by a cold air film". International Developments in Heat Transfer. ASME New York pp 675 - 681.
Opatowski T.	1964	"Calibration of Mach 8 contoured nozzle ". Imperial College Aeronautics Internal Memo.

Pia B.R. Whitelaw J.H. 1967 "The influence of density gradients on the effectiveness of film cooling". I.C. Dept. of Mech Eng. EHT/TN/8.

Pia B.R. 1968 "The applications of the boundary layer model to predict the influence of slot boundary conditions on film cooling". Imperial College Dept. of Mech.Eng. EHT/TN/9.

Pia S.I. 1957 "Viscous flow theory part II - turbulent flow". D. Von Nostrand Co. Inc. Princeton, New Jersey.

Papell S.S. Trout A.M. 1959 "Experimental investigation of air film cooling applied to an adiabatic wall by means of an axially discharging slot". NASA TN D-9.

Papell S.S. 1960 "Effect on gaseous film cooling through angled slots and normal holes". NASA TB D299.

Patel R.B. Newman B.G. 1961 "Self preserving, two dimensional jets and wall jets in a moving stream". McGill University Mech. Eng. Research Laboratory: Aerodynamics Section, Report Ae.5.

Powers J.O. Albacete L.M. 1966 "Effects of foreign gas injection on laminar boundary layer stability at low Mach numbers". Naval Ordnance Laboratory 66 - 155.

Patankar S.V. Spalding P.B. 1967 "A finite difference procedure for solving the boundary layer equations for two dimensional flows". Journal Heat Mass Transfer 10 p.1389.

Ragsdale R.G. Edwards O.J.	1965	"Data comparison and photographic observations of co-axial mixing of dissimilar gases at nearly equal stream velocities". NASA TN D-3131.
Rabinowicz J. Jessey M.E. Bartsch C.A.	1956	"Resistance thermometer for heat transfer measurements in a shock tube". GALCIT Hypersonic Research Project Memo 33 July 2.
Redeker E. Miller D.S.	1966	"Mach 16 film cooling". Proceedings 1966 Heat Transfer Fluid Mechanics Institute, Stanford University.
Richards B.E.	1967	"Film cooling in hypersonic flow". Ph.D. Thesis, University of London.
Robinson J.L.	1967	"Similarity solutions in several turbulent shear flows". NPL Aero. Report 1242 ARC 29 330.
Roland H.C. Pasqua R.F. Stevens P.N.	1966	"Film and transpiration cooling of nozzle throats". AEDC - TR - 66 - 88.
Rotta J.C.	1964	"A review of experimental temperature distribution in supersonic and hypersonic turbulent boundary layers with heat transfer". Aeronautical Research Council 26 485 HYP 465.
Roshko A.	1969	"The problem of density effect on free turbulent mixing". Symposium on turbulence, Seattle 23 - 27 June.
Rubesin M.W.	1951	"The effect of arbitary surface temperature variation along a flat plate on the convective heat transfer in an incompressible turbulent boundary layer". NACA TN 2345.

Schetz J.A, Favin S.	1966	"The ignition of slot injected gaseous hydrogen in a supersonic air stream". AIAA Paper 66-644.
Schetz J.A. Jannone J.	1965	"Initial boundary layer effects on laminar flows with wall slot injection". Journal of Heat Transfer. Trans ASME Series C Vol. 87 p.157
Schlichting H.	1960	"Boundary layer theory 4th edition". McGraw-Hill.
Seban R.A.	1960	"Heat transfer and effectiveness for a turbulent boundary layer with tangential fluid injection". Journal Heat Transfer Trans. ASME Series C.82 pp. 303 - 312.
Seban R.A.	1960	"Effects of initial boundary layer thickness on a tangential injection system". Journal of Heat Transfer Trans ASME C Vol 82. No.4 p.392.
Seban R.A. Back I.H.	1962	"Velocity and temperature profiles in turbulent boundary layer with tangential injection". Journal Heat Transfer. Trans. ASME Series C 84 45 - 54.
Sivasegaram S. Whitelaw J.H.	1967	"Film cooling slots, the importance of lip thickness and injection angle". I.C. Mech Eng. Report EHT/TN/6.
Skinner G.T.	1960	"Analogue network to convert surface temperature to heat flux" Cornell Aero. Lab. CAL-100.
Skinner G.T.	1962	"A new method of calibrating thin film gauge backing materials". Cornell Aero. Lab. CAL-105.

Sommer S.C. Short B.J.	1955	"Free flight measurements of turbulent-boundary-layer skin friction in the presence of severe Aerodynamic heating at Mach numbers 2.8 to 7.0". Ames Aero. Lab. NACA TN 3391.
Spalding D.B.	1962	"Heat and mass transfer in boundary layers, part 2. Film Cooling". Northern Research & Engineering Corp. Report No.1058-2, Sept.
Spalding D.B. Patankar S.V.	1967	"Heat and mass transfer in boundary layers". Morgan-Grampion, London.
Stollery J.L. El-Ehwany	1967	"Shorter communication on the use of a boundary layer model for correlating film cooling data". Int. Journal of Heat & Mass Transfer Vol. 10.
Stollery J.L. El-Ehwany	1965	"A note on the use of a boundary layer model for correlating film-cooling data". Int. J. Heat Mass Transfer 8, 55.
Stollery J.L. Maull D.J. Belcher B.J.	1960	"The Imperial College Gun Tunnel". Journal of the Royal Aeronautical Society Vol. 64 p. 24.
Swenson B.L.	1961	"An approximate analysis of film cooling on blunt bodies by gas injection near the stagnation point". NASA TN D-861.
Tifford	1963	"Surface mass transfer correlations". AIAA Vol. 1. p. 1414.
Tollmien	1945	"As reported in Maydew and Miller (1963) p. 12.
Townsend A.A.	1956	"The structure of turbulent shear flow". University Press, Cambridge.

Townsend A.A.	1966	"The mechanism of entrainment in free turbulent flows". Journal of Fluid Mechanics Vol. 26 Part 4. p. 689.
Tribus M. Klien J.	1953	"Forced convection from non-isothermal surfaces". Heat Transfer, A Symposium. University of Michigan Press. Ann Arbor. Mich.
Van Driest E.R.	1952	"Investigation of the laminar boundary layer in compressible fluids using Crocco method". NACA TN 2597.
Van Driest E.R.	1951	"Turbulent boundary layer in compressible fluids". Journal of Aeronautical Sciences Vol. 18. No.3 p. 145.
Vasiliu J.	1962	"Pressure distribution in regions of step induced turbulent separation". Journal of Aeronautical Sciences Vol. 29. No.5
Vidal R.J.	1962	"Transient surface temperature measurements". CAL Report 114.
Visich M. Libby P.A.	1960	"Experimental investigation of mixing of Mach number 3.95 stream in presence of wall". NASA TN D-247.
Watson G.G.	1964	"A survey of techniques for measuring surface temperatures". NPL Report 153.
Whitelaw J.H.	1967	"The effect of slot height on the effectiveness of the uniform density two dimensional wall jet". I.C. Mech. Eng. Report EHT/TN/4.

Wieghardt K.	1946	"On the blowing of warm air for de-icing devices". F.B. 1900 (1944) Reports and Translations No.315, also "Hot-air discharge for de-icing". American Astronautical Federation Translation F-TS-919-RE.
Wisniewski Jack	1961	"Recent studies on the effect of cooling on boundary layer transition at Mach 4." J. Aero. Space Science Vol. 28 p. 250.
Zakkay V. Fox H.	1966	"Experimental and analytical considerations of turbulent heterogeneous mixing in the wake". 7th AGARD Colloquium, Oslo, Paper NYU-AA-66-54.

APPENDIX A

HEAT TRANSFER MEASUREMENT

INDEX

1. INTRODUCTION AND REVIEW OF LITERATURE

A six channel plug in module system was designed and built for use in a hypersonic gun tunnel which has a steady running time in the order of 50 milliseconds. Thin film surface temperature thermometers were used to measure the transient surface temperatures which were processed by analogue circuits to produce voltages representative of the heat transfer rates. Separate calibration techniques were developed to determine the analogue circuit calibration factor and the thermal characteristics of the backing material.

The first investigation of measurement of transient surface temperatures by Chabai and Emrick (1955), Vidal (1956) and Blackman (1956) using thin film resistance thermometers, determined that the technique was useful for instantaneous temperature measurements. These detectors could be used for accurately timing the passage of shock waves and/or determining heat transfer rates. Hall and Hertzberg (1958) presented a review of instrumentation development which started a period of improving and refining of techniques.

Holden (1964) gives a good survey of surface temperature thermometry as do others like Kurzrock (1963), Vidal (1962), and Watson (1964). The best published bibliography of heat transfer instrumentation was presented by Baylez and Turner (1968). These investigators found that surface thin film resistance thermometers were highly sensitive, gave good frequency response, had response times in the nanosecond range, and were suitable for measurements of heat transfer in the range .01 to 100 Btu/ft^2 sec. for short duration test facilities.

A small current was passed through a metallic strip (resistance thermometer) mounted upon a poor electrical conductor (backing material) and this configuration was mounted in a high stagnation temperature testing facility. The resistance of the thermometer is linearly related to its temperature over the small temperature change experienced and hence a transient voltage was produced. This temperature history had to be numerically or graphically integrated to obtain a heat transfer rate history until Meyer (1960), and Skinner (1960) independently developed a resistance - capacitance network which enabled heat transfer to be recorded directly. The inclusion of this network increases the electrical noise on the output. By using transistorised amplifiers and stabilised power supplies, heat transfer rates of about .01 Btu/ft^2 sec. are still measurable with signal to noise ratios of about 5. Both Meyer and Skinner (1960) recognised that some filtering of the high frequency electrical and aerodynamic noise would be necessary.

The bulk thermal properties of the backing materials may not be reliable. These properties may change from sample to sample due to the manufacturing process and it may be subject to variation during the baking process of gauge preparation since some of the film material may diffuse into the backing material. Vidal (1962) notes that the accuracy of measurements depends upon the knowledge of these thermal properties. The first techniques of calibration employed a pulsing procedure where a known amount of energy was dissipated in the gauge and the temperature rise recorded. This required the knowledge of the effective surface area of the gauge which was not readily available. Holden (1963), Skinner (1960), and Meyer (1960), each produced a step voltage through the gauge and obtained a bulk factor containing the unknown analogue calibration factor, resistance-temperature coefficient, and thermal properties of the

backing material.

The difficulty in measuring the effective gauge area especially if the regions near the connecting leads are not well defined, resulted in not too satisfactory results. Skinner (1962) developed a technique that eliminates this area measurement by referring the thermal characteristics of the backing material to that of a liquid with well known thermal characteristics. His pulsing technique also accounts for nonuniform gauges where resistance, width, and thickness may vary along the gauge length.

2. THEORY OF THIN FILM GAUGES

The response time of a thin metalic film deposited on an insulator (pyrex glass or quartz usually) can be considered as the classical one dimensional heat transfer problem if the width of the film is such that, during the running time of the tunnel, heat flows essentially one dimensionally into the backing material. Vidal (1956) considered this problem in detail. The time, t, taken for heat to diffuse from the upper to lower surface of a film of thickness, l, is a measure of its response time. This time has been shown to be given by :-

$$t = \frac{l^2 \rho c}{k} \qquad 2.1$$

where ρ, c, k, are the density specific heat and thermal conductivity of the metal film. Because of platinums low thermal capacity, c, thinness, l, and high thermal conductivity k, this time will be very low. For the Hanovia X-05 platinum gauges used the thickness was of the order of 10^{-6} inches and t was of the order of 10^{-9} seconds.

The very thin gauge can thus be assumed to be a one dimensional slab mounted on a dissimilar semi infinite heat sink. For the thin film in hypersonic testing facilities the assumption that the film takes up the instantaneous temperature of the backing material surface has been widely accepted. Thus the presence of the film is neglected and the problem of heat transfer to the backing material in terms of the surface temperature must be considered.

In using the method to measure heat transfer from gas streams it is assumed that the change in surface temperature is small compared with the gas temperature.

Carslaw and Jaeger (1959), determined the relationship between an arbitary surface temperature T (t) and a heat transfer rate per unit area per unit time q (t), where t is time, to be :-

$$T(t) = \frac{\sqrt{k}}{\bar{K}\sqrt{\pi}} \int_0^t \frac{q(t-\psi)}{\sqrt{\psi}}\, d\psi \qquad 2.2$$

Here $\bar{K}$ is the thermal diffusivity ($= \frac{k}{c\rho}$), ρ the density, c the heat capacity, and k the thermal conductivity. Inverting this expression and using the boundary condition of T (o) = 0 gives :

$$q(t) = \frac{\sqrt{\rho ck}}{2\sqrt{\pi}} \left[\frac{2\,T(t)}{\sqrt{t}} + \int_0^t \frac{T(t) - T(\psi)}{(t-\psi)^{3/2}}\, d\psi \right] \qquad 2.3$$

For a constant heat transfer rate equation 2.3 reduces to :-

$$q(t) = \frac{\sqrt{\pi}}{2} \sqrt{\rho c k} \quad \frac{T(t)}{\sqrt{t}} \qquad 2.4$$

Since the change in surface temperature is small the resistance of the gauge, R, can be assumed to vary linearly with temperature.

$$\Delta R = \alpha R_o \, T(t) \qquad 2.5$$

where T (t) is the change in temperature, α the temperature coefficient of resistance, and R_o the initial resistance at t = 0.

If a constant current, I, is carried by the gauge, a change in voltage E(t) is related to temperature variation by:-

$$E(t) = I\Delta R = \alpha I R_o \, T(t) \qquad 2.6$$

The initial voltage across the gauge, E_o, was :-

$$E_o = IR_o \qquad 2.7$$

and equation 2.6, for a constant gauge current, becomes :-

$$T(t) = \frac{E(t)}{\alpha E_o} \qquad 2.8$$

Substituting equation 2.8 into equations 2.4 and 2.3 gives for a constant heat transfer rate :-

$$q(t) = \frac{\sqrt{\rho ck}}{\alpha} \frac{\sqrt{\pi}}{2E_o} \frac{E(t)}{\sqrt{t}} \qquad 2.9$$

For an arbitary heat flux :-

$$q(t) = \frac{\sqrt{\rho ck}}{2\alpha\sqrt{\pi}E_o} \left[\frac{2E(t)}{\sqrt{t}} + \int_o^t \frac{E(t) - E(\psi)}{(t-\psi)^{3/2}} d\psi \right] \qquad 2.10$$

3. THEORY OF THE ANALOGUE CIRCUITS

By taking a record of the voltage change E(t), numerical or graphical techniques could be used th evaluate q(t) from equation 2.10. This procedure requires considerable effort and there are no indications of satisfactory results available at the time the information is obtained. Skinner (1960), and Meyer (1960) considered using the analogy between electrical and thermal diffusion as a solution to this problem.

The equation of one dimensional heat diffusion is :-

$$\frac{\partial T}{\partial t} = \frac{k}{\rho c} \frac{\partial^2 T}{\partial x^2} \qquad 3.1$$

where the symbols are the same as those used in Section 2 and x is the distance from the surface. The diffusion of electrical charge through a medium with a capacitance C per unit volume and resistivity r is :-

$$\frac{\partial V}{\partial t} = \frac{1}{rC} \frac{\partial^2 V}{\partial x^2} \qquad 3.2$$

where V is the voltage potential.

These two equations have identical form. Now it is possible to say V is the analogue of T, 1/r is the analogue of k, and C is the analogue of ρc. To overcome the problem of building a circuit with distributed resistivity and capacitance a "lumped" network with specific values of capacitance and resistance was devised.

Meyer (1960) chose a "T" network since its response time was such that for an RC network of infinite length the output voltage reached 99% of its asymptotic value in t = .8 RC seconds.

Although the time resolution would improve by decreasing RC, the output voltage would be smaller. Thus the value of RC required would depend upon the magnitude of heat transfer to be measured and the time during which it is to be measured. Meyer (1960) suggested RC = 100 microseconds for a tunnel with running times between 4 and 50 milliseconds.

Meyer (1960) went on to determine the minimum number of lumps necessary so that the network would seem to be infinite during the useful running time. His calculations for a 50 millisecond running time indicated 50 lumps which seemed to be a large number. By increasing the RC values in an arithmetic progression fewer lumps were required. However, Meyer (1963) stated that high quality resistors and condensers were required and the cost is subsequently higher. Meyer (1963) also stated in his second paper that a time delay on the output voltage equal to $\frac{RC}{8}$ would result and should be considered for accurate time measurements. His second paper acknowledged the fact that the arithmetic increase in RC values would not give an identical output to a uniform lump network but suggested adding two additional lumps, both equal to the first suggested lump, to the beginning of the network. This would bring the output voltage of the arithmetic progression within 1% of the uniform lumped network.

Figure 30 is a representation of the T section analogue network.

Skinner (1960) considered the analogue as a filter which approximated the required transfer function. His analogue required fewer components of non standard accurate values. For this reason the network suggested by Meyer was adopted.

Using the analogy and applying it to equation 2.9 for a steady heat transfer rate the output voltage V_A becomes

$$V_A = \frac{E_o \alpha}{\sqrt{\rho c k}} \quad \frac{\sqrt{RC}}{2} \quad q \qquad 3.3$$

and defining $\frac{2}{\sqrt{RC}}$ as A* and $\sqrt{\rho c k}$ as β gives :-

$$q = A^* \frac{\beta}{\alpha} \quad \frac{V_A}{E_o} \qquad 3.4$$

4. CALIBRATIONS

4.1 Amplifier Calibration

Consider the normal wheatstone bridge below:-

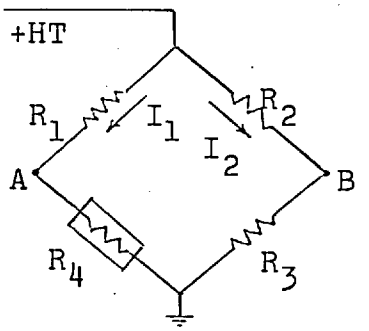

In this case R_4 is the gauge while R_1 is made variable to adjust the current through the left side of

the bridge and hence the voltage drop Eo over the gauge. R_2 is also variable to adjust the current through the right side of the bridge which allows the voltage drop over R_3 to be set equal to that over the gauge R_4.

Heating R_4 results in an out of balance voltage E(t), to be produced between points A and B :-

$$E(t) = I_1 R'_4(t) - I_2 R_3$$

where R'_4 (t) is the new resistance under heating conditions. However E(t) is superimposed on to the normal standing voltage Eo over the gauge and special floating difference amplifier configurations are required. A suitable configuration selected was that shown below:

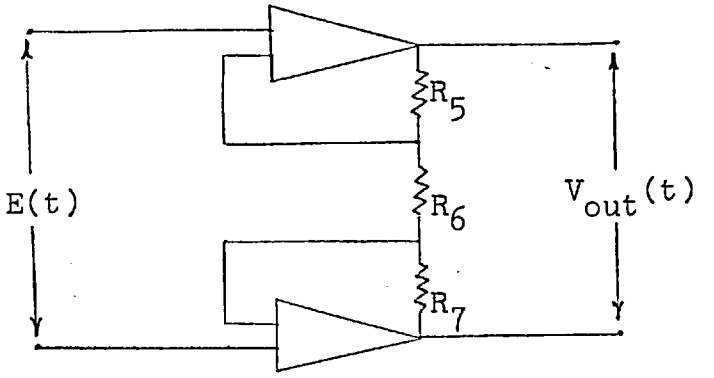

Under these circumstances using the fact that the current through R_6 is not reduced by the feedback loops it is possible to say :

$$E(t) = I_6 R_6$$

$$Vout\ (t) = I_6 (R_5 + R_6 + R_7)$$

$$G = \frac{Vout}{E(t)} = \frac{R_5 + R_6 + R_7}{R_6}$$

It is normal to make the two resistors in the feedback loops R_5 and R_7 equal and by making R_6 variable an adjustable gain configuration is possible. With $R_5 = R_7$ the gain, G, becomes :

$$G = \frac{2R_5}{R_6} + 1$$

By decreasing R_6 to zero an infinite gain is possible but too small a value of R_6 will push the amplifiers to their saturation point with a very small input signal. Although a high gain is desirable it must also be remembered that the bandwidth is inversely proportional to the gain.

The amplifiers chosen were Zeltex transistorized operational amplifiers series 116D. These amplifiers each have a 10 Volt output or 20 Volts in the described configuration, require an input current of 100 nanoamp driving an input impedance of .2 megohms. The power supply required was a nominal $\pm$ 15 Volts and 4 milliamps. The output drift was advertised as 50 μv/1% change in voltage supply which is very suitable for this type of usage.

If a heat transfer rate of 100 Btu/ft^2 sec. were to be measured and nominal values of Eo = 1 Volt, α = .00276, β = .0743, A* = 200 then the input voltage would be approximately 20 millivolts. The gain is thus limited to 1,000 so as not to saturate the amplifiers. In practise a gain setting of about 250 is quite adequate in terms of bandwidth, magnitude of output voltage, and saturation level avoidance.

Since the actual signal to be measured is composed of a DC signal with a superimposed signal upon it, which is itself an increasing voltage with superimposed higher frequency disturbances, it was felt that for the sake of a genuine gain calibration a similar input signal should be used. Thus a low frequency (1 KHZ) sine wave oscillator with a DC output superimposed on the fluctuating voltage was selected. This signal is fed into the amplifier and compared with the output to determine the gain. Both the DC and 1 KC AC gain can be measured be means of comparison of oscilloscope traces or usage of an AC/DC digital voltmeter.

In practise the gains calculated using a real signal will be more representative of the actual gain than the theoretical value.

4.2 Analogue Calibration

By subjecting the gauge to a constant heat flux, q, an out-of-balance voltage, E(t), will appear across the wheatstone bridge such that :-

$$q = \frac{\beta}{\alpha} \frac{\sqrt{\pi}}{2} \frac{E(t)}{Eo \sqrt{t}} \qquad 4.2.1.$$

Analogue theory states that :

$$q = \frac{\beta}{\alpha} A^* \frac{V_A}{Eo} \qquad 4.2.2.$$

Eliminating q from these equations and squaring results in :

$$t = \frac{\pi}{(2A^*V_A)^2} E^2(t) \qquad 4.2.3.$$

Thus the slope of a plot of t versus $E^2(t)$ enables the calculation of A* without the knowledge of β and α.

Another method requires the numerical calculation of the equation for an arbitary heat input, q (t):

$$q\ (t) = \frac{\beta}{2\alpha\sqrt{\pi}\ Eo}\left[\frac{2E(t)}{\sqrt{t}} + \int_o^t \frac{E(t) - E(\psi)}{(t-\psi)^{3/2}}\,d\psi\right] \qquad 4.2.4.$$

With the heat flux known the value of A* could be determined for any time by combining equation 4.2.2. with 4.2.4. to give:

$$A^* = q\ (t)\ \frac{\alpha}{\beta}\ \frac{Eo}{V_A(t)} \qquad 4.2.5.$$

or on direct substitution :

$$A^* = \frac{1}{2\sqrt{\pi}\ V_A(t)}\left[\frac{2E(t)}{\sqrt{t}} + \int_o^t \frac{E(t) - E(\psi)}{(t-\psi)^{3/2}}\,d\psi\right] \qquad 4.2.6.$$

Once again the β/α term drops out and must be determined separately by other techniques.

When this second method is employed the time shift of $\frac{RC}{8}$ on the analogue output voltage, V_A, must be considered.

4.3 Pulse Calibration

The method used was similar to that described by Skinner (June 1962).

The thermal properties of the pyrex backing material β must be accurately known :

$\beta = (\rho ck)^{\frac{1}{2}}$

k = thermal conductivity

c = specific heat

ρ = density

This β may be different from sample to sample of the same material or may change due to the baking process in gauge preparation.

A step current was applied to the gauge and the surface temperature rise recorded. The gauge was then immersed in distilled water at the same temperature and pulsed again. The two resulting temperature records have the same time dependence but different amplitudes since in the second case some I^2R heat generated in the gauge will pass into the water. The amplitude ratio is simply related to the β's of the pyrex and water.

The calibration temperature and the normal model temperature under flow conditions (i.e. room temperature) should be the same since β is a function of temperature.

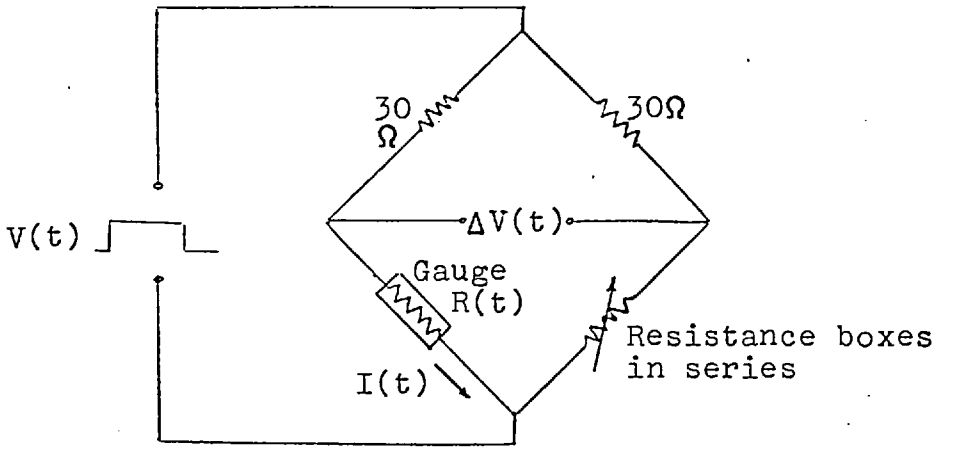

The voltage acorss the gauge is a linear function of gauge current and the change in resistance during a pulse cycle is small compared to the initial resistance. The energy input to the gauge is proportional to $V^2(t)/R(o)$ and if the gauge is always at the same temperature when V(t) is applied then energy dissipation will always be the same.

The bridge is balanced, step voltage V(t) applied and the output voltage $\Delta V(t)$ measured on an oscilloscope. $\Delta V(t)$ is due to the rise of gauge resistance with surface temperature of the pyrex baking. Thus one can say :

$$\Delta V(t) = I(t)\,\Delta R(t) = I(t)\,\alpha_o R_o \quad F(t) \qquad 4.3.1.$$

where

$\Delta V(t)$ = output voltage
$I(t)$ = gauge current
$\Delta R(t)$ = change in gauge resistance from initial value
$F(t)$ = change in gauge temperature from initial value
$\alpha_o R_o$ = slope of R vs T line for this gauge

Quantities relating to pulsing in water will be denoted by a cross. Subscripts g and w will be used to denote

properties and quantities relating to the pyrex glass backing material and water respectively.

Lower case letters denote Laplace transforms of corresponding upper case letters.

i.e. $q(s) = \mathcal{L}Q(t) = \int_0^\infty e^{-st} Q(t)\, dt$

Since the gauge adapts the temperature of the backing material, the flux of heat (when pulsed in air) in relation to temperature:

$$q(s) = \beta_g \sqrt{s}\ f(s) \qquad 4.3.2.$$

assuming one-dimensional heat flow into the glass and neglecting any flux into the air.

The heat flux Q(t) is the total energy dissipated in the gauge divided by the effective gauge area.

When this gauge is immersed into water at the same temperature and the same current pulse is passed through it, heat will flow into both the pyrex and the water. Assuming that the gauge presents the same effective area to both glass and water then:

$$q(s) = q_g^+(s) + q_w^+(s) \qquad 4.3.3.$$

where

$$q_g^+ (s) = \beta_g \sqrt{s}\, f^+ (s) \qquad 4.3.4.$$

and

$$q_w^+ (s) = \beta_w \sqrt{s}\, f^+(s) \qquad 4.3.5.$$

putting 4.3.4. and 4.3.5. into 4.3.3. gives :

$$q (s) = (\beta_g + \beta_w) \sqrt{s}\, f^+(s) \qquad 4.3.6.$$

Compare with 4.3.2.

$$\beta_g \sqrt{s}\, f (s) = (\beta_g + \beta_w) \sqrt{s}\, f^+(s) \qquad 4.3.7.$$

The functional form of F(t) and $F^+(t)$ must be the same if V(t) is repeatable; thus can write:

$$F(t) = A' F_o(t)$$

and

$$F^+(t) = A^+ F_o (t)$$

where A' and A^+ are the amplitude of the air pulse and water pulse temperatures at a given time after pulse application. That is F(t) and $F^+(t)$ differ only in amplitude.

Now 4.3.7. can be written as :

$$\beta_g A' = (\beta_g + \beta_w) A^+$$

or

$$\beta_g = \beta_w \left(\frac{A'}{A^+} - 1\right)^{-1} \qquad 4.3.8.$$

If the water is pure distilled water β_w is known and when the measurements of A' and A^+ are made, the β_g is easily calculated. Other liquids with known properties could be used.

Oscilloscope traces of $\Delta V(t)$ and $\Delta V^+(t)$ are superimposed to give :

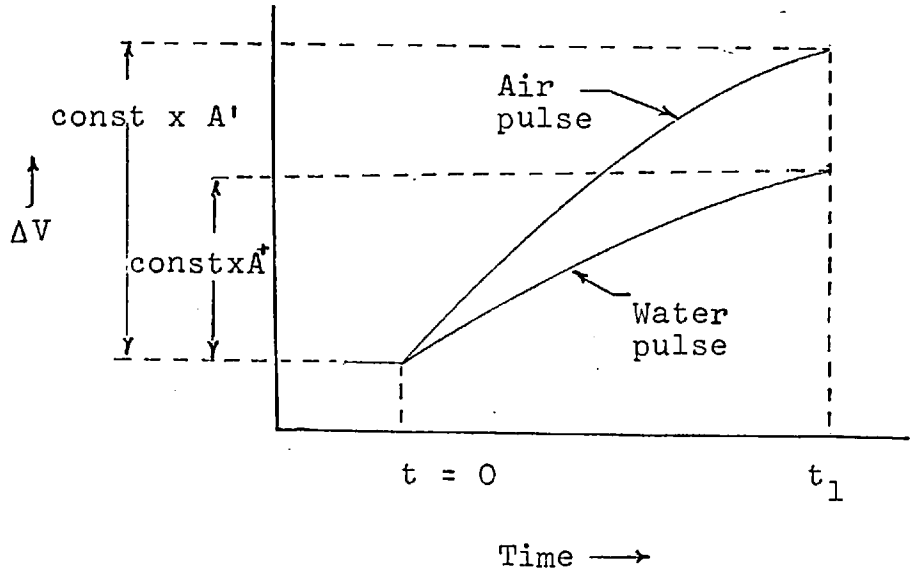

From equation 4.3.1. these voltages are proportional respectively to $I(t)\ F(t)$ and $I(t)\ F^+(t)$. A suitable time t_1 is chosen and the ratio amplitude at t_1 gives A'/A^+.

For pyrex glass past workers have deduced :

$\beta = 0.0745 \pm 18\%$ Btu/ft^2 $^\circ$F sec$^{\frac{1}{2}}$

β for distilled water was taken as 0.0780 Btu/ft^2 $^\circ$F sec$^{\frac{1}{2}}$ derived from properties of water at the test temperature.

5. EXPERIMENTAL WORK

5.1 Preparation of Thin Film Gauges

(1) A metal template and the 1/16 inch pyrex glass were cut to the required size.

(2) The metal template was marked with the locations of the ½ inch long gauges and drilled holes 1/16 inch in diameter were made at the end of each gauge location.

(3) The cold clean pyrex was completely immersed in melted wax and withdrawn quickly such that all surfaces were completely covered with a somewhat uniform wax layer.

(4) With the metal template taped to the wax coated pyrex, a hypodermic tube was used to remove the wax from the gauge end location.

(5) By immersing the wax coated pyrex in a 40% solution of hydroflouric acid for 2½ hours, etched indentations in the wax free areas were obtained.

(6) A protective coating of paint was applied to the etched surface after removal of the wax.

(7) After backing the pyrex with a spare piece of glass, to prevent backside chipping, 0.020 inch holes were drilled through the centre of the etched holes using a Mallard Ultrasonic Drill and 220 grain carborundum and water mixture as the abrasive.

(8) When cleaning the paint off the pyrex surface, care was taken to ensure the holes were clean of all carborundum.

(9) The pyrex was placed on a clean smooth stainless steel plate and heated to 680°C, the pyrex plastic temperature, to relieve the stresses due to the drilling. Annealing at 550°C for three hours completed the baking cycle.

(10) Acetone diluted Hanovia X-05 platinum paint was applied in thin layers between the etched holes using a Rowneys series 56 (sable and ox hair) number 3 brush. The paint was applied to the etched areas as well.

(11) An overnight drying in a dust free atmosphere was allowed prior to a second baking cycle as stated in paragraph 9.

(12) Gauge resistance was measured by pushing soft solder into the holes and connecting an avometer.

(13) Gauges built up in layers have shown to be more abrasive resistant. By reversing the order of paint application for each of the four layers applied, a near uniform gauge resistance was obtained.

(14) Silver paste No.38 was used to fill the drilled holes and make an electrical contact with the platinum. The undersurface silver was spread out in a tongue-like manner to which connecting wires could be soldered.

(15) Hardening of the silver was achieved by another baking cycle at 600°C with the oven door remaining open so the gases produced could escape and not hinder the quality of the gauges.

(16) The hardened silver was coated with an oxide which when scraped away, permitted the tinned wire leads to be connected using low melting point solder and a cool iron. Excess heat could cause local cracking of the pyrex.

5.2 Electronic Circuits

5.2.1. Introduction

During development of this equipment some effort was made to reduce the common sources of electronic noise and maintain flexibility of the equipment.

By the usage of stabalised power supplies the high voltage used to supply all circuits could be reliably assumed to remain constant. The use of transistorised commercially tested operational amplifiers that have been successfully

used in industry and are noted for their stability reduces another common source of noise. Earth loops between the gauges and the bridge circuits were eliminated by using two connecting leads for each gauge with a common earth within the metalic equipment box. Shielded wire was utilized on all circuits outside the main unit and care was taken on all soldered leads to ensure good contact was achieved. High quality component parts were utilized throughout.

Great flexibility of the equipment was achieved by utilizing a plug in module system. Each channel will function in any of the six positions available and the plug-in amplifiers mounted on cards are removable from the channel module for easy replacement. A gauge switching unit which allows any gauge on a model plug to be connected to any desired channel was constructed to further increase flexibility.

The equipment has been calibrated and used successfully to measure heat transfer rates as low as .01 Btu/ft^2 sec. although the signal to noise ratio was low (say 5) for these low signal levels.

Figure 31 shows the assembled equipment with the gauge switching unit and a digital voltmeter in the normal operational configuration.

If one arm of a Wheatstone bridge consists of a temperature sensitive resistance on a model body then an out-of-balance voltage results as heat generated in a hypersonic boundary layer is transferred to the body. This signal is amplified and passed into an analogue system which converts the voltage representing the temperature increase

into a voltage representing the heat transfer rate. This is shown in a block diagram below:

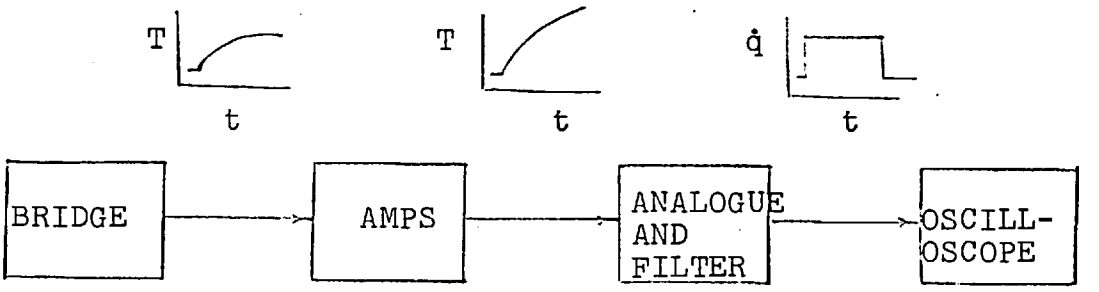

or in a more detailed manner :

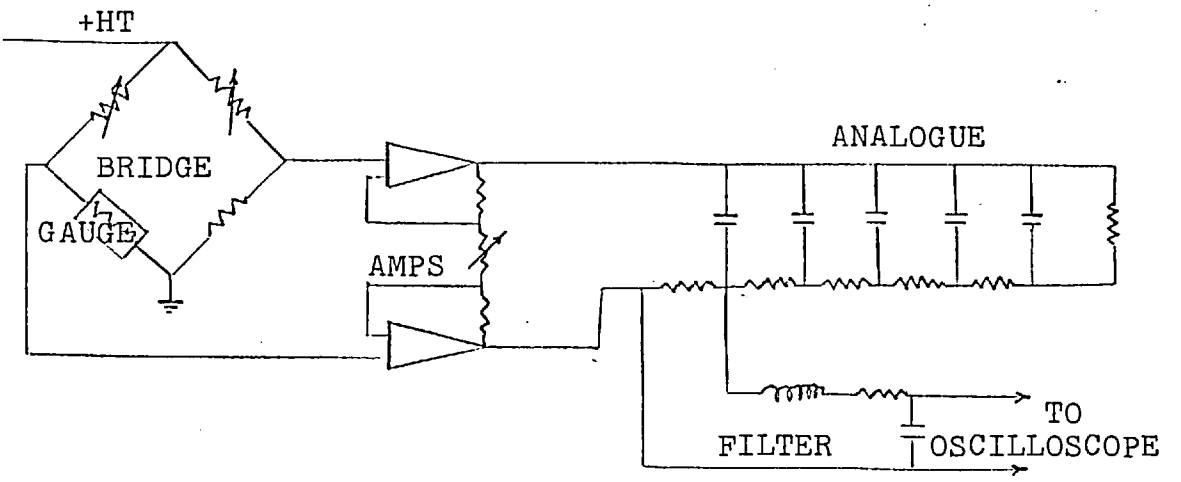

The amplifiers, analogue circuits, and filters used are completely illustrated in figure 32.

5.2.2 Pulse Generator

To calibrate the thermal properties of the pyrex backing material a pulse generator was designed which would allow means of reliably reproducing a square voltage pulse and a reference state to ensure accurate bridge balancing.

Transistorized flip flop monostable pulse circuits were linked such that the rear edge of the output pulse of the first stage triggered the second stage. This was done to enable a time delay to be generated prior to the application of the square pulse to the bridge circuit. This delay appeared on the oscilloscope as a zero voltage and indicated the time when the voltage pulse was generated. Basically the flip flop circuit has one stable and one unstable or quasi-stable state. A trigger pulse flips the circuit into the unstable state and it subsequently flops back into the stable state in a time determined by component values.

The time the circuit (in figure 33a) remains in the quasi stable state is given approximately by $t \approx 0.7\ C_3\ R_3$.

With reference to figure 34, the condenser following the test switch triggers the first stage through a diode. The collector output voltage from the second transistor is used to trigger the oscilloscope and the second flip flop network. The resulting signal from the second stage is passed to a power transistor to increase the current output of the generator. The first time delay is controlled by $C_1\ R_1$ while the time of pulse voltage is controlled by $C_2\ R_2$. This generator produces a square wave as illustrated in figure 33b.

The square wave is applied to a wheatstone bridge containing the gauge and the resulting out-of-balance temperature history monitored (see figure 35c).

5.3 Experimental Measurements

5.3.1. Alpha determination.

The temperature resistance coefficient has been found to be considerably lower than the bulk value of .00276/°F. This is primarily due to very thin layers of the Hanovia X - 05 not behaving as the bulk material. This difference could also be attributed to the platinum sinking into the pyrex substrate during the baking and the mixture of the two substances could have different properties than either of them individually.

Thus it is most important that α be experimentally determined.

5.3.2. Beta determination.

In this calibration 50 gauges were tested using the method described in the previous pages. The results gave a value of $\beta = 0.0743 \pm 10\%$ Btu/ft^2 sec. $\frac{1}{2}$°F which compares well with Bogdan's $\beta = 0.0737$ and Skinner's $\beta = .0745$.

Considering the amount of effort required to obtain this value it is recommended that the bulk value of 0.0743 be used for all pyrex backed thin films used at Imperial College.

5.3.3 Analogue calibration

Temperature and heat transfer histories were made simultaneously on three different runs for each channel. The temperature voltages were recorded for each millisecond and numerically processed by the programme described in section 6 of this appendix. The analogue calibration factor A* was found to vary by $\pm$ 5% of the theoretical value of 200. As a check on how the analogue output compares with the numerical calculation of the heat transfer a computer drawn graph is included in figure 36. The result demonstrates how well the analogue can follow the temperature voltage for increasing, decreasing and steady heat transfer inputs.

6. CALCULATION PROGRAMME FOR THE ANALOGUE CALIBRATION FACTOR AND HEAT TRANSFER RATE HISTORY FROM A TEMPERATURE HISTORY.

The fortran IV programme listed below is complete except for subroutine ART which draws a graph of q(t) against t. An interested reader could use the routine to plot points given in Appendix C or refer to the original card deck.

The method used in calculation of q (t) from T(t) eliminates the indeterminate $\frac{0}{0}$ which occurs in equation 4.2.4 when $t \rightarrow \psi$. Three methods of calculating A* were programmed of which two completed the integration. The third method used equation 4.2.3 for the steady heat input time.

```
$EXECUTE        IBJOB
$IBJOB
$IBFTC ALOG
C       THIS WILL GIVE HEAT TRANSFER FROM TIME TEMPERATURE TRACE
C       SOME OF THE IDEAS USED IN THIS PROGRAMME ORIGINATED WITH JOHN
C       WILSON OF THE NATIONAL PHYSICAL LABRATORIES TEDDINGTON, LONDON
C
C       NF FILM NUMBER/ NR RUN NUMBER /TINT TIME INTERVAL IN MILLISECONDS/
C       FV FILM VOLTAGE/ BETA SQRT RHO C K / ALPHA TEMPERATURE COEFFICIENT
C       OF RESISTANCE/ NS NUMBER OF READINGS /IDAY DAY/IMO MONTH/IYR YEAR/
C       SENST IS SCOPE SENSITIVITY FOR TEMPERATURE TRACE  SENSQ IS SCOPE
C       SENSITIVITY FOR HEAT TRANSFER TRACE BOTH IN VOLTS/CM   E(J) IS
C       THE VOLTAGE REPRESENTING THE TEMPERATURE ABOVE THE DATUM IN CM
C       AMPGN  AMPLIFIER GAIN FOR BOTH TRACES   VA  HEAT TRANSFER
C       VOLTAGE DURING STEADY FLOW FROM SECOND TRACE IN CMS
C
C   EXAMPLE DATA CARD
C110368 103 108 50    1.0 1.0   .00276     .07431      2.0 .05   1000. 5.58
C
        DOUBLE PRECISION CZ(55),P(55),C1,C2,STDY
        DIMENSION Q(2,100),E(55),Z(100),D(100),F(55),QQ(2,97),IVW(50)
        COMMON AVGQ,MR,NF,IDAY,IMO,IYR,NAME
  100   READ(5,1000)IDAY,IMO,IYR,NR,NF,NS,TINT,FV,ALPHA,BETA,SENST,SENSQ,
       1AMPGN,VA
 1000   FORMAT(1X,I2,I2,I2,1X,I3,1X,I3,1X,I2,2X,F5.0,F5.0,F10.0,F10.0,F5.0
       1,F5.0,F6.0,F4.0)
        INT=TINT
        READ(5,1001) (E(J),J=1,NS)
 1001   FORMAT (10F7.0)
        MR=NR
        DO 1 I=1,100
        Z(I)=SQRT(FLOAT(I)*TINT)
      1 CONTINUE
        D(1)=Z(1)
```

```
      DO 2 I=2,100
      D(I)=Z(I)-Z(I-1)
    2 CONTINUE
C
C     FINDS THE START OF THE TRACE
C
      DELTAZ=E(1)
      M=1
      IF(DELTAZ.LT.0.005) GO TO 3
      IF(DELTAZ.GT.0.005) GO TO 75
    3 M=M+1
      AELTAZ=E(M)-E(M-1)
      IF(AELTAZ.LT.0.005) GO TO 3
   75 L=M+1
      J=NS-2
C
C     SMOOTHING OF THE MEASURED READINGS BY DRAWING A CUBIC THROUGH 5
C     POINTS THUS FIRST TWO AND LAST TWO READINGS UNABLE TO BE SMOOTHED
C
      DO 4 K=L,J
      F(K)=.5*E(K)-1./12.*E(K+2)+1./3.*E(K+1)+1./3.*E(K-1)-1./12.*E(K-2)
    4 CONTINUE
      DO 93 K=L,J
      E(K)=F(K)
   93 CONTINUE
      A=SQRT(.001*TINT)*ALPHA*FV
      CONST=SQRT(3.1415926)
      B=CONST*SENST*BETA/A
      NS=NS-1
      DO 5 I=1,NS
      F(I)=E(I+1)-E(I)
    5 CONTINUE
```

```
      IF(NS.LE.4) GO TO 444
C
C     HEAT TRANSFER FOR THE FIRST FOUR MILLISECONDS NOT CALCULATED
C
      IF(INT.EQ.1)IBA=6
      IF(INT.EQ.2)IBA=3
      IF(INT.EQ.3)IBA=2
      DO 7 IP=IBA,NS
      SUM=0.0
      DO 8 K=1,IP
      M=IP-K+1
      SUM=SUM+F(K)*D(M)
    8 CONTINUE
C
C     GRAPH PLOTTING ARRANGMENTS
C
      Q(2,IP)=B*SUM/AMPGN
      Q(1,IP)=.001*TINT*FLOAT(IP)-.001*TINT
    7 CONTINUE
      DO 9 J=1,2
      DO 10 I=IBA,NS
      IF(IBA.EQ.6)IPA=I-5
      IF(IBA.EQ.3)IPA=I-2
      IF(IBA.EQ.2)IPA=I-1
      IF(IBA.EQ.1)IPA=I
      QQ(J,IPA)=Q(J,I)
   10 CONTINUE
    9 CONTINUE
      DO 40 I=IBA,NS
      IVW(I)=INT*(I-1)
   40 CONTINUE
C     FIND QDOT OVER 11MS TO 19 MS FOR A* DETERMINATION
```

```
      NO=1
      QSUM=0.0
      DO 70 I=12,20
   76 QSUM=QSUM+Q(2,I)
      NO=NO+1
   70 CONTINUE
      QSTAR=QSUM/FLOAT(NO-1)
C     FOUR INTERATIONS WITH AAA AND BBB SETTING SCATTER LIMITS FOR QSTAR
      DO 202 J=1,4
      QAGE=0.0
      NEV=0
      DO 200 I=12,NS
      AAA=1.05*QSTAR
      BBB=.95*QSTAR
      IF(Q(2,I).LT.BBB.OR.Q(2,I).GT.AAA) GO TO 200
      QAGE=QAGE+Q(2,I)
      NEV=NEV+1
      IF(NEV.EQ.1)ICU=I
      IF(NEV.GE.1)ICUT=I
  200 CONTINUE
      QSTAR=QAGE/FLOAT(NEV)
  202 CONTINUE
C
C     DETERMINE ANALOGUE CALIBRATION FACTOR A*
C
      ASTAR=QSTAR*ALPHA*FV*AMPGN/(BETA*VA*SENSQ)

C     CALCULATES ANALOUGE FACTOR FROM SLOPE OF TIME VS E(T) SQUARED
C
      CZ(1)=0.0
      P(1)=0.0
      DO 41 I=ICU,ICUT
```

```
      TEEV=E(I)*SENST/AMPGN
      IAH=I-ICU+2
      CZ(IAH)=TEEV**2
      P(IAH)=FLOAT(I-1)*TINT*.001
   41 CONTINUE
      ID=ICUT-ICU+2
      CALL ALINE(ID,P,CZ,C1,C2,STDY)
      CC1=C1
      ASTAR1=SQRT(CC1)*3.1415926*AMPGN/(2.*VA*SENSQ)
C
      NB=NS-IBA+2
      QQ(1,NB)=0.0
      QQ(2,NB)=QSTAR
      CALL ART(QQ,NB)
C
C     NUMBERS IN BRACKETS FOR QDOT(I) INDICATE TIME IN MILLISECONDS FROM
C     START OF MEASUREMENTS OF E(J)
C
      WRITE(6,1020)IDAY,IMO,IYR,NR,NF,SENST
 1020 FORMAT(//1X,5HDATE ,I2,1H/,I2,1H/,I2,5X,11HRUN NUMBER ,I3,5X,12HFI
     1LM NUMBER ,I3,5X,18HSCOPE SENSITIVITY ,F6.4,2X,8HVOLTS/CM,///)
      WRITE(6,1009)(IVW(IP),Q(2,IP),IP=IBA,NS)
 1009 FORMAT(5(1X,5HQDOT(,I2,2H)=,1X,1PE11.4))
      ICU=ICU-1
      ICUT=ICUT-1
      WRITE(6,1070)ICU,ICUT,QSTAR
 1070 FORMAT(/1X,33H AVERAGE QDOT DURING STEADY FLOW(,I2,4H TO ,I2,17H M
     1S FROM START)= ,F10.6,/)
      WRITE(6,2082)ASTAR
 2082 FORMAT(//1X,33HANALOGUE CALIBRATION FACTOR A* = ,F9.4,//)
      WRITE(6,11) ASTAR1
   11 FORMAT(/1X,32HANANOGUE FACTOR A* FROM SLOPE = ,F10.4,/)
```

```
      APH=0.0
      BQTEST=0.0
      DO 993 I=ICU,ICUT
      T=FLOAT(I)*.001
      AQTEST=3.1415962*E(I+1)*SENST/(SQRT(T)*VA*SENSQ*2.)
      APH=APH+1.
      BQTEST=BQTEST+AQTEST
  993 CONTINUE
      AWANS=BQTEST/APH
      WRITE(6,1942)AWANS
 1942 FORMAT(1X,27HTHIRD METHOD GIVES ASTAR = ,F10.4)
      GO TO 100
  444 STOP
      END
```

```
$IBFTC STLINE
      SUBROUTINE ALINE(N,X,Y,C1,C2,STDY)
      DOUBLE PRECISION X(N),Y(N),C1,C2,STDV,S(4),B(4),ST,BN,XM,YM,STDY
C
C  THERE ARE N X AND Y POINTS. A LINE Y=C1X+C2 IS FITTED TO THEN
C*
      XM=DABS(X(1))
      YM=DABS(Y(1))
      DO 1 I=2,N
      IF(DABS(X(I)).GT.XM)XM=DABS(X(I))
      IF(DABS(Y(I)).GT.YM)YM=DABS(Y(I))
    1 CONTINUE
      DO 2 I=1,N
      X(I)=X(I)/XM
      Y(I)=Y(I)/YM
    2 CONTINUE
      DO 3 I=1,4
      S(I)=0.0
    3 CONTINUE
      DO 4 I=1,N
      S(1)=S(1)+X(I)
      S(2)=S(2)+Y(I)
      S(3)=S(3)+X(I)*X(I)
      S(4)=S(4)+X(I)*Y(I)
    4 CONTINUE
      BN=N
      C2=S(3)*S(2)-S(1)*S(4)/(BN*S(3)-(S(1)**2))
      C1=BN*S(4)-S(1)*S(2)/(BN*S(3)-(S(1)**2))
C IF STRAIGHT LINE PASSES THROUGH 0-0 THEN C1  =S(4)/S(3)
      C1=S(4)/S(3)
      ST=0.0
      DO 5 I=1,N
      ST=ST+(Y(I)-C1*X(I)-C2)**2
    5 CONTINUE
      STDV=DSQRT(ST/BN)
      C1=C1*YM/XM
      C2=C2*YM
      STDY=STDV*YM
      RETURN
      END
```

7. CONCLUSIONS

The equipment was used to measure laminar heat transfer on a flat plate at Mach 8.2 to compare the output signals with that predicted by Eckerts reference temperature method. With proper experimental technique the equipment is estimated to provide a maximum of 10% error with the actual heat transfer rate.

Calibration of the platinum thin film gauge temperature coefficient of resistance is essential as the bulk property values are unreliable for very thin layers of material.

The analogue calibration factor can be taken to equal the theoretical $A^* = 2/\sqrt{RC} = 200$ and the thermal properties of the pyrex backing material, β, can be assumed equal to 0.0743 $Btu/ft^2/sec^{\frac{1}{2}}/^oF$.

APPENDIX B

MAINSTREAM FLOW CONDITIONS

Mainstream flow conditions were calculated for the five nozzles used in the Imperial College gun tunnel. The Mach 8.2, and Mach 12.25 nozzles were contoured and calibrations by Opatowski (1963) and Mohammadian (1968) showed only a slight favourable Mach number gradient in each. The conical nozzles of Mach numbers 7.5, 9.7, and 14.9, were calibrated by Needham (1963). The ratio of specific heat, for air as the processed gas, was considered constant at 1.4 for the calculations shown on the following listing.

```
$EXECUTE        IBJOB
$IBJOB          MAP
$IBFTC MAIN

C  GUN TUNNEL CONDITIONS FOR ANY MACH NUMBER

      DOUBLE PRECISION PRATIO(40),TSTAG(30),A(900),C(30),SMOOTH(30),SUMX
     1(60),SMYX(30),AMEANX(30),RES(30),TINF(40),P4(40),PINF(40),DENS(40)
     2,VISC(40),VEL(40),P(40),REXIN(40),REXFT(40),AMACH,TAM,TB,TEMP,CO,S
     3,SUM,TEMPER(40),SM(30),SMIN
      DIMENSION IP(30),DSTAG(30),KX(50),AMA(5),TIMF(40),TAMPER(40)
C  STAGNATION TEMPERATURES FROM GRAPH
      DATA(DSTAG(J),J=1,26)/662.,725.,760.,820.,860.,890.,925.,950.,985.
     1,1010.,1040.,1065.,1095.,1120.,1130.,1150.,1175.,1190.,1215.,1235.
     2,1250.,1260.,1270.,1285.,1305.,1325./
C  MACH NUMBERS FOR CALCULATIONS
      DATA(AMA(I),I=1,5)/7.5,8.2,9.7,12.25,14.9/
      DO 3 I=1,26
C  DRIVE PRESSURE  INCREASE IN STEPS OF 100 PSI
      IP(I)=500+(I-1)*100
C  CHANGE STAG TEMP SO VARIES FROM 0 TO 1 --NORMALIZED
      TSTAG(I)=(DSTAG(I)-662.)/663.
C  ACTUAL DRIVE PRESSURE USED INCLUDES ATMOSPHERIC PRESSURE
      P4(I)=500.+FLOAT(I-1)*100.+14.7
C  PRESSURE RATIOS THAT MATCH WITH STAG TEMPS FROM GRAPH
    3 PRATIO(I)=FLOAT(I-1)*5.
C  POLYFT PUTS A CUBIC THROUGH THE POINTS
      NA=26
      NOUT=6
      KOR=3
      KTOR=2*KOR
      KR=KOR*KOR
      CALL POLYFT(PRATIO,TSTAG,NA,KOR,C,CO,A,NOUT,SMOOTH,KTOR,KR,S,SUMX,
     1SMYX,AMEANX,RES)
C  CONVERSION FACTORS FOR AIR AS PERFECT GAS
```

```
      TEMP=32.17*144./1716.
      TAM=DSQRT(1.4*1716.)
      TB=32.17*12.
      DO 8 IMA=1,5
      AMACH=AMA(IMA)
    6 DO 8 M=1,21
C   MAINSTREAM PRESSURE FOR A GIVEN DRIVE PRESSURE
      PINF(M)=0.8*P4(M)/((1.+((AMACH**2.)/5.))**3.5)
      K=0
      DO 160 I=1,21
C   BARREL PRESSURE  GAUGE READING
      P(I)=5.*FLOAT(I-1)
      PRATIO(I)=P4(M)/(P(I)+14.7)
C   INSURES CALCULATIONS ARE CONDUCTED ONLY OVER THE CALIBRATED RANGE
      IF(PRATIO(I).GT.20.)GO TO 100
      GO TO 160
  100 K=K+1
      KX(K)=I
  160 CONTINUE
      K1=KX(1)
      K2=KX(K)
      DO 10 I=K1,K2
      SUM=CO
      DO 9 NBC=1,KOR
    9 SUM=SUM+(C(NBC)*((PRATIO(I)-20.)**NBC))
C   STAGNATION TEMPERATURE IN DEGREES R
      TEMPER(I)=((SUM*663.)+662.)*1.8
C   MAINSTREAM TEMPERATURE
      TINF(I)=TEMPER(I)/(1.+((AMACH**2.)/5.))
C   VISCOSITY
      VISC(I)=2.27*(TINF(I)**(3./2.))/(TINF(I)+198.6)*1.E-8
C   VELOCITY IN FT/SEC
```

```
    5 VEL(I)=AMACH*TAM*DSQRT(TINF(I))
C   DENSITY
      DENS(I)=PINF(M)*TEMP/TINF(I)
C   REYNOLDS NUMBER PER INCH
      REXIN(I)=DENS(I)*VEL(I)/(VISC(I)*TB)
C   REYNOLDS NUMBER PER FOOT
      REXFT(I)=REXIN(I)*12.
C   CONVERSION OF TEMPERATURES TO DEGREES K
      TIMF(I)=TINF(I)/1.8
      TAMPER(I)=TEMPER(I)/1.8
      IF(PRATIO(I).LT.20.)GO TO 20
   10 CONTINUE
   20 CONTINUE
C   WRITE OUT ALL THE DESIRED PARAMETERS
      WRITE(6,1000)AMACH,IP(M)
 1000 FORMAT(1H1,43X,45HVARIOUS GUN TUNNEL FREE STREAM CONDITIONS FOR,//
     1,37X,18H A MACH NUMBER OF ,F4.1,25H AND A DRIVE PRESSURE OF I4,5H
     2PSIG,///,6X,2HP1,11X,2HP4,5X,10HSTAGNATION,5X,4HFLOW,8X,4HFLOW,9X,
     34HFLOW,9X,4HFLOW,9X,4HFLOW,7X,8HREYNOLDS,5X,8HREYNOLDS,/,19X,2HP1,
     45X,11HTEMPERATURE,2X,8HPRESSURE,5X,7HDENSITY,5X,9HVISCOSITY,4X,8HV
     5ELOCITY,4X,11HTEMPERATURE,4X,6HNUMBER,7X,6HNUMBER,/,4X,6H(PSIG),19
     6X,3H(K),8X,6H(PSIA),6X,8H(LB/FT3),3X,12H(LB SEC/FT2),2X,8H(FT/SEC)
     8,8X,
     73H(K),7X,8HPER INCH,5X,8HPER FOOT,//)
      WRITE(6,1001)(P(I),PRATIO(I),TAMPER(I),PINF(M),DENS(I),VISC(I),VEL
     I(I),TIMF(I),REXIN(I),REXFT(I),I=K1,K2)
 1001 FORMAT(4X,0PF5.1,8X,F5.1,6X,F5.0,6X,F7.4,4X,1PE11.4,2X,E11.4,2X,
     1E11.4,5X,0PF5.1,5X,1PE11.4,2X,E11.4)
      PD=PINF(M)/14.7*760.
      WRITE(6,1005) PD
 1005 FORMAT(5X,////,38H DUMP TANK PRESSURE MUST BE LESS THAN ,F5.3,
     123H MILLIMETERS OF MERCURY)
    8 CONTINUE
      STOP
      END
```

APPENDIX C

COMPUTER PROGRAMME USED TO CALCULATE FILM COOLING EFFECTIVENESS AND HEAT TRANSFER RATE

INTRODUCTION

This type of calculation is easily handled by a relatively small machine and is quite economical on time. A computer programme is a necessary tool to solve the equations presented by the mathematical models in order to predict heat transfer and film cooling effectiveness for both laminar and turbulent hypersonic flows.

The programme is written in Fortran IV and has been run on IBM 7090, IBM 7094, and CDC 6600 computers. No changes should be necessary for any machine that can compile this language. The flexibility of the programme depends largely upon the ingenuity of the user but is presented in a form which should make further modifications relatively easy. The subroutine names, variable names, and function definitions have been given symbols which, in general, are self explanatory as to the algebraic symbol the storage location represents.

DESCRIPTION OF THE SUBROUTINES

The main programme (MAIN) initiates the calculation by reading in the initial conditions and the title of the calculation. The constants required are first calculated by calling subroutine CONST and then the location of each calculation position is determined. The first calculation occurs at the end of the potential core region with subsequent x locations selected by the value of the variable NOUT in subroutine CONST. For each of the selected

locations downstream of the slot subroutine CHANGE is called to conduct the required calculation. A table of the final calculated values is given and is followed by a graph of heat transfer rate vs distance from the slot.

Up to and including the end of the potential core region subroutine POTCOR is called which sets the relative parameters for no wall heat transfer.

The bulk of the required calculations were conducted in subroutine CHANGE. An interation method was used to calculate the adiabatic wall temperature, T_{aw}.

Integration of the required function FN, was conducted in subroutine BODE. The function was first evaluated at 11 locations over the integration limits XI to X2 using the BODE RULE weighting method as given by Abramowitz and Stegun (1965) pp. 887. The integration was then conducted in two parts by doubling the number of steps between the integration limits. Evaluating the first half was added to the calculation of the second half. A comparison with the first 10 step calculation resulted in a percent difference, ERROR, which dictated if a further doubling of the numbers of steps should be taken. The number of recalculations and comparisons with the last integral evaluation was terminated by the error being less than that specified in ERROR or by the number of recalculations permitted, MAXCAL.

The velocity profiles use the error function which was also numerically determined by a formula given in Abramowitz and Stegan (1965). This appears as an external function called ERFN.

Function UDU determines the non dimensionallised velocity profile u/u_∞ while function CPW was used to determine the specific heat at the wall.

There are two control locations which determine which mathematical boundary layer model is to be used. The location "LAMNAR" controls which of the turbulent film cooling models to use while "LFC" controls the selection of the laminar film cooling case.

LAMNAR = 1 the delayed mixing model selected
LAMNAR = 0 the complete mixing model selected and the value of x_{pc} must be included as an additional data card
LAMNAR = -1 the simple mixing model used
LFC = 0 turbulent film cooling
LFC = 1 laminar film cooling and automatically sets LAMNAR = 1

CONVENTIONS AND SYMBOLS USED

The following is a list of the symbols used to enable calculation of the film cooling effectiveness for the complete mixing and delayed mixing mathematical models. The British FPS units convention is used throughout except where stated :

Fortran Symbol	Algerbraic Symbol	Meaning
AA	$\alpha' = \frac{u_c + u_\infty}{2\, u_\infty}$	used in velccity profile calculation
ADD		amount to add on to the last estimate of the adiabatic wall temperature (^oR).
ALAM	$\lambda = \frac{u_\infty - u_c}{u_\infty + u_c}$	used in velocity profile calculation
AMACH	M_∞	mainstream Mach number
AMC	M_c	coolant Mach number
ANETA	η''	film cooling effectiveness parameter
CF	C_f	coefficient of friction
CFR	$(\frac{.0286}{\frac{\rho_\infty u_\infty}{\mu_\infty}})^{.2}$	constant used in calculation of C_f - the coefficient of friction
CONV	g x J	conversion factor (32.176 x 778)
CP	Cp	specific heat of mixture (Btu/lb^oR)
CPC	Cp_c	coolant - specific heat constant pressure (Btu/lb ^oR)
CPM	Cp_∞	specific heat at constant pressure of main stream (Btu/lb^oR)
CPW	Cp_w	specific heat at the wall
CPX	Cp(x)	specific heat of gas mixture (Btu/lb^oR)
D1		$D_1 = (Cp_c/Cp_\infty) - 1$
D2		$D_2 = (W_\infty / W_c) - 1$
D3		$D_3 = \rho_\infty u_\infty \delta \int_0^1 \frac{u/u_\infty}{h/h_\infty}\, dz$

Fortran Symbol	Algebraic Symbol	Meaning
DEL		constant used in calculation of δ the height of the hypothetical layer (inches)
DELS		constant used to determine how the wall affects the velocity profile
DELPC	δ_{pc}	height of the mixing layer at the end of the potential core region
DELTA	δ	height of mixing layer (inches)
DT1	$\rho_\infty u_\infty$	
E	ϵ	percent error limitation for use in the integration
ERFN	$\mathrm{erf}(x) = \frac{2}{\sqrt{\pi}}\int_0^x e^{-t^2}dt$	error function
FAC		fraction of velocity profile affected by presence of the wall
FN	$f(u/u_\infty, h/h_\infty)$	function to determine mass flow in the mixing layer
GAMC	γ_c	coolant ratio of specific heats
GAMM	γ_∞	mainstream ratio of specific heats
GRAV	g	gravity acceleration (32.176 ft/sec^2)
HAW	h_{aw}	adiabatic wall enthalpy (Btu/lb)
HINF	h_∞	mainstream enthalpy (Btu/lb)
HOC	h_{oc}	coolant stagnation enthalpy (Btu/lb)
HOM	$h_{o\infty}$	mainstream stagnation enthalpy (Btu/lb)
HWALL	h_w	wall enthalpy (Btu/lb)

Fortran Symbol	Algebraic Symbol	Meaning
IGAS		dummy coolant gas identifier
IW		dummy subscript for each calculation station
KS		maximum number of calculation stations
LAMNAR		dummy variable: if = 0 then complete mixing model used: if = 1 then delayed mixing model used: if = -1 then simple boundary layer model used
LFC		if = 0 turbulent case if = 1 laminar mainstream case
MAX		maximum number of recalculations for the integration subroutine
NOUT		increase of spacing (in slot heights) downstream of the slot to conduct calculations
P	$(u/u_\infty)=(y/\delta)^p$	turbulent velocity profile power dependance
PC	P_c	coolant layer pressure (psi)
PINF	P_∞	mainstream pressure (psi)
PP	Pp	coolant plenum pressure (psia)
PR	Pr	Prandtl number - both streams
Q	q	heat transfer rate Btu/ft^2 sec
RC	R_c	coolant gas constant
RECOV	r	recovery factor
RES	Re_c	slot reynolds number

Fortran Symbol	Algebraic Symbol	Meaning
REPIN	$\frac{\rho_\infty u_\infty}{\mu_\infty}$	Reynolds number per inch of mainstream
RHOINF	ρ_∞	density of mainstream (lb/ft^3)
RINF	R_∞	mainstream gas constant (Btu/lb^oR)
ROC	ρ_c	coolant density (lb/ft^3)
ROSTAA	ρ_c^*	reference density of coolant
ROSTAR	ρ^*	reference density (lb/ft^3)
RM	$m = \frac{\rho_c u_c}{\rho_\infty u_\infty}$	mass velocity ratio
SK	K'	constant used in equation 5.8.1.
SLOT	s	height of slot (inches)
SP	s'	height coolant would expand to if underexpanded and no mixing (inches)
SPREAD	σ	rate of jet spread parameter
STNO	St	Stanton number
TADW	$T_{aw}(x)$	adiabatic wall temperature (^oR)
TAW	T_{aw}	adiabatic wall temperature (^oR) temporary location
TC	T_c	coolant temperature (^oR)
TITLE		title to appear on top of output graph - for reference
TINF	T_∞	mainstream temperature (^oR)
TOCO	T_{oc}	stagnation temperature of coolant(^oR)
TOM	$T_{o\infty}$	mainstream stagnation temperature(^oR)
TRECOV	T_r	recovery temperature (^oR)
TSTAR	T*	reference temperature (^oR)

Fortran Symbol	Algebraic Symbol	Meaning
TWALL	T_w	wall temperature (^oR)
UC	u_c	coolant velocity (ft/sec)
UDU	u/u_∞	velocity profile
UINF	u_∞	mainstream velocity (ft/sec)
UL	u_L	maximum velocity in the velocity profile which is affected by the presence of the wall
UR	G	universal gas constant
VISC	μ_c	coolant viscosity (lb/ft sec)
VISINF	μ_∞	viscosity of mainstream (lb/ft sec)
VISSTA	μ_c	reference viscosity of coolant
VISSTR	μ^*	reference viscosity (lb/ft sec)
WDOC	$\dot{m}_c$	mass flow of coolant (lb/min)
WDOT	$\dot{m}_c$	mass flow of coolant - initially units of lb/min but changes to lbs/sec ft
WIDTH	L	width of slot injection station (inches)
WL	$\dot{m}_L$	mass flow in layer (lb/sec ft)
WTMOLC	W_c	molecular weight of coolant
WTMOLM	W_∞	molecular weight of mainstream
X	x	distance downstream from slot (inches)
X1,X2	$\int_{x_1}^{x_2} f(x)dx$	integration limits
XDS	x/s	number of slot heights
X1	x"	distance from slot to start of layer affected by the presence of the

Fortran Symbol	Algebraic Symbol	Meaning
XL		maximum length of plate for calculation to be conducted (inches)
XONE	x_1	distance from slot for the start of the hypothetical mixing layer (inches)
XPC	x_{pc}	distance from slot to end of potential core region (inches)

LISTING OF COMPUTER PROGRAMME

This section comprises of a complete listing of the computer programme used. The input data cards must be arranged such that the title (60 characters in length) card preceeds the numbered information. The units used on the second card are as follows :-

UINF	-	u_∞	mainstream velocity - ft/sec
TWALL	-	T_w	wall temperature - ^oR
TINF	-	T_∞	mainstream temperature - ^oR
SLOT	-	s	slot height - inches
CPC	-	Cp_c	coolant specific heat Btu/lb^oR
WTMOLC	-	W_c	molecular weight - lb/Mole
WDOT	-	$\dot{m}_c$	coolant mass flow - lb/min.
PINF	-	P_∞	mainstream pressure - lb/in^2.

```
$IBFTC MAIN
      COMMON/BLOCK5/LAMNAR,XIL,XIT,XONE,LFC
      COMMON/CONST1/P,XL,PR,WIDTH,UR,WTMOLM,CPM,CONV,GRAV,NOUT,RECOV,KS,
     1IGAS,RC,RINF,GAMC,GAMM,TOCO,ROINF,VISINF,REPIN,TRECOV,TSTAR,PP,
     2WDOC,AMC,SP,TC,ROC,UC,VISC,RES,ROSTAR,VISSTR,DEL,CFR,RM,TOM,AA,
     3ALAM,HINF,HOC,HAW,HOM,HWALL,PC,AMACH,DT1,IA,UINF,TWALL,TINF,SLOT,
     4CPC,WTMOLC,WDOT,PINF,XPC,SPREAD,D1,D2,D3,WL,DELTA,CPX,TAW,XVO,
     5XI,RHOINF,IW,DELS,FAC,DELPC,UL,IBL,HDH
      COMMON/MAINP/TITLE(10),XDS(200),X(200),NVAL(1),B(2,200),ANETA(200)
     1,Q(200),TADW(200),CP(200),SK(200),STNO(200)
      COMMON/BODE1/MAX,INTI,E,X1,X2
C  ERFN IS THE ERROR FUNCTION
      EXTERNAL ERFN,UDU,CPW,FN
   10 CONTINUE
      READ(5,101)(TITLE(I),I=1,10)
  101 FORMAT(10A6)
C  UINF - MAINSTREAM VELOCITY  FT/SEC  TWALL - WALL TEMPERATURE RANKINE
C  TINF - MAINSTREAM TEMPERATURE (R)  SLOT - HIEGHT OF INJECTION SLOT
C  (INCHES)   CPC - SPECIFIC HEAT CONST PRESSURE  BTU/LB R
C  WTMOLC - COOLANT MOLECULAR WEIGHT   WDOT - COOLANT MASS FLOW RATE
C  (LB/MIN)   PINF - MAINSTREAM PRESSURE PSI
      READ(5,100)UINF,TWALL,TINF,SLOT,CPC,WTMOLC,WDOT,PINF
  100 FORMAT(8F10.0)
      IF(UINF.LT.0.0)STOP
      CALL CONST
      IF(LAMNAR.EQ.-1) GO TO 400
C  IW IS COUNTER FOR NUMBER OF CALCULATIONS
      IW=1
      X(IW)=XPC
      XDS(IW)=XPC/SLOT
C  SUBROUTINE TO CALCULATE CONDITIONS IN THE POTENTIAL CORE REGION
      CALL POTCOR
```

```
      DO 1 IX=1,KS,NOUT
      IW=(IX-1)/NOUT+2
      ID=IFIX(XDS(IW-1))+IX
      IF(ID.GT.KS) GO TO 3
C  XDS IS X DIVIDED BY SLOT HIEGHT
      XDS(IW)=FLOAT(ID)
C  X ARRAY OF DISTANCE FROM SLOT IN INCHES
      X(IW)=XDS(IW)*SLOT
      IF(X(IW)-XPC)11,11,12
   11 CALL POTCOR
      GO TO 1
   12 CONTINUE
C  HIEGHT OF HYPOTHETICAL  BOUNDARY LAYER
      DELTA=DEL*(X(IW)+XONE)**.8
      IF(LFC.EQ.1)DELTA=DEL*SQRT(X(IW)+XONE)
C  HIEGHT OF WALL EFFECT BOUNDARY LAYER
      DELTAS=DELS*(X(IW)-XI)**.8
      FAC=DELTAS/DELTA
C  UL IS THE VELOCITY AT EDGE OF WALL EFFECT REGION
      UL=AA*(1.+ALAM*ERFN(SPREAD*(FAC*DELTA-SLOT)/X(IW)))*UINF
C  CALCULATES THE ADIABATIC WALL TEMPERATURE IN MIXING REGION
      CALL CHANGE
    1 CONTINUE
      GO TO 3
  400 CONTINUE
      IW=1
      XDS(IW)=0.0
      X(IW)=0.0
      CALL POTCOR
      DO 401 IX=1,KS,NOUT
      IW=(IX-1)/NOUT+2
```

```
      ID=IFIX(XDS(IW-1))+IX
      IF(ID.GT.KS) GO TO 3
      XDS(IW)=FLOAT(ID)
      X(IW)=XDS(IW)*SLOT
      DELTA=DEL*(X(IW)+XONE)**.8
      CALL POTCOR
  401 CONTINUE
    3 WRITE(6,200)
  200 FORMAT(1H1,/////////////,15X,1HX,9X,3HX/S,9X,1HK,9X,2HCP,9X,3HTAW,
     18X,2HST,8X,4H ETA,9X,1HQ,//)
      IW=IW-1
      WRITE(6,201)(X(I),XDS(I),SK(I),CP(I),TADW(I),STNO(I),
     1ANETA(I),Q(I),I=1,IW)
  201 FORMAT(10X,1P8E11.3)
C   PLOT RESULTS
      NVAL(1)=IW
      CALL CURVES(X,Q,IW,8,NVAL,1,TITLE,1)
      WDOT=WDOC
      GO TO 10
      END
```

```
$IBFTC CONSTA
      SUBROUTINE CONST
      DOUBLE PRECISION W,TEMP,TEMP1,TEMP2,PHI,SUM
      COMMON/BLOCK5/LAMNAR,XIL,XIT,XONE,LFC
      COMMON/CONST1/P,XL,PR,WIDTH,UR,WTMOLM,CPM,CONV,GRAV,NOUT,RECOV,KS,
     1IGAS,RC,RINF,GAMC,GAMM,TOCO,ROINF,VISINF,REPIN,TRECOV,TSTAR,PP,
     2WDOC,AMC,SP,TC,ROC,UC,VISC,RES,ROSTAR,VISSTR,DEL,CFR,RM,TOM,AA,
     3ALAM,HINF,HOC,HAW,HOM,HWALL,PC,AMACH,DT1,IA,UINF,TWALL,TINF,SLOT,
     4CPC,WTMOLC,WDOT,PINF,XPC,SPREAD,D1,D2,D3,WL,DELTA,CPX,TAW,XVO,
     5XI,RHOINF,IW,DELS,FAC,DELPC,UL,IBL,HDH
      COMMON/BODE1/MAX,INTI,E,X1,X2
      COMMON/MAINP/TITLE(10),XDS(200),X(200),NVAL(1),B(2,200),ANETA(200)
     1,Q(200),TADW(200),CP(200),SK(200),STNO(200)
C  WORK OUT THE SYSTEM CONSTANTS
      LFC=1
      LFC=0
      LAMNAR=1
      IF(LFC.EQ.1)LAMNAR=1
C  DISTANCE IN INCHES FOR CALCULATION TO BE CONDUCTED
      XL=12.
C  INITIAL NUMBER OF SLOT HIEGHTS TO START AT AND INTERVAL BETWEEN REST
      NOUT=1
C  PRANDTL NUMBER
      PR=.7
      IF(LFC.EQ.1)PR=.72
C  VELOCITY  PROFILE POWER
      P=1./7.
C  WIDTH OF SLOT IN INCHES
      WIDTH=4.5
C  UNIVERSAL GAS CONSTANT  R
      UR=1.986
C  MOL WT OF MAIN STREAM
      WTMOLM=28.96
C  SPECIFIC HEAT CONSTANT PRESSURE MAIN STREAM
      CPM=.24
      GRAV=32.174
```

```
      CONV=778.*GRAV
C     CONSTANT USED TO FIND LAYER GROWTH (46.165 DEPENDS ON MACH NUMBER)
      AK=0.029/0.8*46.165
C     RECOVERY FACTOR
      RECOV=PR**(1./3.)
      IF(LFC.EQ.1)RECOV=SQRT(PR)
C     MAX NUMBER OF SLOT HIEGHTS FOR CALCULATION
      KS=XL/SLOT
      IF(KS.GT.200)KS=200
C     FOREIGN GAS IDENTIFIER
      IGAS=WTMOLM-WTMOLC
C     GAS CONSTANT FOR COOLANT
      RC=UR/WTMOLC
C     GAS CONSTANT MAIN STREAM
      RINF=UR/WTMOLM
C     RATIO OF SPECIFIC HEATS OF COOLANT
      GAMC=CPC/(CPC-RC)
C     RATIO OF SPECIFIC HEATS MAIN STREAM
      GAMM=CPM/(CPM-RINF)
      RC=RC*CONV
      RINF=RINF*CONV
C     STAGNATION TEMPERATURE OF COOLANT EQUALS WALL TEMPERATURE
      TOCO=TWALL
C     MAIN STREAM DENSITY
      RHOINF=PINF*144.*GRAV/(TINF*RINF)
C     MAIN STREAM VISCOSITY
      VISINF=2.27*(TINF**1.5)/(TINF+198.6)*GRAV*1.E-08
C     MAIN STREAM REYNOLDS NUMBER
      REPIN=RHOINF*UINF/(VISINF*12.)
C     RECOVERY TEMPERATURE
      TRECOV=TINF+(.5*RECOV*UINF**2/6006.)
C     ECKERTS REFERENCE TEMPERATURE
      TSTAR=.5*(TINF+TWALL)+.22*(TRECOV-TINF)
```

```
C  REFERENCE DENSITY AND VISCOSITY
      ROSTAR=RHOINF*TINF/TSTAR
      VISSTR=2.27*(TSTAR**1.5)/(TSTAR+198.6)*GRAV*1.E-08
C  USED TO FIND DELTA -- HIEGHT OF LAYER
      DEL=AK*REPIN**(-0.2)*(VISSTR/VISINF)**(0.2)*(ROSTAR/RHOINF)**(0.8)
      IF(LFC.EQ.1)DEL=16./SQRT(REPIN)
C  COEFFICIENT OF FRICTION CONSTANT
      CFR=.0286/(REPIN**.2)
      IF(LFC.EQ.1) CFR=0.332/SQRT(REPIN )
      WDOC=WDOT
C  MASS FLOW/MIN CHANGED TO MASS FLOW/SEC/FT WIDTH
      WDOT=WDOT*12./(60.*WIDTH)
C  COOLANT MACH NUMBER
      SIDER=WDOC*SQRT(RC*TOCO/GAMC)/(PINF*SLOT*WIDTH*60.*32.174)
      AMC=0.0
      K=0
   80 CONTINUE
      AMC=AMC+.1**K
      SIDEL=AMC*SQRT(1.+(GAMC-1.)/2.*AMC**2)
      IF(SIDEL-SIDER)80,82,81
   81 CONTINUE
      AMC=AMC-.1**K
      K=K+1
      IF(K.EQ.6) GO TO 82
      GO TO 80
   82 CONTINUE
      IF(AMC.GT.0.999) GO TO 83
C  PRESSURE IN PLENUM CHAMBER (PSI)
      PP=PINF*((1.+(GAMC-1.)/2.*AMC**2)**(GAMC/(GAMC-1.)))
      GO TO 84
   83 CONTINUE
      PP=WDOC/(SLOT*WIDTH)*SQRT(RC*TOCO/GAMC)*((GAMC+1.)/2.)**((GAMC+1.)
     1/(2.*(GAMC-1.)))/(32.174*60.)
```

```
      AMC=SQRT(ABS(2./(GAMC-1.)*((PP/PINF)**((GAMC-1.)/GAMC)-1.)))
C  HIEGHT COOLANT WOULD EXPAND  TO IF NO MIXING
      SP=SLOT*(1.+(GAMC-1.)/2.*AMC**2)**((GAMC+1.)/(2.*(GAMC-1.)))/
     1(AMC*((GAMC+1.)/2.)**((GAMC+1.)/(2.*(GAMC-1.))))
   84 CONTINUE
C  COOLANT TEMPERATURE
      TC=TOCO/(1.+(GAMC-1.)/2.*AMC**2)
C  COOLANT DENSITY
      ROC=PINF*GRAV*144./(RC*TC)
C  VELOCITY OF COOLANT
      UC=AMC*SQRT(GAMC*RC*TC)
      TRECOV=TC+(.5*RECOV*UC**2/(CPC*CONV))
      TSTAR=.5*(TC+TWALL)+.22*(TRECOV-TC)
      ROSTAA=ROC*TC/TSTAR
C  VISCOSITY CALCULATIONS
      IF(IGAS)30,33,31
C  COOLANT IS AIR
   33 VISC=2.27*(TC**1.5)/(TC+198.6)*GRAV*1.E-08
      VISSTA=2.27*(TSTAR**1.5)/(TSTAR+198.6)*GRAV*1.E-08
      GO TO 32
C  COOLANT IS FREON
   30 CONTINUE
      VISREF=113.*6.72E-08
      TREF=460.
      VISC=VISREF*(TC/TREF)**.650
      VISSTA=VISREF*(TSTAR/TREF)**.650
      GO TO 32
C  COOLANT IS HELIUM
   31 CONTINUE
      VISREF=228.1*6.72E-08
      TREF=672.
      VISC=VISREF*(TC/TREF)**.662
```

```
      VISSTA=VISREF*(TSTAR/TREF)**.662
   32 CONTINUE
C  CALCULATE THE SLOT REYNOLDS NUMBER
      RES=ROC*UC*SLOT/(12.*VISC)
      DELS=DEL*11./46.165
      RM=ROC*UC/(RHOINF*UINF)
C  USED IN CALCULATION OF VELOCITY PROFILES
      AA=(UINF+UC)/(2.*UINF)
      ALAM=(UINF-UC)/(UINF+UC)
C  MAIN STREAM STAGNATION TEMPERATURE
      TOM=TINF+UINF**2/(2.*CPM*CONV)
      HINF=CPM*TINF
C  COOLANT STAGNATION ENTHALPY
      HOC=TOCO*CPC
      HAW=TOCO*CPC
C  MAIN STREAM STAGNATION ENTHALPY
      HOM=TOM*CPM
C  WALL ENTHALPY
      HWALL=TWALL*CPC
      HDH=HOC/HINF
      PC=ROC*RC*TC/(GRAV*144.)
C  MACH NUMBER OF MAIN STREAM
      AMACH=UINF/SQRT(GAMM*RINF*TINF)
      DT1=RHOINF*UINF
      D1=CPC/CPM-1.
      D2=WTMOLM/WTMOLC-1.
      IW=1
C  MAX IS THE MAXIMUM NUMBER OF RECALCULATIONS DUING INTEGRATION
      MAX=5
C  E  IS THE MAXIMUM PERCENT ERROR ALLOWED BETWEEN LAST AND PRESENT INTEGRATION
      E=1.0
```

```
C   INTEGRATION LIMITS
      X1=0.0
      X2=1.0
C   FIND FALSE ORIGIN OF HYPOTHETICAL LAYER
      XIL=-2.
      IF(LAMNAR.NE.0) GO TO 20
      READ(5,153)XPC
  153 FORMAT(F10.0)
      K=1
   53 CONTINUE
      SPREAD=XPC/SLOT*(-XIL)
      DELPC=DELS*XPC**.8
      IF(DELPC.GT.SLOT) GO TO 55
      X(IW)=XPC
      DELTA=0.0
      M=2
   56 CONTINUE
      DELTA=DELTA+.1**M
      IF(DELTA.LE.DELPC) GO TO 56
      FAC=DELPC/DELTA
      UL=AA*(1.+ALAM*ERFN(SPREAD*(FAC*DELTA-SLOT)/X(IW)))*UINF
      INTI=1
      CALL BODE(X1,X2,PCI,E,PHI,MAX)
      D3=DT1*DELTA*PCI/12.
      WL=D3*(1.+D1)/(D2+1.)
      IF(ABS(WDOT-WL)/WDOT.LT..01) GO TO 55
      IF(WDOT-WL)58,55,56
   58 CONTINUE
      DELTA=DELTA-.1**M
      M=M+1
      IF(M.GT.5) GO TO 55
```

```
      GO TO 56
   55 CONTINUE
   54 CONTINUE
      XI=0.0
      XONE=(DELTA/DEL)**1.25-XPC
      GO TO 94
   20 CONTINUE
      IZ=1
C  DETERMINE THE RATE OF JET SPREAD
      SPREAD=12./(.25*(RHOINF+ROC))*RHOINF
C  XPC IS THE DISTANCE TO THE END OF THE POTENTIAL CORE FROM THE SLOT
      XPC=SPREAD*SLOT/(-XIL)
      X(IW)=XPC
C  XI IS THE DISTANCE FROM THE SLOT TO POINT WHERE WALL EFFECT LAYER STARTS
      SB=2.*XPC+(9.5/SQRT(RES/SLOT)*XPC/SLOT)**2
      SC=XPC**2
      XI=(SB-SQRT(SB**2-4.*SC))/2.
      DELPC=DELS*(XPC-XI)**.8
      M=2
      DELTA=0.0
   21 CONTINUE
      DELTA=DELTA+.1**M
      IF(DELTA.LT.DELPC) GO TO 21
      FAC=DELPC/DELTA
      UL=AA*(1.+ALAM*ERFN(SPREAD*(FAC*DELTA-SLOT)/X(IW)))*UINF
      INTI=1
      CALL BODE(X1,X2,PCI,E,PHI,MAX)
      IF(LAMNAR.EQ.-1)PCI=8./7.
      D3=DT1*DELTA*PCI/12.
C  MASS FLOW IN LAYER
      WL=D3*(1.+D1)/(1.+D2)
```

```
      IF(ABS(WDOT-WL)/WDOT.LT..01) GO TO 23
      IF(WDOT-WL)22,23,21
   22 CONTINUE
      DELTA=DELTA-.1**M
      M=M+1
      IF(M.GT.5) GO TO 23
      GO TO 21
   23 CONTINUE
      SK(1)=DT1*DELTA/(DEL*WDOT*12.*REPIN**.2)
C  XONE IS THE DISTANCE UPSTREAM TO THE ORIGIN OF THE HYPOTHETICAL LAYER
      XONE=(DELTA/DEL)**1.25-XPC
      IF(LFC.EQ.1)XONE=(DELTA/DEL)**2-XPC
   94 CONTINUE
      TRECOV=.5*RECOV*UINF**2/(CPM*CONV)+TINF
      TSTAR=.5*(TINF+TWALL)+.22*(TRECOV-TINF)
      VISSTR=2.27*(TSTAR**1.5)/(TSTAR+198.6)*GRAV*1.E-08
C  WRITE OUT THE RELEVANT PARAMETERS THUS  FAR CALCULATED
      IF(LFC)260,261,260
  260 WRITE(6,262)
  262 FORMAT(1H1,/////////////,34X,31HLAMINAR HYPERSONIC FILM COOLING)
      GO TO 263
  261 WRITE(6,101)
  101 FORMAT(1H1,/////////////,33X,33HTURBULENT HYPERSONIC FILM COOLING)
  263 CONTINUE
      IF(IGAS)250,251,252
  251 WRITE(6,102)
  102 FORMAT(40X,19HWITH AIR AS COOLANT)
      GO TO 253
  250 WRITE(6,103)
  103 FORMAT(39X,21HWITH FREON AS COOLANT)
      GO TO 253
  252 WRITE(6,104)
```

```
104 FORMAT(39X,22HWITH HELIUM AS COOLANT)
253 IF(LAMNAR)257,254,255
254 WRITE(6,105)
105 FORMAT(38X,23H-COMPLETE MIXING MODEL-)
    GO TO 256
255 WRITE(6,106)
106 FORMAT(38X,22H-DELAYED MIXING MODEL-)
    GO TO 256
257 WRITE(6,107)
107 FORMAT(36X,27HSIMPLE BOUNDARY LAYER MODEL)
256 CONTINUE
    WRITE(6,100)WTMOLM,WTMOLC,CPM,CPC,TOM, TOCO,UINF,UC,AMACH,AMC,TINF
   1,TC,PINF,PC,RHOINF,ROC,VISINF,VISC  ,REPIN,RES,GAMM ,GAMC,SPREAD,
   2PP,WDOC,SLOT,       RM,TWALL,XONE
100 FORMAT(//,50X,10HMAINSTREAM,15X,7HCOOLANT,///,15X,16HMOLECULAR WEI
   ,GHT,
   221X,F5.2,16X,F7.3,/,15X,13HSPECIFIC HEAT,22X,F9.4,13X,F9.4,/,15X,
   322HSTAGNATION TEMPERATURE,13X,F7.2,15X,F7.2,/,15X,8HVELOCITY,27X,
   4F7.2,15X,F7.2,/,15X,11HMACH NUMBER,24X,F7.2,15X,F7.2,/,15X,
   511HTEMPERATURE,24X,F7.2,15X,F7.2,/,15X,8HPRESSURE,26X,F12.6,10X,
   6F12.6,/,15X,7HDENSITY,28X,1PE12.3,10X,E12.3,/,15X,9HVISCOSITY,26X,
   7E12.3,10X,E12.3,/,15X,15HREYNOLDS NUMBER,20X,E12.3,10X,E12.3,/,
   815X,27HSPECIFIC HEAT RATIO (GAMMA),8X,0PF8.3,14X,F8.3,///,30X,
   916HOTHER PARAMETERS,///,15X,18HRATE OF JET SPREAD,14X,F5.2,/,15X,
   ,15HPLENUM PRESSURE,15X,1PE12.3,/,15X,29HCOOLANT MASS FLOW (LB/MIN
   1)  ,1X,E12.3,/,15X,11HSLOT HIEGHT,19X,0PF8.3,/,
   2             15X,19HMASS VELOCITY RATIO,11X,1PE12.3,/,15X,16HWALL T
   3EMPERATURE,14X,0PF6.1,/,15X,27HFALSE BOUNDARY LAYER ORIGIN,F9.3,
   417H INCHES FROM SLOT,/,1H1)
    RETURN
    END
```

```
$IBFTC POTCO1
      SUBROUTINE POTCOR
      COMMON/BLOCK5/LAMNAR,XIL,XIT,XONE,LFC
      COMMON/CONST1/P,XL,PR,WIDTH,UR,WTMOLM,CPM,CONV,GRAV,NOUT,RECOV,KS,
     1IGAS,RC,RINF,GAMC,GAMM,TOCO,ROINF,VISINF,REPIN,TRECOV,TSTAR,PP,
     2WDOC,AMC,SP,TC,ROC,UC,VISC,RES,ROSTAR,VISSTR,DEL,CFR,RM,TOM,AA,
     3ALAM,HINF,HOC,HAW,HOM,HWALL,PC,AMACH,DT1,IA,UINF,TWALL,TINF,SLOT,
     4CPC,WTMOLC,WDOT,PINF,XPC,SPREAD,D1,D2,D3,WL,DELTA,CPX,TAW,XVO,
     5XI,RHOINF,IW,DELS,FAC,DELPC,UL,IBL,HDH
      COMMON/MAINP/TITLE(10),XDS(200),X(200),NVAL(1),B(2,200),ANETA(200)
     1,Q(200),TADW(200),CP(200),SK(200),STNO(200)
      IF(IW.GT.1.AND.LAMNAR.EQ.-1) GO TO 1
    2 CONTINUE
C   IN THE POTENTIAL CORE  THE FOLLOWING  ARE USED
      TADW(IW)=TOCO
C   SK IS THE CONSTANT MENTIONED IN THE MODEL
      IF(IW.NE.1)SK(IW)=0.0
C   STANTON NUMBER
      STNO(IW)=0.0
C   SPECIFIC HEAT AT THE WALL
      CP(IW)=CPC
C   HEAT TRANSFER RATE
      Q(IW)=0.0
C   FILM COOLING EFFECTIVENESS
      ANETA(IW)=1.0
      RETURN
    1 CONTINUE
      WL1=DT1*DELTA/12.*7./8.
      CP(IW)=CPW(WL1)
      SK(IW)=SK(1)
      EF=SK(IW)*(X(IW)/(RM*SLOT))**(-.8)*(RES*VISC/VISINF)**.2
      ANETA(IW)=EF*CPC/CPM/(1.+(CPC/CPM-1.)*EF)
      TEMP=(1./ANETA(IW)-1.)*CPM/CPC
      TADW(IW)=(TOCO+TEMP*TOM)/(TEMP+1.)
      XVO=CFR/(.5+TWALL/(2.*TINF)+.22*(TADW(IW)/TINF-1.))**.65
      CF=XVO/((X(IW)+XONE)**.2)
```

```
      STNO(IW)=CF/(PR**(2./3.))
      Q(IW)=DT1*STNO(IW)*CP(IW)*(TADW(IW)-TWALL)
      RETURN
      END
```

```
$IBFTC CHANGA
      SUBROUTINE CHANGE
      DOUBLE PRECISION SUM,PHI
      COMMON/BLOCK5/LAMNAR,XIL,XIT,XONE,LFC
      COMMON/CONST1/P,XL,PR,WIDTH,UR,WTMOLM,CPM,CONV,GRAV,NOUT,RECOV,KS,
     1IGAS,RC,RINF,GAMC,GAMM,TOCO,ROINF,VISINF,REPIN,TRECOV,TSTAR,PP,
     2WDOC,AMC,SP,TC,ROC,UC,VISC,RES,ROSTAR,VISSTR,DEL,CFR,RM,TOM,AA,
     3ALAM,HINF,HOC,HAW,HOM,HWALL,PC,AMACH,DT1,IA,UINF,TWALL,TINF,SLOT,
     4CPC,WTMOLC,WDOT,PINF,XPC,SPREAD,D1,D2,D3,WL,DELTA,CPX,TAW,XVO,
     5XI,RHOINF,IW,DELS,FAC,DELPC,UL,IBL,HDH
      COMMON/MAINP/TITLE(10),XDS(200),X(200),NVAL(1),B(2,200),ANETA(200)
     1,Q(200),TADW(200),CP(200),SK(200),STNO(200)
      COMMON/BODE1/MAX,INTI,E,X1,X2
      ADD=0.0
      C2=DEL*REPIN**.2
      DT2=DT1*DELTA/12.
      IF(LFC.EQ.0)TEM=((X(IW)+XONE)/(RM*SLOT))**(-.8)*(RES*VISC/VISINF)
     1**.2
      IF(LFC.EQ.1)TEM=SQRT(RES*VISC/VISINF*RM*SLOT/(X(IW)+XONE))
      IBL=0
      TAW1=TADW(IW-1)
    2 CONTINUE
      TAW1=TAW1+ADD
C  WALL SPECIFIC HEAT
      IF(IBL.EQ.0)CPX=CP(IW-1)
      IBL=1
C  FIRST MUST FIND THE SPECIFIC HEAT  USING PRESENT TAW
    3 CONTINUE
C  TAW USED IN INTEGRATION -- PUT FIRST GUESS INTO TAW
      TAW=TAW1
      INTI=3
      CALL BODE(X1,X2,SUM,E,PHI,MAX)
      D3=DT2*SUM
      SB=WDOT*D2-D3
      SC=-D1*D3*WDOT
      TEMP=SQRT(SB**2-4.*SC)
      WL1=(-SB+TEMP)/2.
      WL2=(-SB-TEMP)/2.
```

```
      IF(WL2.GT.WL1)WL1=WL2
      ERR=(WL1-WL3)/WL1
      IF(ABS(ERR).LT..05) GO TO 4
      IF(IGAS.EQ.0)GO TO 4
      WL3=WL1
      CPX=CPW(WL3)
      GO TO 3
    4 CONTINUE
      C1=WL1/DT2
      CPX=CPW(WL1)
      HAW=TAW*CPX
      HWALL=TWALL*CPX
C   CONSTANT  MENTIONED IN MODEL
      SK(IW)=1./(C1*C2)
      ETA=SK(IW)*TEM
      ANETA(IW)=CPC/CPM*ETA/(1.+(CPC/CPM-1.)*ETA)
C   CALCULATED TAW
      EF=WDOT/WL1
      TAW2=(EF*(HOC-HOM)+HOM)/CPX
      ERROR=TAW2-TAW1
C   DIFFERENCE BETWEEN GUESS AND CALCULATED TAW
      ADD=ERROR
C   LIMITATION ON THE DIFFERENCE BETWEEN CALCULATED AND GUESSED TAW
      IF(ABS(ERROR).LT.1.0) GO TO 5
      GO TO 2
    5 CONTINUE
      IF(LFC.EQ.1)ANETA(IW)=EF
C   SPECIFIC HEAT AT THE WALL
      CP(IW)=CPW(WL1)
C   COEFFICIENT OF FRICTION
      IF(LFC.EQ.1)AP=.25
      IF(LFC.NE.1)AP=.65
      XVO=CFR/(.5+TWALL/(2.*TINF)+.22*(TAW/TINF-1.))**AP
C   CF  IS THE COEF OF FRICTION DIVIDED BY 2
```

```
      CF=XVO/((X(IW)+XONE)**.2)
      IF(LFC.EQ.1)CF=XVO/SQRT(X(IW)+XONE)
C   STANTON NUMBER.
      STNO(IW)=CF/(PR**(2./3.))
C   TADW IS THE ADIABATIC WALL TEMPERATURE
      TADW(IW)=TAW2
      IF(LFC.EQ.1) GO TO 6
C   HEAT TRANSFER RATE (BTU/FT2/SEC
      Q(IW)=DT1*STNO(IW)*(HAW-HWALL)
      RETURN
    6 CONTINUE
      CFD2=0.332*SQRT(TINF/TSTAR*VISSTR/VISINF)/SQRT(REPIN)
      TEMP=DT1*CPM*(TRECOV-TWALL)*CFD2/PR**(2./3.)
      Q(IW)=(TADW(IW)-TWALL)/(TOM-TWALL)*TEMP/SQRT(X(IW)+.895)
      RETURN
      END
```

```
$IBFTC ART1
      SUBROUTINE BODE(X1,X2,SUM,ERROR,SUM1,MAXCAL)
      DOUBLE PRECISION H,A,B,U,ERR,SUM1,X(11),C(6),E
C  BODES RULE FOR 11 POINTS OR 10 STEPS INTEGRATION
C  INTEGRATION ROUTINE FOR ANY CONTINUOUS FUNCTION BETWEEN X1 AND X2
C  WILL DO MAXCAL RECALCULATIONS OF THE INTEGRAL OF FN UNTIL THE PERCENT
C  DIFFERENCE (ERR) BETWEEN THE LAST PREVIOUS CALCULATION SUM1 AND THE
C  PRESENT SUM IS LESS THAN ERROR
      IF(X1.EQ.X2) STOP
      C(1)=16067.
      C(2)=106300.
      C(3)=-48525.
      C(4)=272400.
      C(5)=-260550.
      C(6)=427368.
      D=.2
      E=1./299376.
      SUM1=0.0
      N=0
      M=0
      IMAX=MAXCAL
      IF(IMAX.LT.3)IMAX=2
      IF(ERROR.EQ.0.0)ERROR=.01
      IMAX=8
      IF(IMAX.GE.10)IMAX=10
      DO 4 N=1,IMAX
      SUM=SUM1
      SUM1=0.0
      M=2*M
      IF(N.EQ.1)M=10
      K=M/10
      H=(X2-X1)/FLOAT(K)
      DO 2 I=1,K
```

```
      A=X1+H*FLOAT(I-1)
      B=X2-H*FLOAT(K-I)
      DO 1 J=1,11
      U=-1.+D*FLOAT(J-1)
      X(J)=(B-A)*U/2.+(B+A)/2.
    1 CONTINUE
      SUM1=(C(1)*(FN(X(1))+FN(X(11)))  +C(2)*(FN(X(2))+FN(X(10)))+
     1C(3)*(FN(X(3))+FN(X(9)))+C(4)*(FN(X(4))+FN(X(8)))+C(5)*(FN(X(5))+
     2FN(X(7)))+C(6)*FN(X(6)))*E*(B-A)/2.+SUM1
    2 CONTINUE
      ERR=DABS((SUM1-SUM)/SUM1*100.)
      IF(ERR.LT.ERROR) GO TO 3
    4 CONTINUE
    3 CONTINUE
      H=H/10.
      A=SUM
      SUM=SUM1
      SUM1=A
      RETURN
      END
```

```
$IBFTC ERFNT
      DOUBLE PRECISION FUNCTION ERFN(W)
      DOUBLE PRECISION P,A(5),T,E,X,W
C  NUMERICAL CALCULATION OF ERROR FUNCTION
      X=W
      SIGN=1.
      IF(W.LT.0.) GO TO 2
      GO TO 3
    2 X=DABS(X)
      SIGN=-1.
    3 CONTINUE
      P=0.3275911
      A(1)=0.254829592
      A(2)=-0.284496736
      A(3)=1.421413741
      A(4)=-1.453152027
      A(5)=1.061405429
      T=1./(1.+P*X)
      X=-1.0*X**2
      E=1.-(A(1)*T+A(2)*T**2+A(3)*T**3+A(4)*T**4+A(5)*T**5)*DEXP(X)
      ERFN=E*SIGN
      RETURN
      END
```

```
$IBFTC FUNFN
      DOUBLE PRECISION FUNCTION FN(W)
      DOUBLE PRECISION W,TEMP,TEMP1,TEMP2
      COMMON/BODE1/MAX,INTI,E,X1,X2
      COMMON/CONST1/P,XL,PR,WIDTH,UR,WTMOLM,CPM,CONV,GRAV,NOUT,RECOV,KS,
     1IGAS,RC,RINF,GAMC,GAMM,TOCO,ROINF,VISINF,REPIN,TRECOV,TSTAR,PP,
     2WDOC,AMC,SP,TC,ROC,UC,VISC,RES,ROSTAR,VISSTR,DEL,CFR,RM,TOM,AA,
     3ALAM,HINF,HOC,HAW,HOM,HWALL,PC,AMACH,DT1,IA,UINF,TWALL,TINF,SLOT,
     4CPC,WTMOLC,WDOT,PINF,XPC,SPREAD,D1,D2,D3,WL,DELTA,CPX,TAW,XVO,
     5XI,RHOINF,IW,DELS,FAC,DELPC,UL,IBL,HDH
C  FUNCTION DEFINITIONS FOR THE INTEGRATIONS   INTI DECIDES ON WHICH
C  FN TO USE
      TEMP=UDU(W)
      TEMP1=1.-TEMP
      TEMP2=TEMP**2
      IF(INTI.EQ.1)FN=HDH*(1.-TEMP2)+TEMP2
      IF(INTI.EQ.3)FN=TWALL*CPX/HINF*TEMP1+TAW*CPX/HINF*TEMP1*TEMP+TEMP2
      FN=TEMP/FN
      RETURN
      END
```

```
$IBFTC FUNUDU
      DOUBLE PRECISION FUNCTION UDU(ETA)
      DOUBLE PRECISION ETA
      COMMON/BLOCK5/LAMNAR,XIL,XIT,XONE,LFC
      COMMON/CONST1/P,XL,PR,WIDTH,UR,WTMOLM,CPM,CONV,GRAV,NOUT,RECOV,KS,
     1IGAS,RC,RINF,GAMC,GAMM,TOCO,ROINF,VISINF,REPIN,TRECOV,TSTAR,PP,
     2WDOC,AMC,SP,TC,ROC,UC,VISC,RES,ROSTAR,VISSTR,DEL,CFR,RM,TOM,AA,
     3ALAM,HINF,HOC,HAW,HOM,HWALL,PC,AMACH,DT1,IA,UINF,TWALL,TINF,SLOT,
     4CPC,WTMOLC,WDOT,PINF,XPC,SPREAD,D1,D2,D3,WL,DELTA,CPX,TAW,XVO,
     5XI,RHOINF,IW,DELS,FAC,DELPC,UL,IBL,HDH
      COMMON/MAINP/TITLE(10),XDS(200),X(200),NVAL(1),B(2,200),ANETA(200)
     1,Q(200),TADW(200),CP(200),SK(200),STNO(200)
C  UDU  IS VELOCITY PROFILE   PATCH ON THE 1/7 PROFILE
      IF(ETA.GT.FAC) GO TO 1
      UDU=(ETA/FAC)**P*UL/UINF
      RETURN
    1 CONTINUE
      UDU=AA*(1.+ALAM*ERFN(SPREAD*(ETA*DELTA-SLOT)/X(IW)))
      RETURN
      END
```

```
$IBFTC CPWFUN
      FUNCTION CPW(WL)
      COMMON/CONST1/P,XL,PR,WIDTH,UR,WTMOLM,CPM,CONV,GRAV,NOUT,RECOV,KS,
     1IGAS,RC,RINF,GAMC,GAMM,TOCO,ROINF,VISINF,REPIN,TRECOV,TSTAR,PP,
     2WDOC,AMC,SP,TC,ROC,UC,VISC,RES,ROSTAR,VISSTR,DEL,CFR,RM,TOM,AA,
     3ALAM,HINF,HOC,HAW,HOM,HWALL,PC,AMACH,DT1,IA,UINF,TWALL,TINF,SLOT,
     4CPC,WTMOLC,WDOT,PINF,XPC,SPREAD,D1,D2,D3,WL,DELTA,CPX,TAW,XVO,
     5XI,RHOINF,IW,DELS,FAC,DELPC,UL,IBL,HDH
      COMMON/MAINP/TITLE(10),XDS(200),X(200),NVAL(1),B(2,200),ANETA(200)
     1,Q(200),TADW(200),CP(200),SK(200),STNO(200)
C  FUNCTION TO CALCULATE SPECIFIC HEAT AT THE WALL  COULD BE MODIFIED
C  TO INCLUDE VARIATION OF CP WHEN NOT COMPLETE MIXING AT EACH DOWNSTREAM
C  STATION
      CPX=WDOT/WL*CPC+(WL-WDOT)/WL*CPM
      CPW=CPX
      RETURN
      END
```

```
$IBFTC GRAPH
      SUBROUTINE CURVES(X,Y,NR,DIN,NV,KD,TITLE,ICODE)
      DIMENSION X(NR),Y(NR),DIN(2,NR)
      DIMENSION NMIN(2),TENP(2),DEL(2),VAL(2,13),TITLE(10),TIT(10),
     1LM(2),S(2),KA(2),SIZE(2),DMAX(2),DMIN(2),R(2),AXIS(2),TOP(2),
     2NZERO(2),POINT(111,56),P(111),W(15),NV(15)
C     MUST USE NR X AND Y POINTS WITH DIN AS 2 DIMENSIONAL ARRAY
C     NV IS 1D ARRAY WITH NUMBER OF LAST VALUE OF SYMBOL RANGE
C     KD IS NUMBER OF SYMBOLS REQUIRED
C     TITLE IS ALPHANUMERIC 10A6
C     ICODE SLEECTS THE RESOLUTION FOR THE GRAPH
C      ICODE=0 GIVES MINIMUM RESOLUTION BUT SENSIBLE AXIS LABLES
C      ICODE=1 WILL USE ALL THE SPACE AVAILABLE ON A 50X100 PAGE  BUT
C     THE LABLES ARE ONLY FAIR AND RESOLUTION BEST
C      ICODE=2 NO IMPROVEMENT IN RESOLUTION AND WORSE LABLES
C      ICODE.GT.2 NO BENIFIT IN RESOLUTION OR LABLES THUS SUPRESS
C      MAXIMUM OF 15 CURVE SYMBOLS  I.E. KD=15 MAX LIMIT
C            SYMBOLS
      DATA(W(I),I=1,15)/1H1,1H2,1H3,1H4,1H5,1H6,1H7,1H8,1H9,1H0,1HX,1H.,
     11H+,1HA,1HQ/
      DATA BLANK,ZERO,PLUS,PHEN,UPRT,STAR/1H ,1H0,1H+,1H-,1HI,1H*/
      IF(ICODE.GT.2)ICODE=2
      DO 61 I=1,2
      DMAX(I)=0.0
      DMIN(I)=0.0
      R(I)=0.0
      AXIS(I)=0.0
      NMIN(I)=0
      LM(I)=0
      TEMP(I)=0.0
      DEL(I)=0.0
      KA(I)=0
```

```
      TOP(I)=0.0
   61 CONTINUE
      LM(2)=5
C    IF LESS THAN 5 SYMBOLS REQUIRED USE 4 BEST LOOKING ONES AVAILABLE

      IF(KD.GT.5) GO TO 60
      W(1)=STAR
      W(2)=W(11)
      W(3)=W(12)
      W(4)=PLUS
      W(5)=ZERO
   60 CONTINUE
      NQ=NR
      IF(NQ.GT.5000)NQ=5000
      IF(KD.GT.15)KD=15

C       NOT DESTROY X AND Y VALUES PUT INTO DIN

      DO 1  I=1,NR
      DIN(1,I)=X(I)
    1 DIN(2,I)=Y(I)

C    SIZE OF GRAPH TO FIT ONTO PAGE

      SIZE(1)=101.
      SIZE(2)=51.
      S(1)=111.
      S(2)=55.
      LT=SIZE(1)
      LS=SIZE(2)-1.

C     MAIN DO LOOP
```

```
      DO 15 I=1,2

      NZERO(I)=S(I)

C     FIND MAX AND MINIMUM VALUES OF DIN

      DMAX(I)=DIN(I,1)
      DMIN(I)=DMAX(I)
      DO 10 J=1,NQ
      IF(DIN(I,J).GT.DMAX(I))DMAX(I)=DIN(I,J)
   10 IF(DIN(I,J).LT.DMIN(I))DMIN(I)=DIN(I,J)
      R(I)=DMAX(I)-DMIN(I)

C     RANGE IS R(I)    TEST FOR ZERO RANGE

      IF(R(I).NE.0.) GO TO 12
      IF(DMAX(I).NE.0.) GO TO 11
      AXIS(I)=-1.
      TOP(I)=1.
      GO TO 15
   11 ABSARG=10.*DMAX(I)
      R(I)=ABS(ABSARG)

   12 CONTINUE
      DO 13 NN=1,76
   13 IF(R(I).LT.10.**(NN-38)) GO TO 14
   14 CONTINUE
      NMIN(I)=NN-39
      TENP(I)=10.**(NMIN(I)-ICODE)

C     FOR GREATER RESOLUTION USE TENP=10.**(NMIN-1)
```

```
      AXARG=DMIN(I)/TENP(I)

C     AXARG IS NOW A NUMBER OF FORM 5.273 SUITABLE FOR TRUNCATION
C     AXIS(I) IS VALUE CONVERTED TO 5.0*10**N-1  A SUITABLE ROUND NUMBER
C     AXIS(I) ARE THE MINIMUM VALUES FOR GRAPH COORIDINATES

      AXIS(I)=TENP(I)*AINT(AXARG)
      IF(DMIN(I)-AXIS(I).LE.R(I)/100.)AXIS(I)=AXIS(I)-TENP(I)
      IF(DMIN(I)-AXIS(I).LE.R(I)/100.)AXIS(I)=AXIS(I)-TENP(I)
      AXIS(I)=AINT(AXIS(I)/TENP(I))*TENP(I)
      TOP(I)=AXIS(I)
    9 TOP(I)=TOP(I)+(SIZE(I)-1.)*TENP(I)/100.
      IF(TOP(I)-DMAX(I).LE.R(I)/100.) GO TO 9
      TOP(I)=AINT(TOP(I)/TENP(I))*TENP(I)
      IF(TOP(I).GT.0..AND.AXIS(I).LT.0..AND.AINT(R(I)).EQ.10.**(NN-39))
     1NMIN(I)=NMIN(I)-1

C     FIND PRINT POSITION OF ZERO-ZERO IF ANY

      IF(TOP(I).GE.0..AND.AXIS(I).LE.0.) GO TO 21
      GO TO 121
   21 NZERO(I)=-AXIS(I)*(SIZE(I)-1.)/(TOP(I)-AXIS(I))+1.5
      IF(I.EQ.1) GO TO 1115
      KA(2)=NZERO(2)/5+1
      LM(2)=5*KA(2)-NZERO(2)
      GO TO 1116
 1115 KA(1)=NZERO(1)/10+1
      LM(1)=10*KA(1)-NZERO(1)+1
 1116 CONTINUE
      NZERO(I)=NZERO(I)+LM(I)
  121 CONTINUE
C     DEL(I) IS VALUE BETWEEN AXIS LABLES
```

```
      DEL(I)=(TOP(I)-AXIS(I))/10.
   15 CONTINUE

C     VAL(I,J) ARE VALUE OF LABLES

      DO 200 I=1,2
      IF(TOP(I).GE.0..AND.AXIS(I).LE.0.) GO TO 201
      DO 222 MMH=1,13
      VAL(I,MMH)=(TOP(I)-FLOAT(MMH-1)*DEL(I))/10.**NMIN(I)
  222 CONTINUE
      GO TO 202
  201 DO 122 MMH=1,13
      VAL(I,MMH)=(FLOAT(12-KA(I)-MMH)*DEL(I))/10.**NMIN(I)
  122 CONTINUE
  202 CONTINUE
      NMIN(I)=-NMIN(I)
  200 CONTINUE

C   REPLACE DIN VALUES WITH ROW COLUMN COORDINATES

      DO 17 I=1,2
      DO 16 J=1,NQ
      INTSTO=(DIN(I,J)-AXIS(I))*(SIZE(I)-1.)/(TOP(I)-AXIS(I))+1.5
   16 DIN(I,J)=INTSTO
   17 CONTINUE
      N=1

C    DOO LOOP TO PUT THE REQUIRED SYMBOL INTO POINT(I,J)

      DO 51 IA=1,KD

C   SINGLE SYMBOL RANGE FROM NC TO NB IN ORIGINAL X AND Y ARRAYS
```

```
      NB=NV(IA)
      IF(IA.EQ.1) GO TO 52
      NC=NV(IA-1)+1
      GO TO 53
   52 NC=1

C     SORT SINGLE SYMBOL RANGE INTO DESCENDING ORDER

   53 JJ=NB-1
      DO 19 K=NC,JJ
      IT=NB-NC-K
      DO 19 J=NC,IT
      IF(DIN(2,J).GE.DIN(2,J+1))GO TO 19
      DO 18 I=1,2
      RLSTO=DIN(I,J+1)
      DIN(I,J+1)=DIN(I,J)
   18 DIN(I,J)=RLSTO
   19 CONTINUE

C     PUT REQUIRED SYMBBOL W(IA) INTO POINT
C    **(NOTE...LATER SYMBOLS INSERTED WILL OVERWRITE ALL OTHERS***)

      DO 54 IB=NC,NB
      MXA=DIN(1,IB)
      MYA=DIN(2,IB)
      POINT(MXA,MYA)=W(IA)
   54 CONTINUE
   51 CONTINUE

C    NOW SORT COMPLETE ARRAY DIN INTO DESCENDING ORDER
```

```
      IF(KD.EQ.1) GO TO 58
      KK=NQ-1
      DO 55 K=1,KK
      JJ=NQ-K
      DO 56 J=1,JJ
      IF(DIN(2,J).GE.DIN(2,J+1))GO TO 56
      DO 57 I=1,2
      RLSTO=DIN(I,J+1)
      DIN(I,J+1)=DIN(I,J)
   57 DIN(I,J)=RLSTO
   56 CONTINUE
   55 CONTINUE
C     WRITE THE TITLE OF GRAPH AT TOP OF A NEW PAGE

   58 CONTINUE
      IY=1
      J=1
      WRITE(6,123)(TITLE(I),I=1,10)
  123 FORMAT(1H1,45X,10A6)

C    DO LOOP FOR EACH LINE

      DO 31 LL=1,55
      L=56-LL

C    PUT SYMBOLS AND BLANKS INTO ARRAY P

      DO 30 M=1, 111
   30 P(M)=BLANK

C    TEST FOR THE PRESENCE OF THE Y=ZERO LINE
```

```
      IF(L.EQ.55) GO TO 429
      IF(NZERO(2).NE.L) GO TO 39
  429 CONTINUE

C    IF ZERO PRESENT FILL WITH --------

      DO 29 M=1,111
   29 P(M)=PHEN

C    PUT + IN EVERY 10TH LOCATION

      DO 129 M=1,111,10
  129 P(M)=PLUS
      GO TO 24

C     PUT I IN LOCATION CORRESPONDING TO X=0 OR + IF LINE IS AN EVEN
C     MULTIPLE OF 5

   39 M=NZERO(1)
      P(M)=UPRT
      P(111)=UPRT
      DO 139 MA=5,111,5
      IF(L.EQ.MA)P(111)=PLUS
  139 IF(L.EQ.MA)P(M)=PLUS
   24 IF(J.GT.NQ) GO TO 25

C    CHECK ALL POINTS ON LINE EQUAL TO L


C     MAKE SURE CORRECT SYMBOL IS INSERTED IN CORRECT X LOCATION

      MY=DIN(2,J)
```

```
      MX=DIN(1,J)
      MX1=MX+LM(1)
      IF(MY.LT.L-LM(2)) GO TO 25
      P(MX1)=POINT(MX,MY)
      J=J+1
      GO TO  24
   25 IF(NZERO(2).EQ.L) GO TO 27
      TAZ=FLOAT(L)/5.
      TAZZ=AINT(TAZ)
      IZ=(TAZ-TAZZ)*10.
      IF(IZ)125,125,126
  125 WRITE(6,26)VAL(2,IY),(P(M),M=2,111)
   26 FORMAT(11X,F8.3,1X,1H+,110A1)
      IY=IY+1
      GO TO 31
  126 CONTINUE
      IF(L.EQ. 26) GO TO 150
      IF(L.EQ.24) GO TO 152
      GO TO 151
  150 WRITE(6,153)(P(M),M=2,111)
  153 FORMAT(3X,5HTIMES,12X,1HI,110A1)
      GO TO 31
  152 WRITE(6,154) NMIN(2),(P(M),M=2,111)
  154 FORMAT(2X,4H10**,I3,11X,1HI,110A1)
      GO TO 31
  151 CONTINUE
      WRITE(6,127)(P(M),M=2,111)
  127 FORMAT(20X,1HI,110A1)
      GO TO 31
   27 CONTINUE
      WRITE(6,34)VAL(2,IY),(P(M),M=2,111)
      IY=IY+1
```

```
 31 CONTINUE
    DO 33 M=1,111
 33 P(11)=PHEN
    DO 133 MA=1,111,10
133 P(MA)=PLUS
    M=NZERO(1)
    P(M)=PLUS
    WRITE(6,34)VAL(2,12),(P(M),M=2,111)
 34 FORMAT(11X,F8.3,1X,1H+,110A1)
    DO 140I=1,13
    J=14-I
140 DIN(1,J)=VAL(1,I)
    DO 141 I=1,13
141 VAL(1,I)=DIN(1,I)
    N=2
    IF(LM(1).EQ.0)N=3
    M=N+10
    WRITE(6,142)(VAL(1,I),I=N,M)
142 FORMAT(14X,11(2X,F8.3))
    WRITE(6,143) NMIN(1)
143 FORMAT(  64X,10HTIMES 10**,I3)
    VERT=(TOP(2)-AXIS(2))/(SIZE(2)-1.)
    HORIZ=(TOP(1)-AXIS(1))/(SIZE(1)-1.)
    WRITE(6,37)VERT,HORIZ
 37 FORMAT(30X,9HDELTA Y =,1PE9.2,54X,9HDELTA X =,E9.2)
C     WRITE OUT THE PLOTTED VALUES AND SYMBOL USED  INCREASING  X
    DO 228 I=1,NR
    DIN(1,I)=X(I)
228 DIN(2,I)=Y(I)
    WRITE(6,337)(TITLE(I),I=1,10)
337 FORMAT(//,1X,19HPLOTTED VALUES FOR ,10A6)
    DO 351 IA=1,KD
```

```
      NB=NV(IA)
      IF(IA.EQ.1) GO TO 352
      NC=NV(IA-1)+1
      GO TO 353
  352 NC=1
  353 CONTINUE
      JJ=NB-1
      DO 319 K=NC,JJ
      IT=NB-NC-K
      DO 319 J=NC,IT
      IF(DIN(1,J).LE.DIN(1,J+1)) GO TO 319
      DO 318 I=1,2
      RLSTO=DIN(I,J+1)
      DIN(I,J+1)=DIN(I,J)
  318 DIN(I,J)=RLSTO
  319 CONTINUE
      WRITE(6,338)W(IA)
  338 FORMAT(///,10X,13HSYMBOL USED -,A1,1H-,//,6X,5(1HX,10X,1HY,12X),//
     1)
      WRITE(6,339)(DIN(1,I),DIN(2,I),I=NC,NB)
  339 FORMAT(5(2X,1PE9.2,2X,E9.2,2X))
  351 CONTINUE
      WRITE(6,999)
  999 FORMAT(1H1)
      RETURN
      END
```

MODEL STATISTICS		
	A - LAMINAR	B - TURBULENT
Width	5 inches	5 inches
Complete Length	12.9 inches	18.5 inches
Largest thickness	0.5 inches	1 inch
Leading Edge Bevel	30 degrees	17 degrees
Plenum Chamber Length	2.5 inches	5 inches
Plenum Chamber Depth	0.25 inches	0.625 inches
Slot Height (Variable)	0.083 inches	0.080 inches
Leading edge to slot	0.895 inches	6.5 inches
Width of slot	4.5 inches	4.5 inches
Splitter Plate Edge thickness	0.005 inches	0.005 inches
Feed Tubes	2	5

TABLE 1

MODEL STATISTICS

TABLE 2

LAMINAR FILM COOLING

SUMMARY OF TEST CONDITIONS

Mainstream conditions - laminar air

Cp_∞ = .24 Btu/lb°R T_o = 1040°K

u_∞ = 4570 ft/sec M = 8.2

T_∞ = 71.6°K P_∞ = 0.0708 psi.

ρ_∞ = 1.478×10^{-3} lb/ft^3 μ_∞ = 3.275×10^{-6} lb/ft sec.

$\frac{\rho_\infty u_\infty}{\mu_\infty}$ = 1.72×10^{-5} per inch. T_w = 289°K.

Coolant conditions for $P_c = P$ = .0708 psi T_{oc} = 289°K.

GAS	$\dot{m}_c$ lb/min	u_c ft/sec	M_c	T_c °K	Re_c	P_p psi	m
Air	.072	1040	1.02	239	309	.138	.0685
Air	.066	978	.95	244	278	.127	.0628
Air	.060	910	.87	251	248	.117	.0571
Air	.054	838	.80	256	219	.108	.0514
Air	.029	488	.44	278	110	.081	.0276

Nose attachment A on the flat plate with the slot height fixed at 0.083 inches.

TABLE 3

LAMINAR FILM COOLING

MEASURED HEAT TRANSFER RATES

NB S=0 for this column

DISTANCE FROM SLOT INCHES	COOLANT MASS FLOW RATE LBS/MIN					
	0.072	0.066	0.060	0.540	0.029	0.0
	HEAT TRANSFER RATE BTU/SEC/FT^2					
0.625	0.0577	0.0290	0.0526	0.0102	0.0910	1.6010
0.875	0.0552	0.0890	0.0875	0.0456	0.2300	1.3070
1.375	0.0892	0.0950	0.1210	0.1250	0.4310	1.6910
1.875	0.1600	0.2640	0.2180	0.2150	0.5350	1.2900
2.125	0.0960	0.3330	0.2840	0.2890	0.6300	1.4050
2.625	0.2300	0.2710	0.3040	0.3020	0.7480	1.2240
3.125	0.3280	0.4080	0.3840	0.3520	0.8100	1.1730
3.375	0.4310	0.4400	0.4030	0.4580	0.7900	1.0830
4.625	0.6840	0.5150	0.5860	0.4730	0.8000	1.1030
5.125	0.5400	0.5850	0.6230	0.5770	0.8720	0.7700
6.375	0.6780	0.6470	0.6780	0.6370	0.7260	0.7980
6.875	0.9860	0.8930	0.7800	0.6800	1.0300	0.8510
7.125	0.9500	1.0650	0.7150	0.6520	0.8400	0.8130
7.875	0.9480	0.8920	0.7800	0.7830	0.8050	0.6540
8.625	1.2470	1.0800	0.9660	0.9180	0.9360	0.7150
9.375	1.2700	1.2400	1.1100	0.9650	0.8020	0.7700

Distance from leading edge to slot = 0.895 inches

Slot height = 0.083 inches.

TABLE 4

TURBULENT FILM COOLING

SUMMARY OF TEST CONDITIONS

MAINSTREAM CONDITIONS - TURBULENT AIR

Cp_∞	= .24 Btu/lb$^\circ$R	$T_{o\infty}$	= 786°K
u_∞	= 3714 ft/sec	M_∞	= 8.2
T_∞	= 47.4°K	P_∞	= 0.1266 psi.
ρ_∞	= 4.001 x 10^{-3} lb/ft^3	μ_∞	= 2.030 x 10^{-6} lb/ft sec.
$\frac{\rho_\infty u_\infty}{\mu_\infty}$	= 6.102 x 10^5 per inch	T_w	= 289°K

COOLANT CONDITIONS FOR

Pc = P_∞ = .1266 psi T_{oc} = 289°K

GAS	$\dot{m}_c$ lb/min.	u_c ft/sec	M_c	T_c $^\circ$K	Re_c	P_p psi	m
Air	.121	1022	1.00	240	516	0.240	.0543
Air	.0955	855	.81	255	389	0.196	.0428
Air	.0655	623	.58	271	254	0.159	.0294
Freon	.124	294	.61	282	680	0.155	.0556
Freon	.101	242	.50	284	551	0.145	.0453
Freon	.0785	189	.39	286	427	0.138	.0352
Helium	.0515	2842	1.00	217	214	0.260	.0231
Helium	.04275	2523	.86	232	170	0.219	.0192
Helium	.02925	1906	.62	256	109	0.171	.0131

Nose attachment B on the flat plate with slot height fixed at 0.080 inches.

TURBULENT FILM COOLING DATA MACH 8.2

COOLANT GAS	C_{p_c} cal/gm°F	W_c	S in	$\dot{m}_c$ gm/min	V_c ft/sec	m $\frac{\rho_c u_c^2}{\rho_\infty u_\infty^2}$	WALL HEAT TRANSFER RATE $\dot{q}_w$ BTU/FT²/SEC — DISTANCE FROM SLOT X INCHES																																		
							0.375	0.625	0.875	1.125	1.375	1.625	1.875	2.125	2.375	2.625	2.875	3.125	3.375	3.625	3.875	4.125	5.125	5.375	5.625	5.875	6.375	6.625	6.875	7.125	7.375	7.625	7.875	8.125	8.625	8.875	9.125	9.375	9.625	9.875	10.125	10.375	10.625
AIR	.24	28.36	.080	.321	1022	.054	0.00	0.00	0.00	0.00	0.00	0.32	0.43	0.73	1.04	1.11	1.15	1.18	1.16	1.17	1.19	1.32	1.23	1.31	1.32	1.31	1.35	1.40	1.28	1.41	1.37	1.48	1.48	1.54	1.36	1.61	1.54	1.34	1.58	1.60	1.51
			.080	.0955	855	.043	0.00	0.00	0.00	0.00	0.36	0.49	0.57	0.66	0.87	1.08	1.05	1.24	1.30	1.31	1.23	1.27	1.35	1.30	1.34	1.32	1.35	1.39	1.36	1.29	5.25	1.35	1.25	1.24	1.40	1.58	1.45	1.41	1.44	1.57	1.43
			.080	.0655	423	.029	0.00	0.00	0.00	0.00	0.10	0.45	0.70	0.88	1.02	1.09	1.29	1.17	1.36	1.25	1.24	1.35	1.29	1.41	1.41	1.32	5.44	1.55	1.37	1.35	1.37	1.43	1.50	1.66	5.47	1.61	1.69	1.60	1.58	1.66	1.64	
FREON	.1476	130.62	.060	.124	194	.056	0.00	0.00	3.00	0.00	0.00	0.20	0.53	0.38	0.50	0.71	0.85	0.87	0.80	1.01	0.86	0.88	0.90	1.08	1.08	1.08	1.83	0.99	0.98	1.86	1.14	1.19	1.83	1.14	1.01	1.18	1.36	1.18	1.19	1.24	1.22
			.080	.101	241	.045	0.00	0.00	0.00	0.00	0.00	0.36	0.50	0.60	0.98	1.00	1.27	1.18	1.14	1.30	1.33	1.36	1.25	1.35	1.25	1.42	1.23	1.34	5.38	1.24	1.35	1.31	1.47	1.34	1.42	1.53	1.61	1.47	1.51	1.61	1.44	
			.080	.0785	149	.035	0.00	0.00	0.00	0.00	0.10	0.55	0.71	0.72	1.15	1.22	1.34	1.30	1.25	1.32	1.33	1.50	1.41	1.55	1.40	1.53	1.45	1.55	1.60	1.54	1.70	1.48	1.60	1.58	1.52	1.54	1.70	1.54	1.47	1.68	1.45	
HELIUM	1.35	4.003	.080	.0515	3841	.023	0.35	0.45	0.52	0.71	0.46	1.00	0.90	1.20	1.42	1.32	1.32	1.30	1.45	1.84	1.73	1.43	1.86	1.90	1.92	1.90	1.73	1.87	1.77	1.75	1.90	1.80	1.89	1.91	1.73	1.95	1.94	1.95	1.94	2.00	1.90
			.080	.04375	2523	.019	0.21	0.33	0.42	1.02	1.22	1.42	1.84	1.70	1.89	1.83	1.79	2.00	1.87	1.90	1.78	1.91	1.89	1.79	1.99	1.94	1.93	1.97	1.78	1.73	1.95	1.80	2.89	1.94	1.71	1.98	2.00	2.00	1.91	2.00	1.45	
			.080	.02925	1906	.013	0.28	0.81	0.83	1.27	1.44	1.41	1.60	1.82	2.00	1.46	1.77	1.86	1.76	1.80	1.75	1.90	1.79	2.02	1.82	1.82	1.75	1.73	1.81	1.83	1.90	1.68	1.83	1.73	1.79	1.95	1.83	1.81	1.80	2.00	1.94	
NO COOLANT INJECTION							2.38	2.41	2.36	2.21	2.00	2.27	2.25	2.28	2.25	2.12	2.03	3.07	2.22	2.28	3.18	3.26	2.18	2.19	2.11	1.98	2.00	2.19	2.12	1.82	2.14	2.00	2.08	2.11	2.05	2.00	1.95	2.00	1.95	2.05	1.58	

TABLE 5

TABLE 6

BOUNDARY LAYER MODEL PARAMETER CALCULATION RESULTS FOR THREE GASES INJECTED INTO A TURBULENT BOUNDARY LAYER.

Coolant Gas	$m = \frac{\rho_c u_c}{\rho_\infty u_\infty}$	K'	σ	X_1 Inches
Air	.0543	23.2	40.09	0.414
Air	.0428	29.6	40.47	0.282
Air	.0294	42.8	40.85	0.122
Freon	.0556	17.6	28.21	0.320
Freon	.0453	21.5	28.30	0.244
Freon	.0352	27.6	28.37	0.149
Helium	.0231	54.3	46.59	- 0.664
Helium	.0192	68.1	46.68	- 0.429
Helium	.0131	100.2	46.80	- 0.153

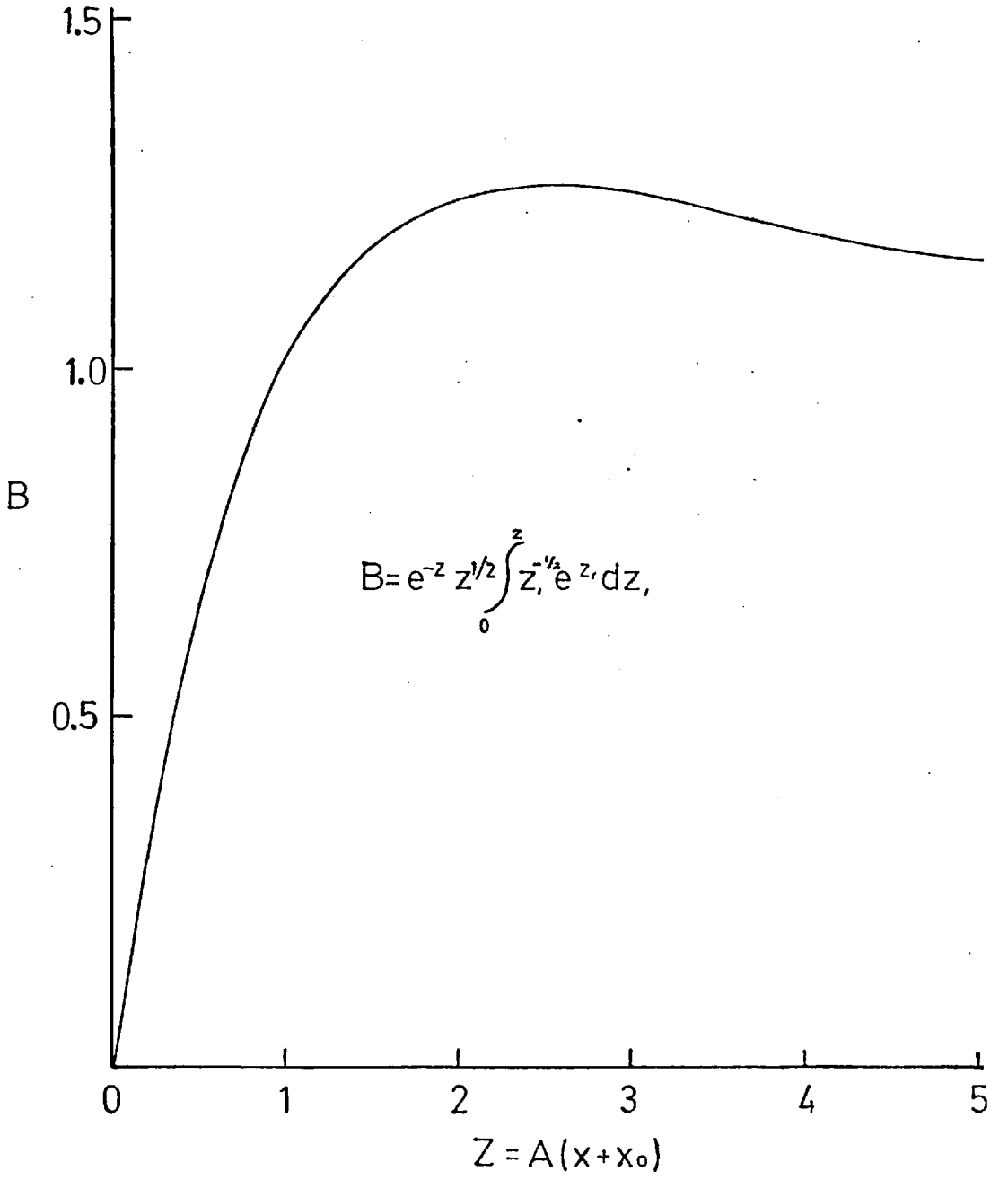

FIGURE 1 LAMINAR FILM COOLING DISCRETE LAYER FUNCTION EVALUATION

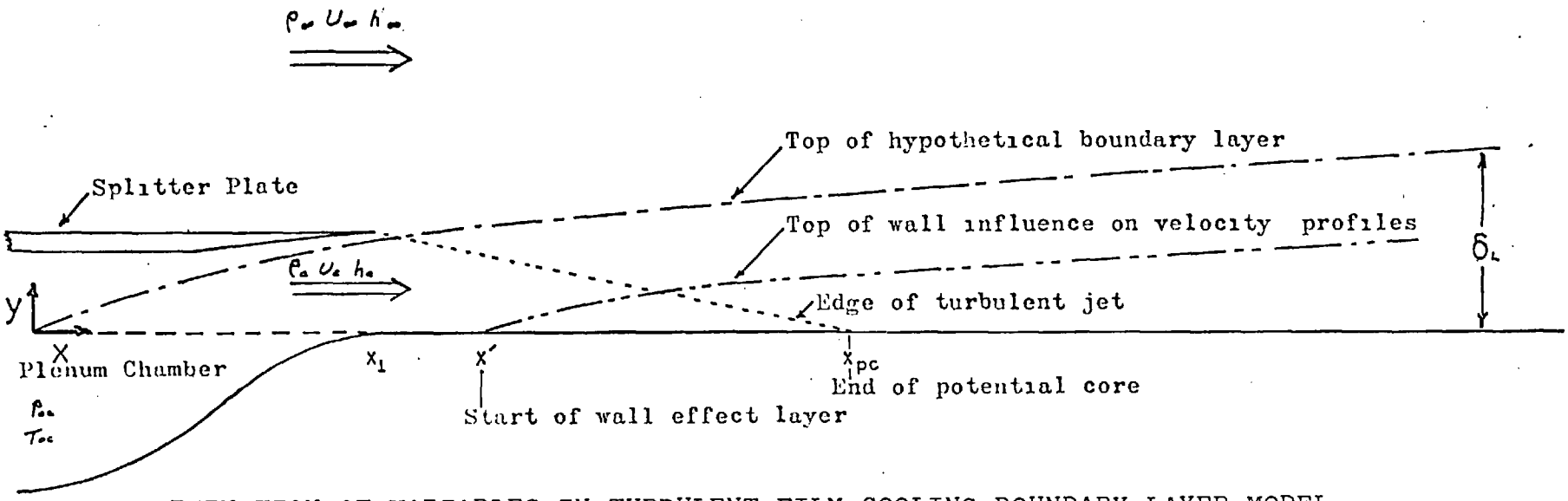

FIG 2a DEFINITION OF VARIABLES IN TURBULENT FILM COOLING BOUNDARY LAYER MODEL

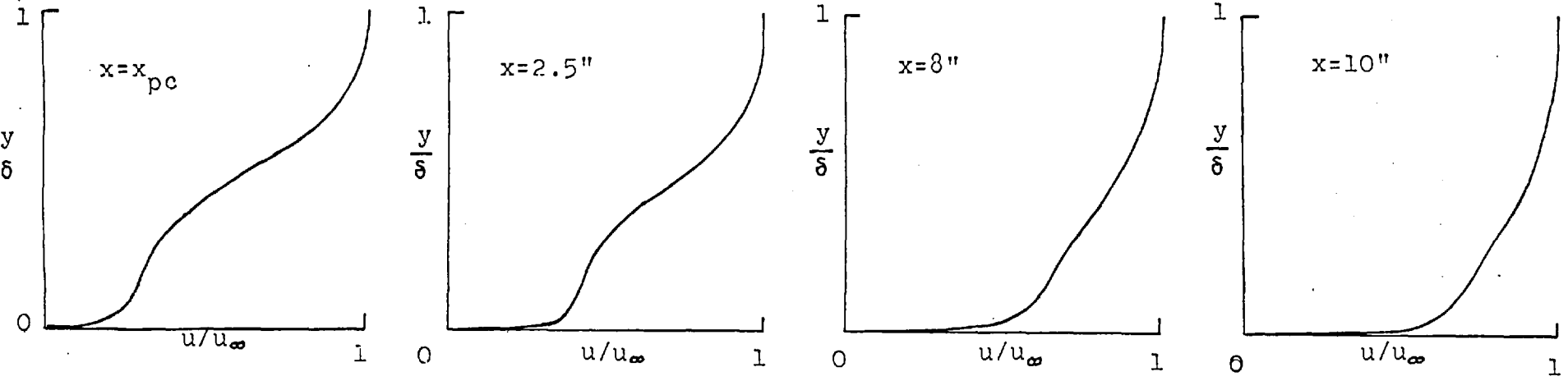

FIG 2b TYPICAL VARIATION OF ASSUMED VELOCITY PROFILES USED IN THE BOUNDARY LAYER MODEL

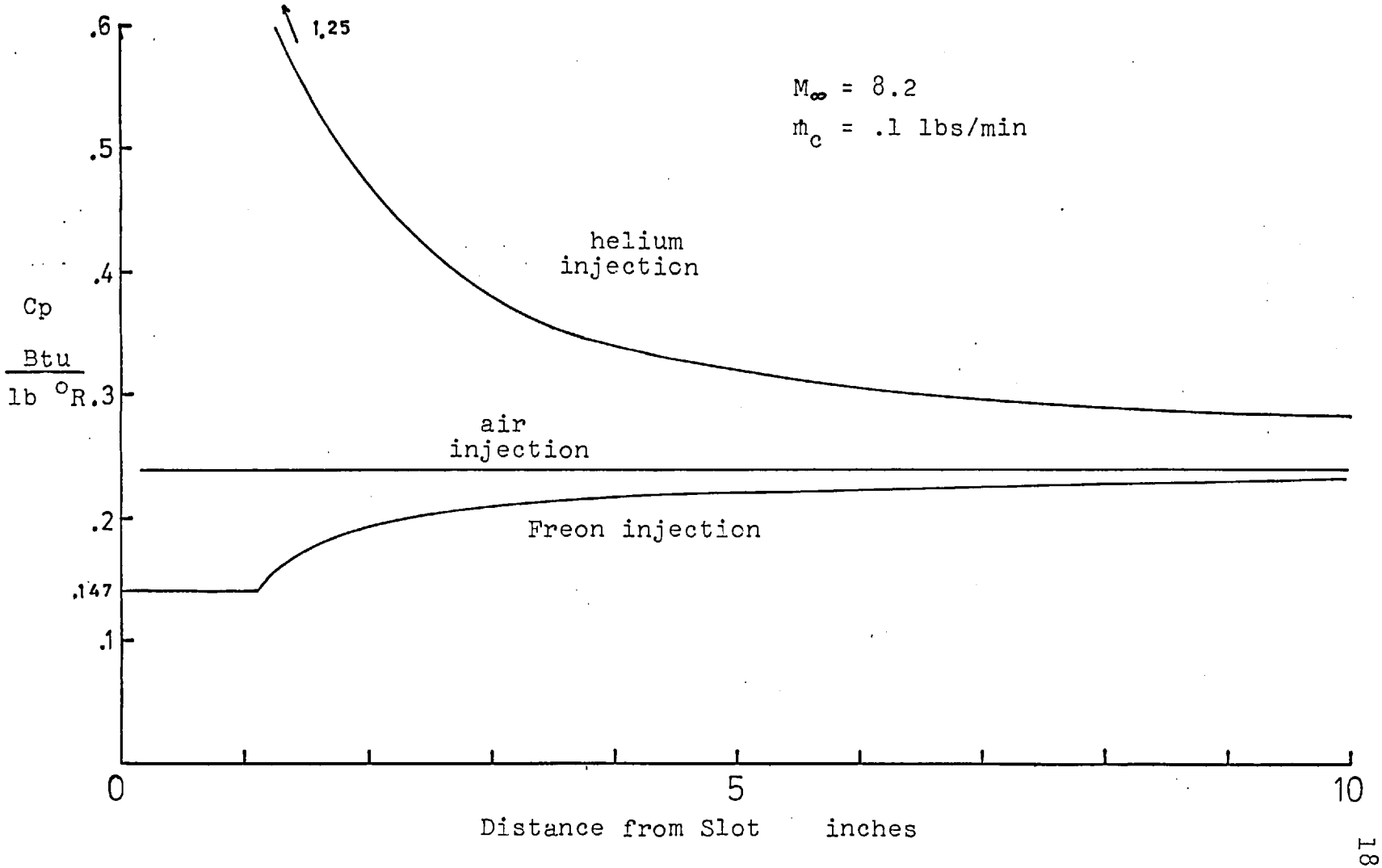

Fig. 3 - BOUNDARY LAYER MODEL SPECIFIC HEAT VARIATION FOR THREE INJECTION GASES.

FIG 4. MODEL NOSE CROSS SECTIONS

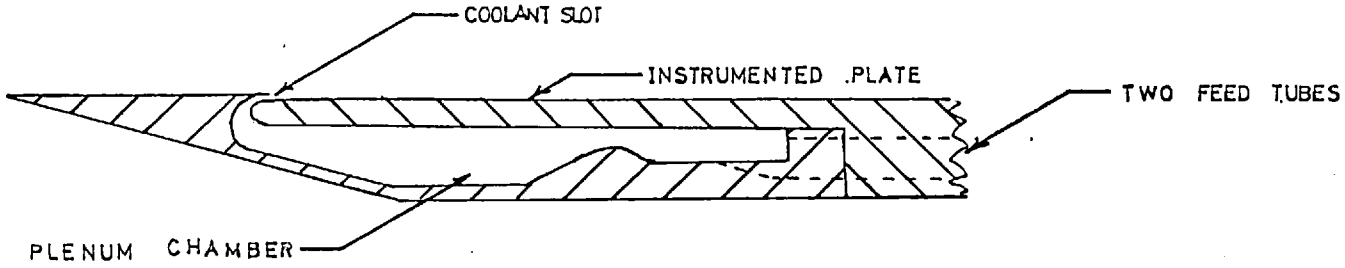

MODEL A LAMINAR

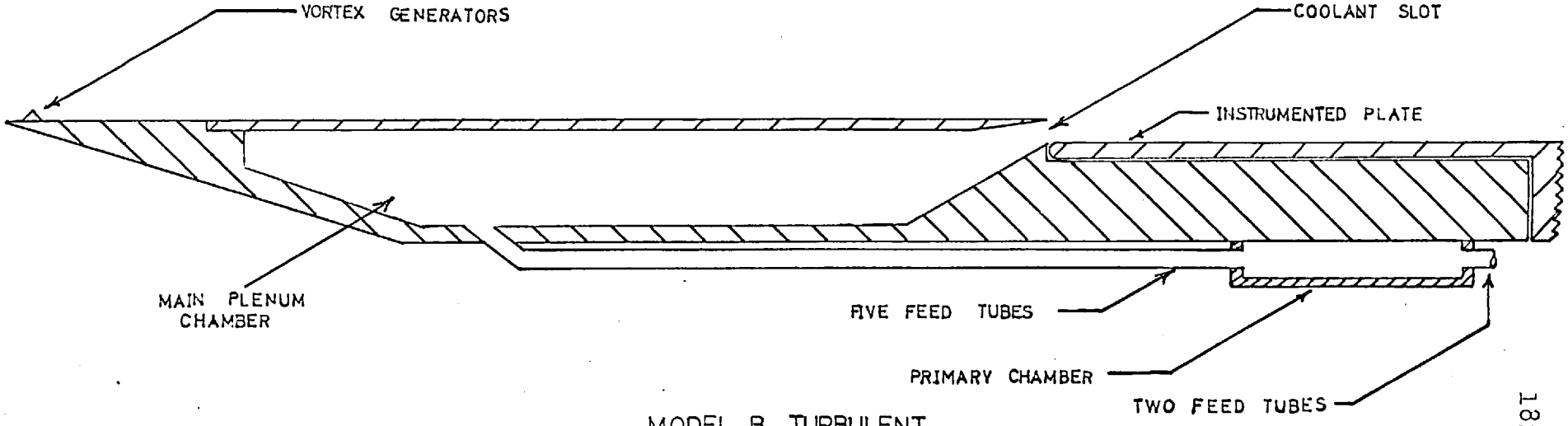

MODEL B TURBULENT

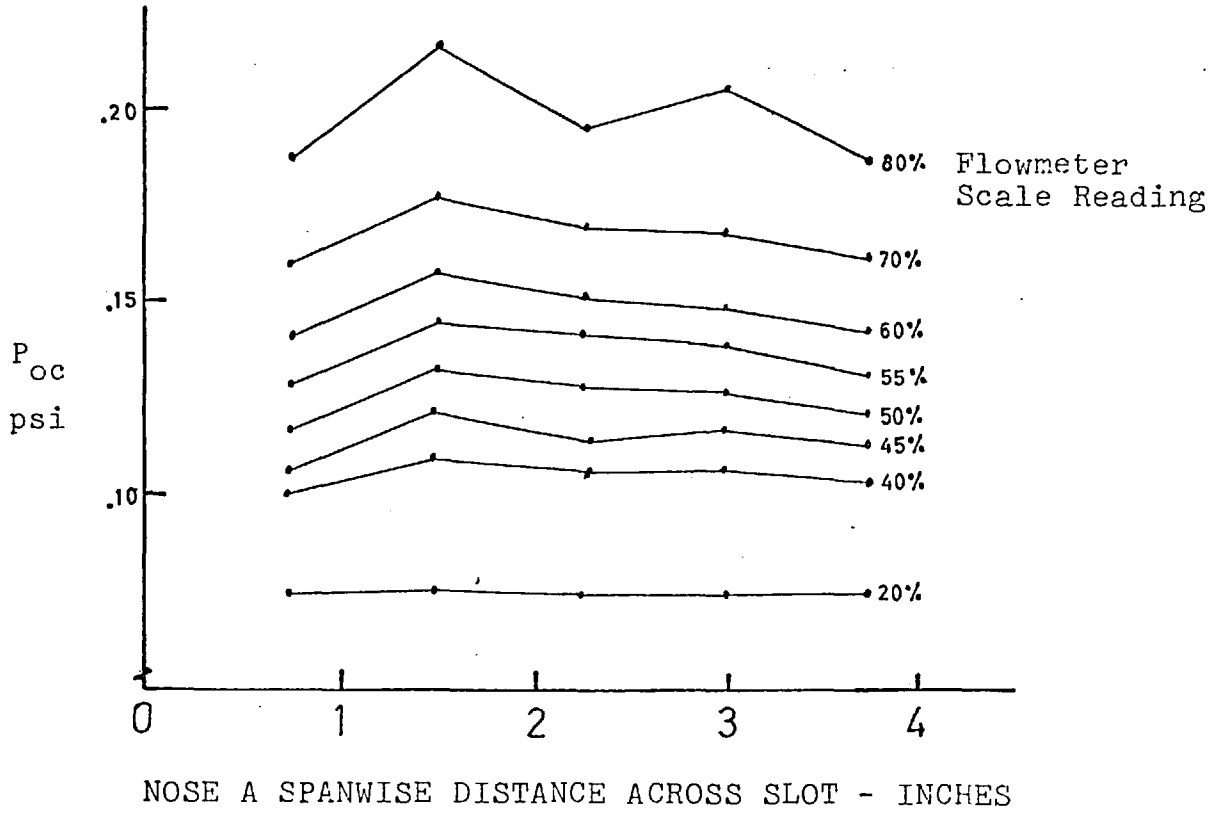

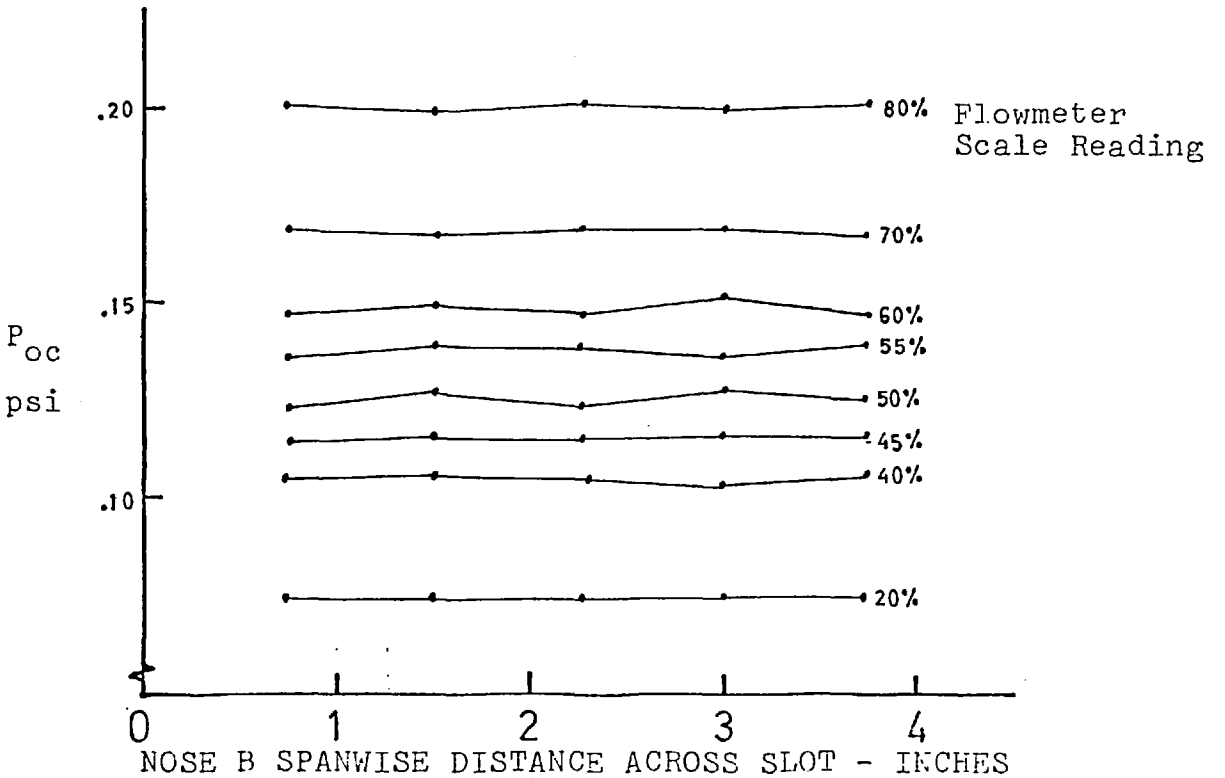

Fig. 5 . AIR COOLANT STAGNATION PRESSURE VARIATION ACROSS SLOT FOR BOTH NOSE EXTENSIONS.

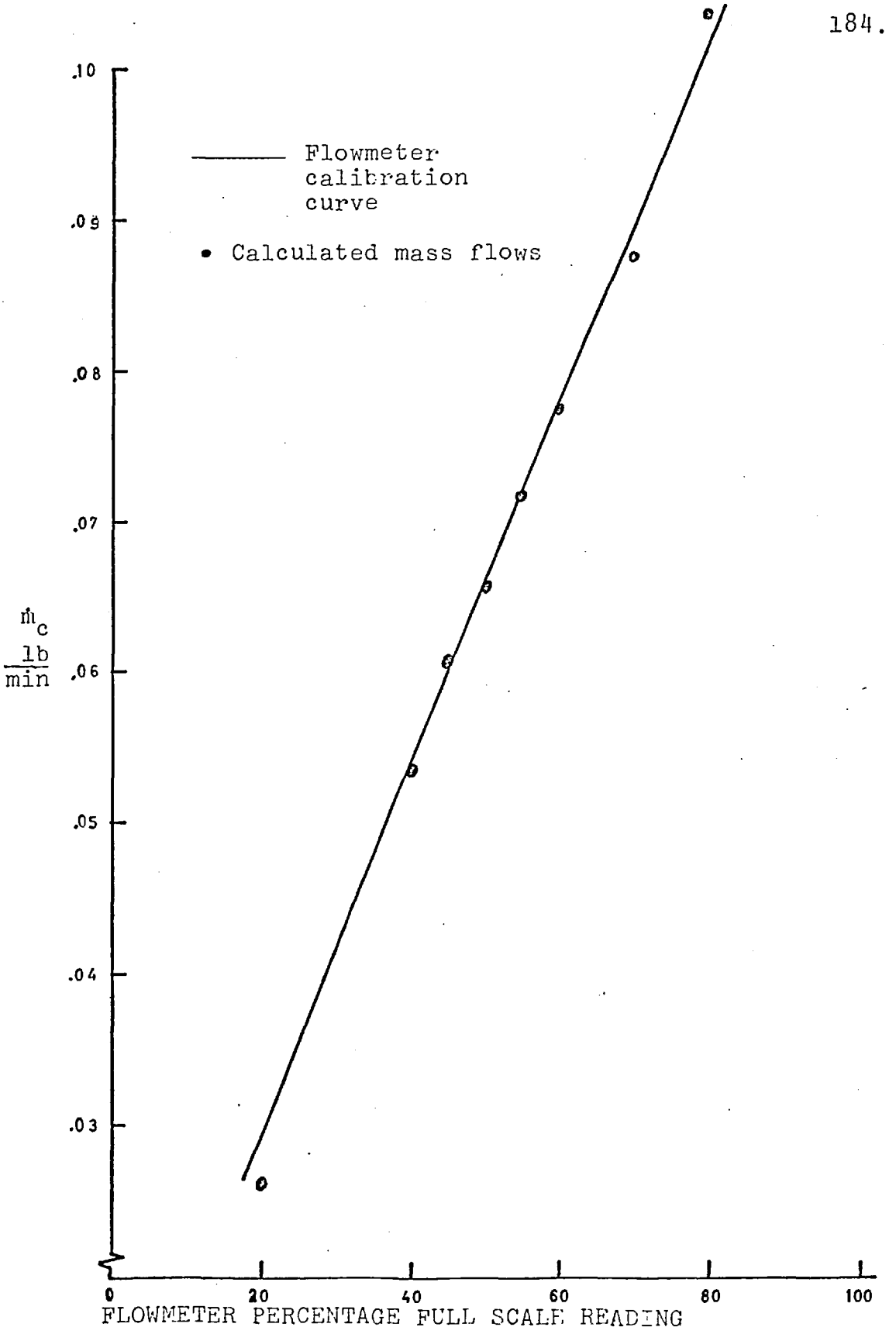

Fig. 6. FLOWMETER CALIBRATION

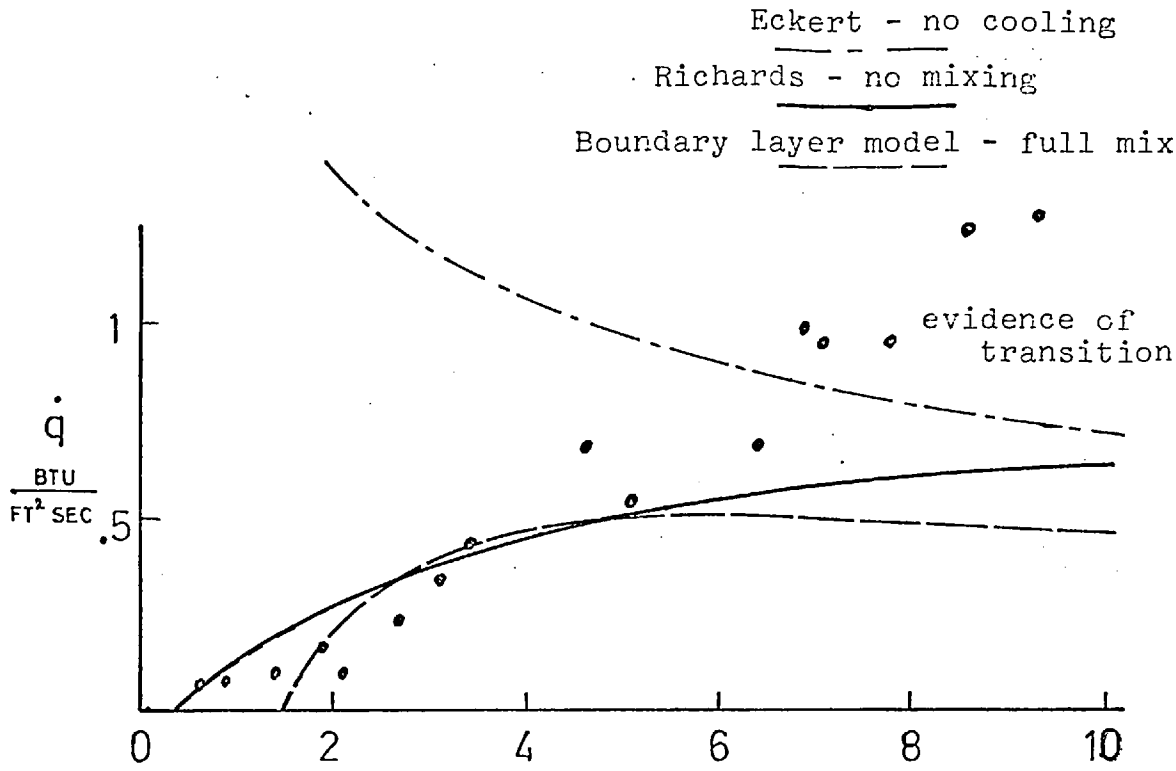

LAMINAR FILM COOLING s = 0.083 inches $\dot{m}_c$ = .072 lb/min

FIG 7a

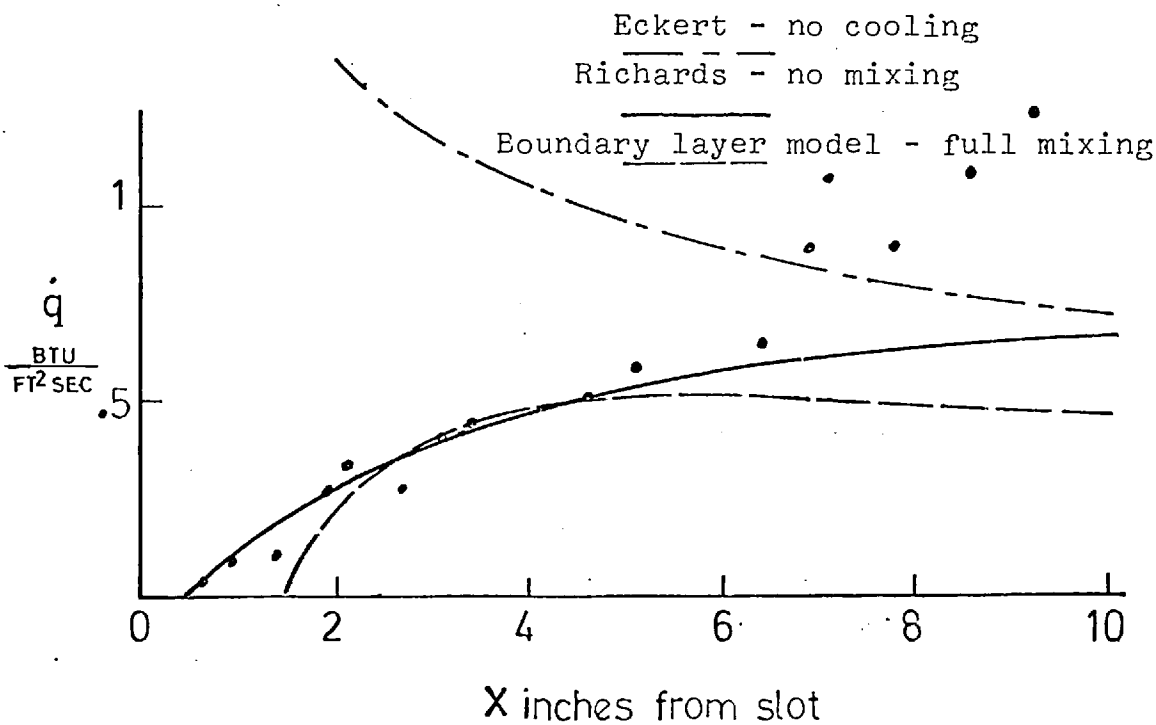

LAMINAR FILM COOLING s = 0.083 inches $\dot{m}_c$ = .066 lb/min

FIG 7b

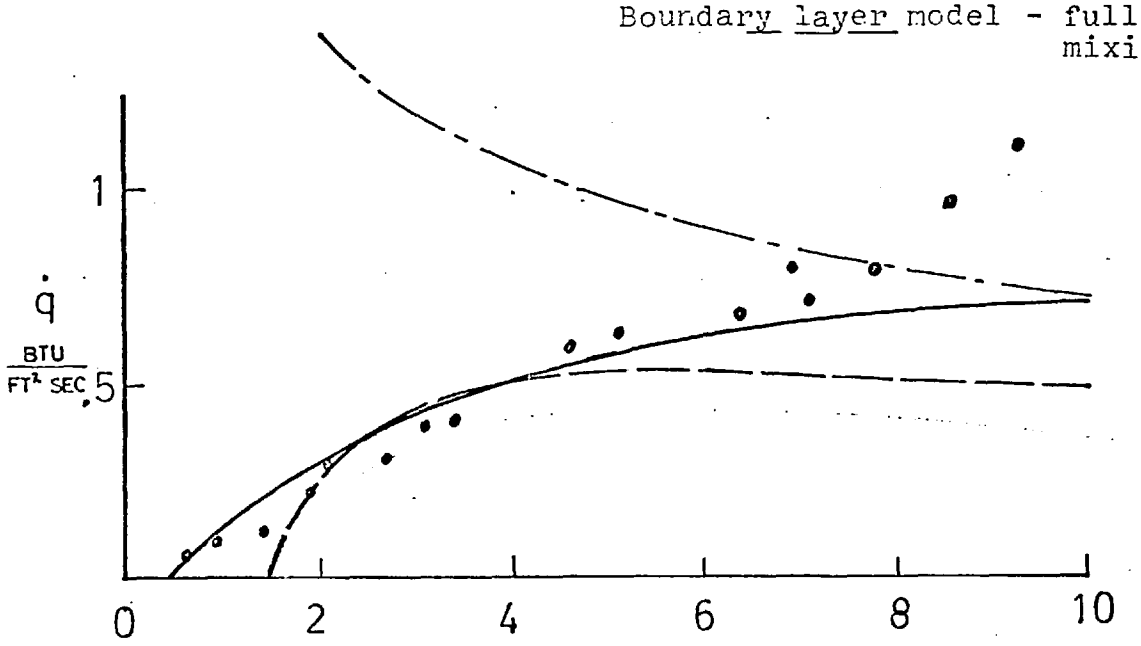

LAMINAR FILM COOLING s = 0.083 $\dot{m}_c$ = 060 lb/min

FIG 7c

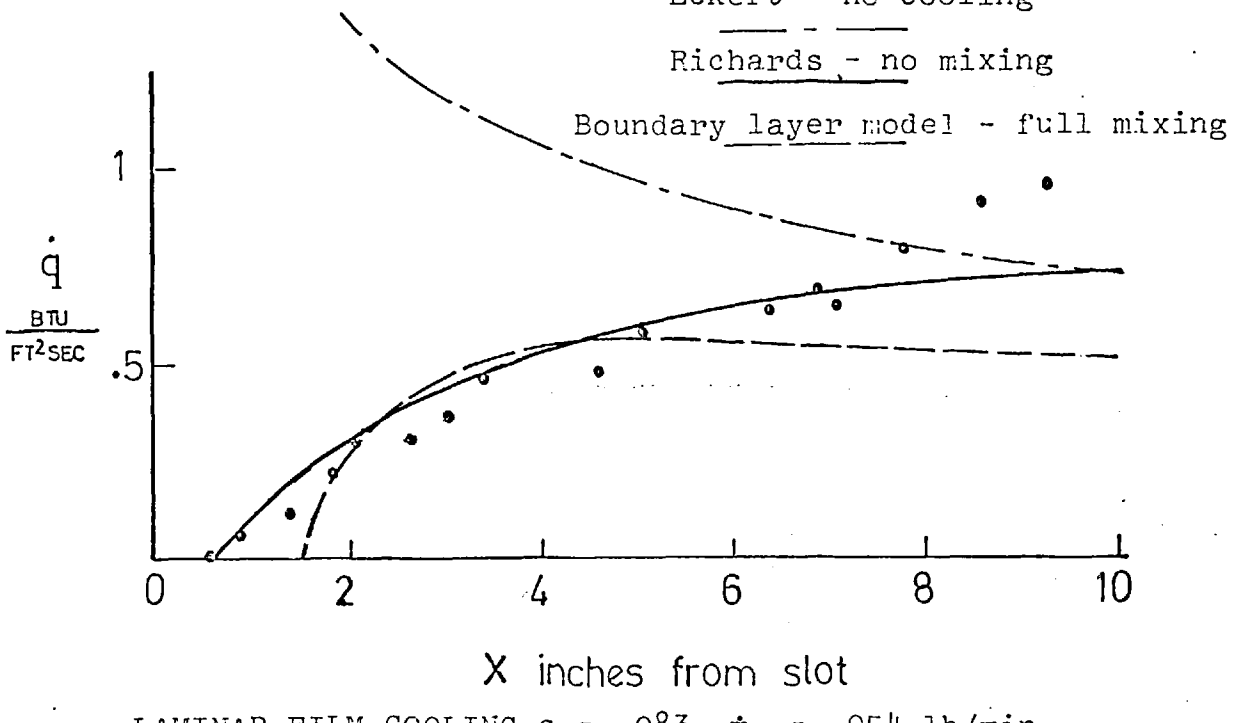

LAMINAR FILM COOLING s = .083 $\dot{m}_c$ = .054 lb/min

FIG 7d

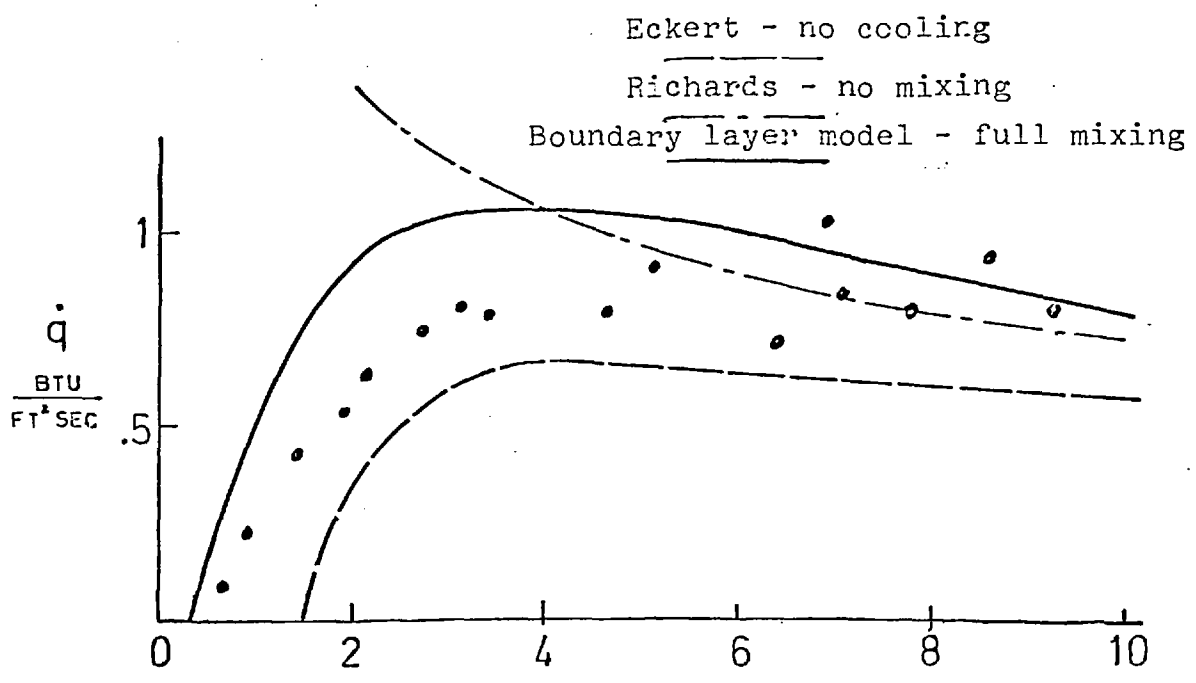

LAMINAR FILM COOLING s = 0.083 inches $\dot{m}_c$ = 0.029 lb/min

FIG 7e

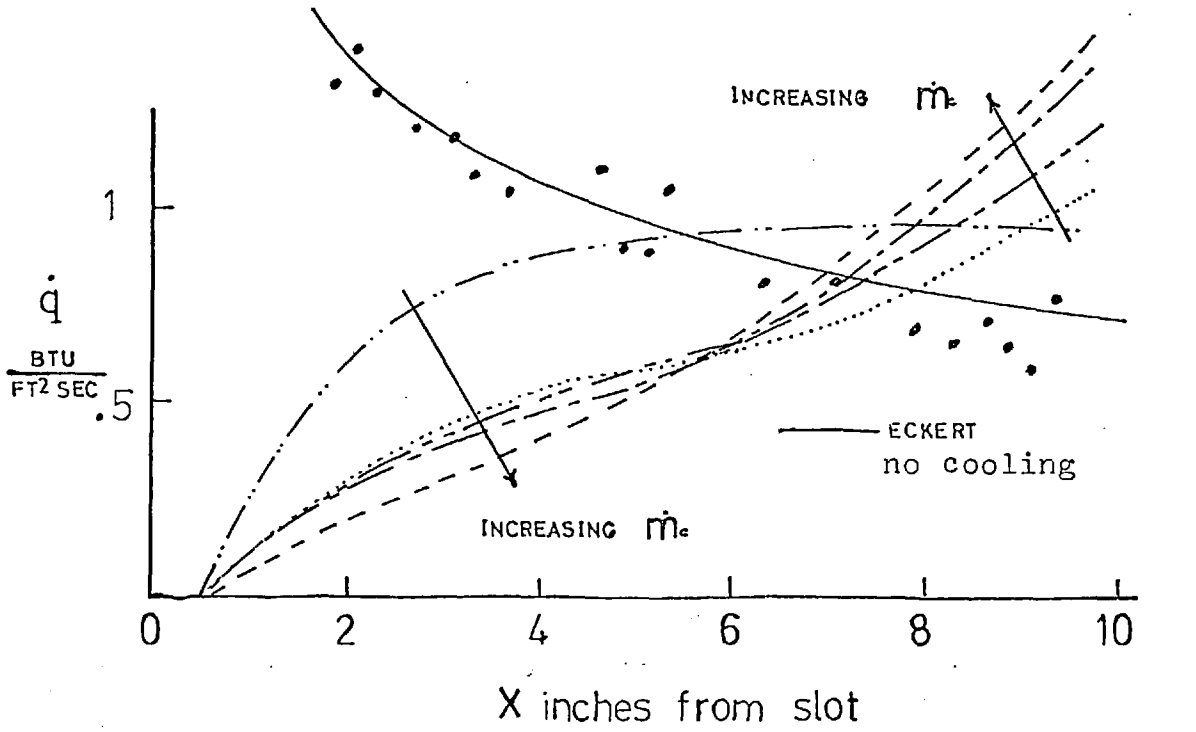

Fig. 7f. LAMINAR FLAT PLATE HEAT TRANSFER DISTRIBUTION s = 0 $\dot{m}_c$ = 0 COMPARED WITH MEAN LINES THROUGH MEASURED DISTRIBUTIONS FOR FIVE COOLANT MASS FLOWS.

Fig. 8a. $\dot{m}_c$ = .078 lb/min

Fig. 8b. $\dot{m}_c$ = .072 lb/min

Fig. 8c. $\dot{m}_c$ = .066 lb/min

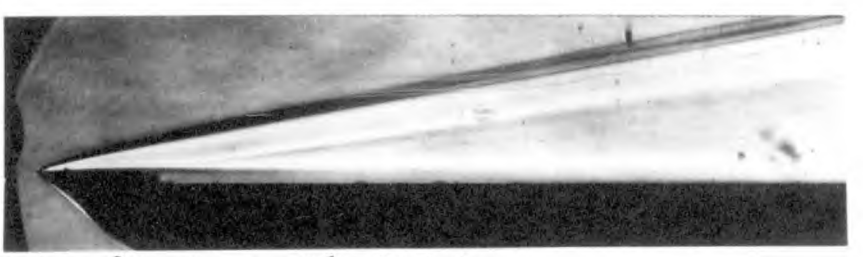

Fig. 8d. $\dot{m}_c$ = .060 lb/min

Fig. 8e. $\dot{m}_c$ = .054 lb/min

Fig. 8. LAMINAR FILM COOLING SCHLIEREN PHOTOGRAPHS FOR AIR INJECTION AT VARIOUS MASS FLOW RATES M_∞ = 8.2

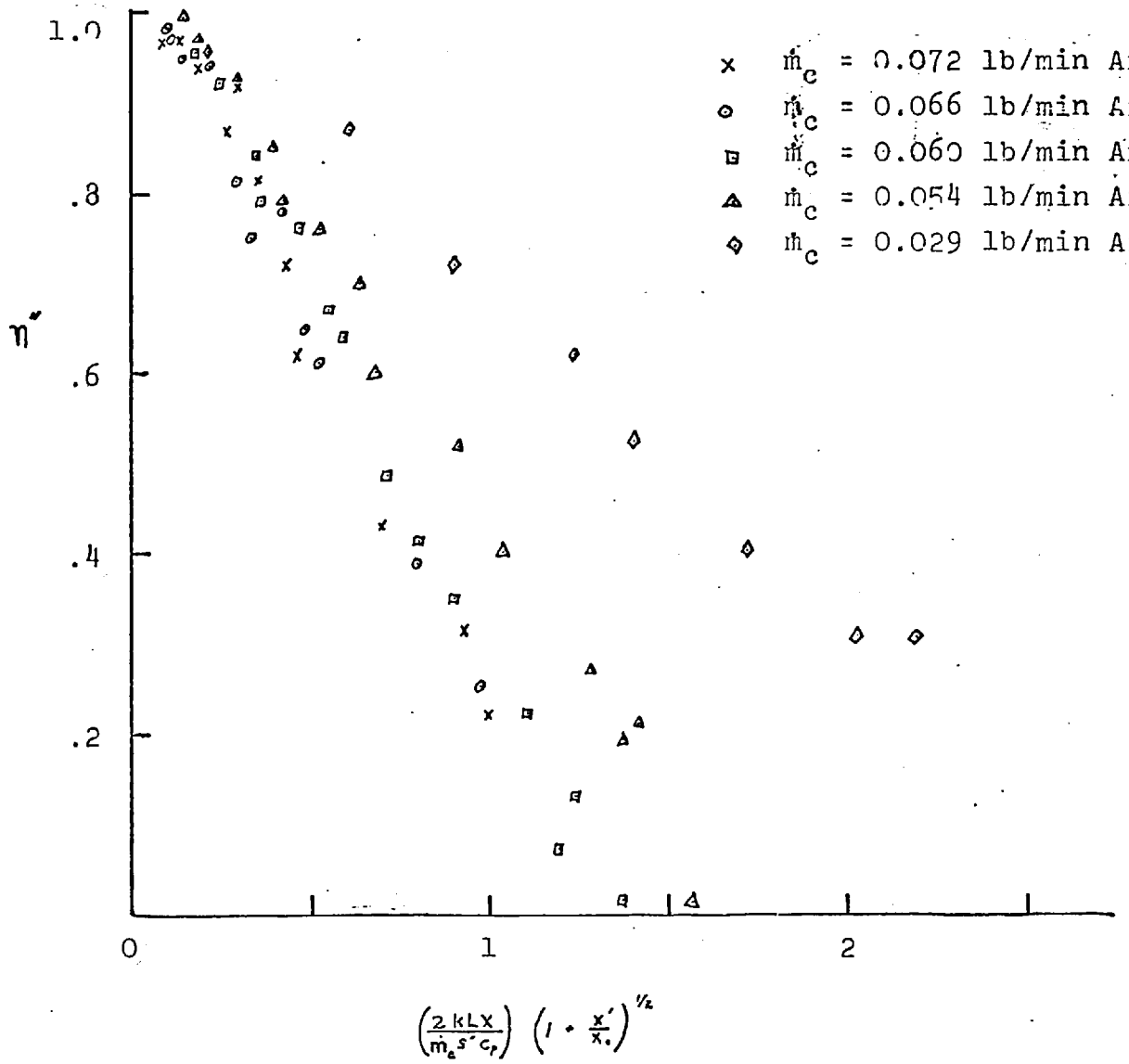

Fig. 9 RICHARDS CORRELATION PARAMETER vs LAMINAR FILM COOLING EFFECTIVENESS

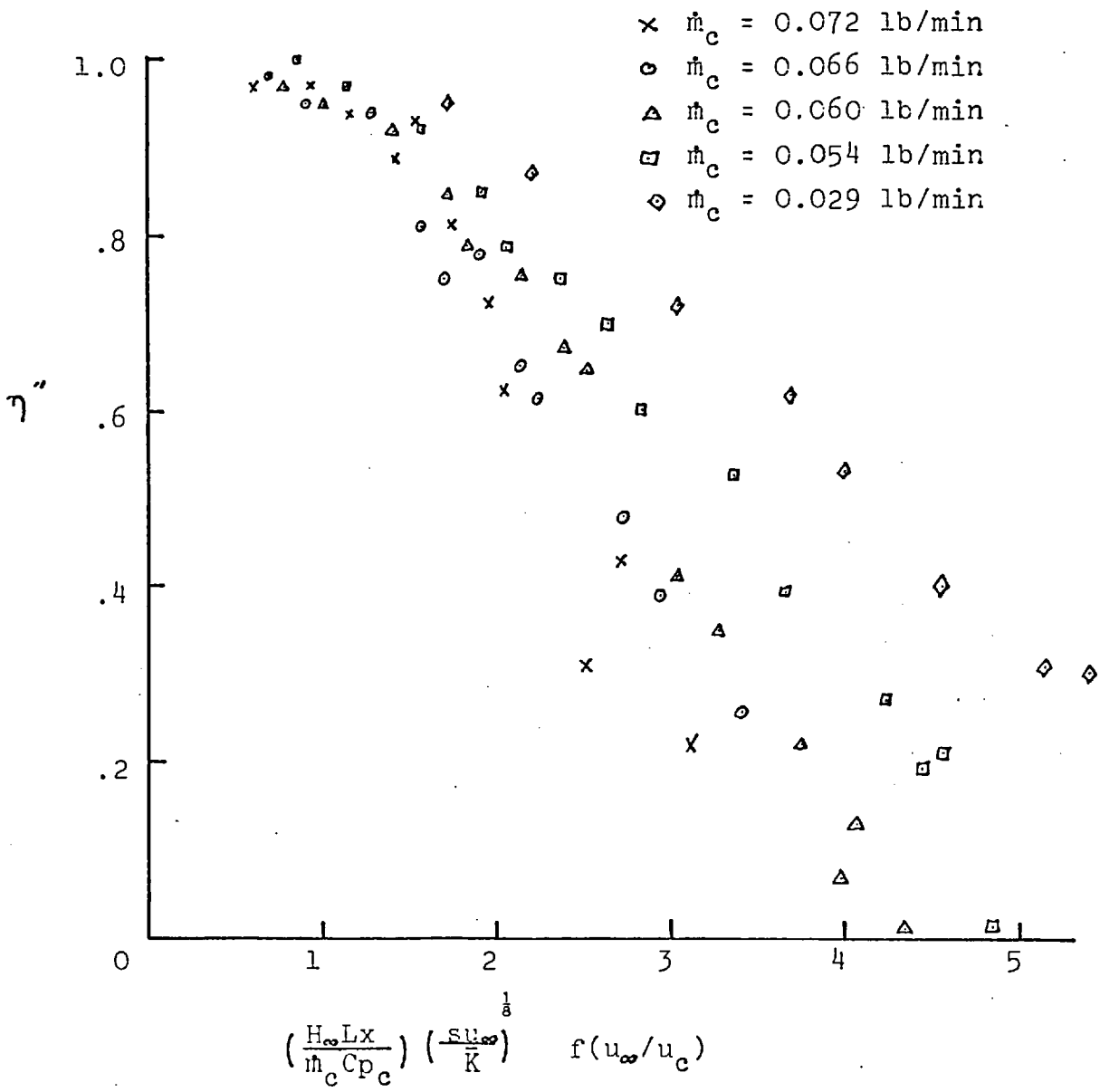

Fig 10. LAMINAR FILM COOLING EFFECTIVENESS CORRELATION SUGGESTED BY LUCAS AND GOLLADAY (1967)

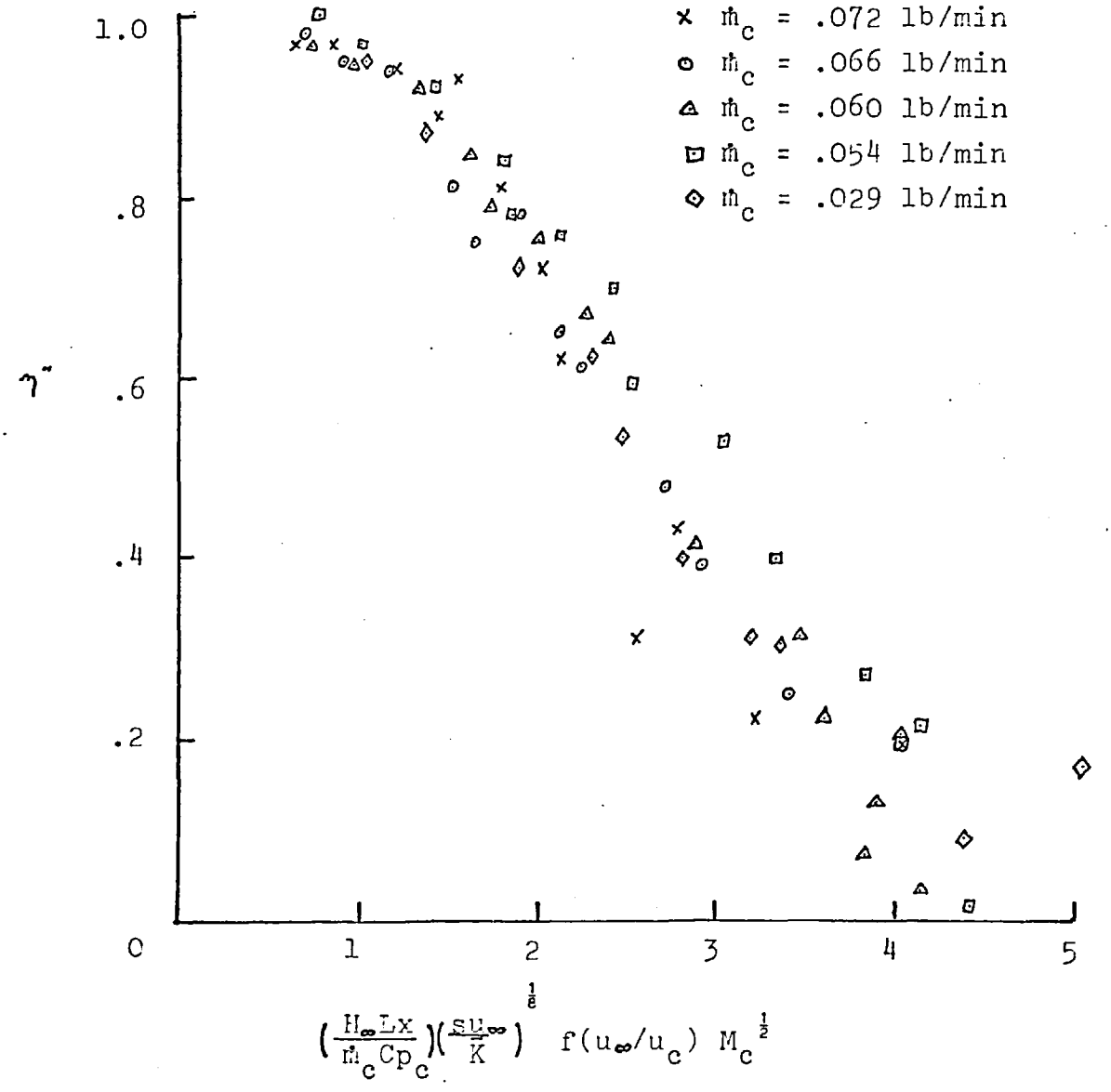

Fig. 11. LAMINAR FILM COOLING EFFECTIVENESS CORRELATION WITH MODIFIED LUCAS AND GOLLADAY (1967) PARAMETER

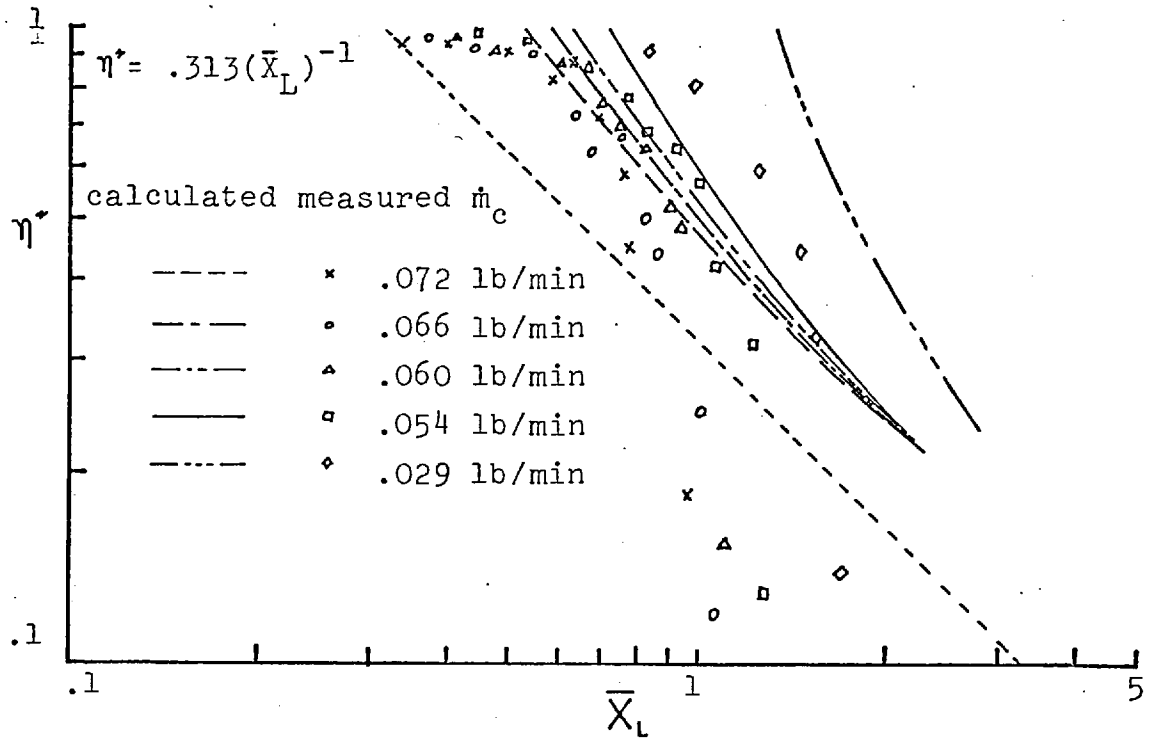

Fig.12 LAMINAR FILM COOLING BOUNDARY LAYER MODEL DATA CORRELATION

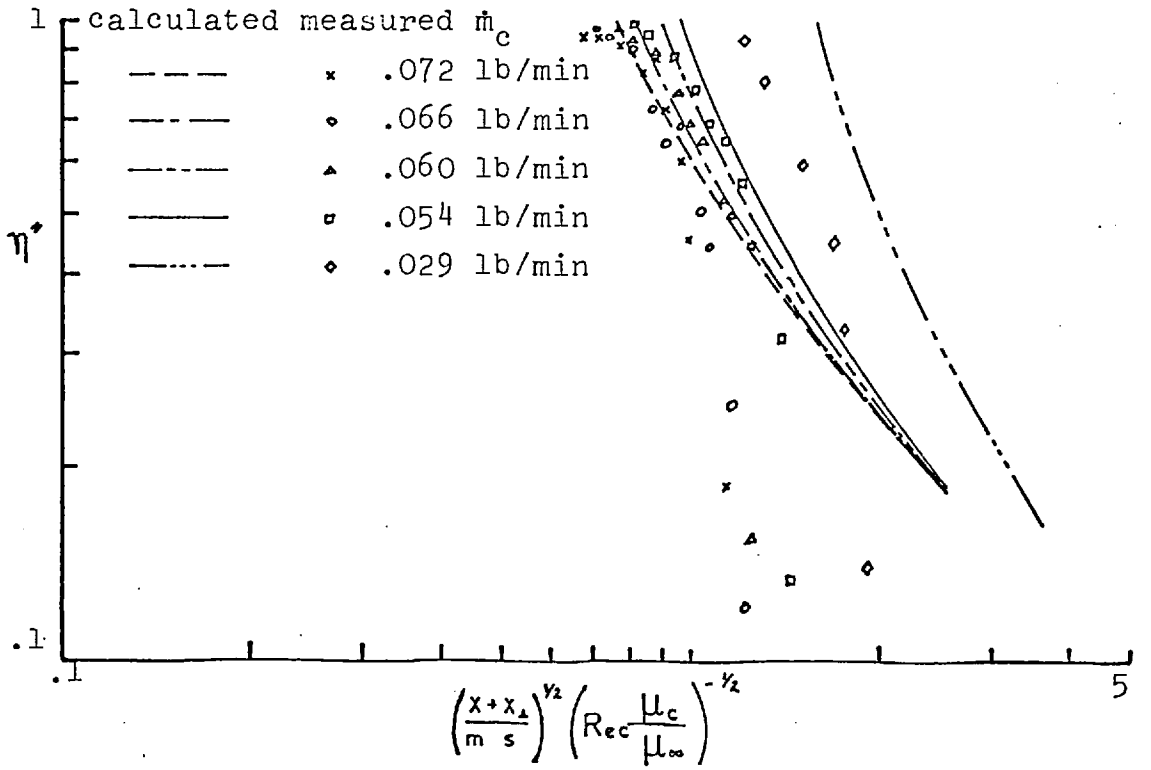

Fig. 13. LAMINAR FILM COOLING BOUNDARY LAYER MODEL DATA CORRELATION WITH STARTING LENGTH CORRECTION

no coolant flow — with slot

no coolant flow — without slot

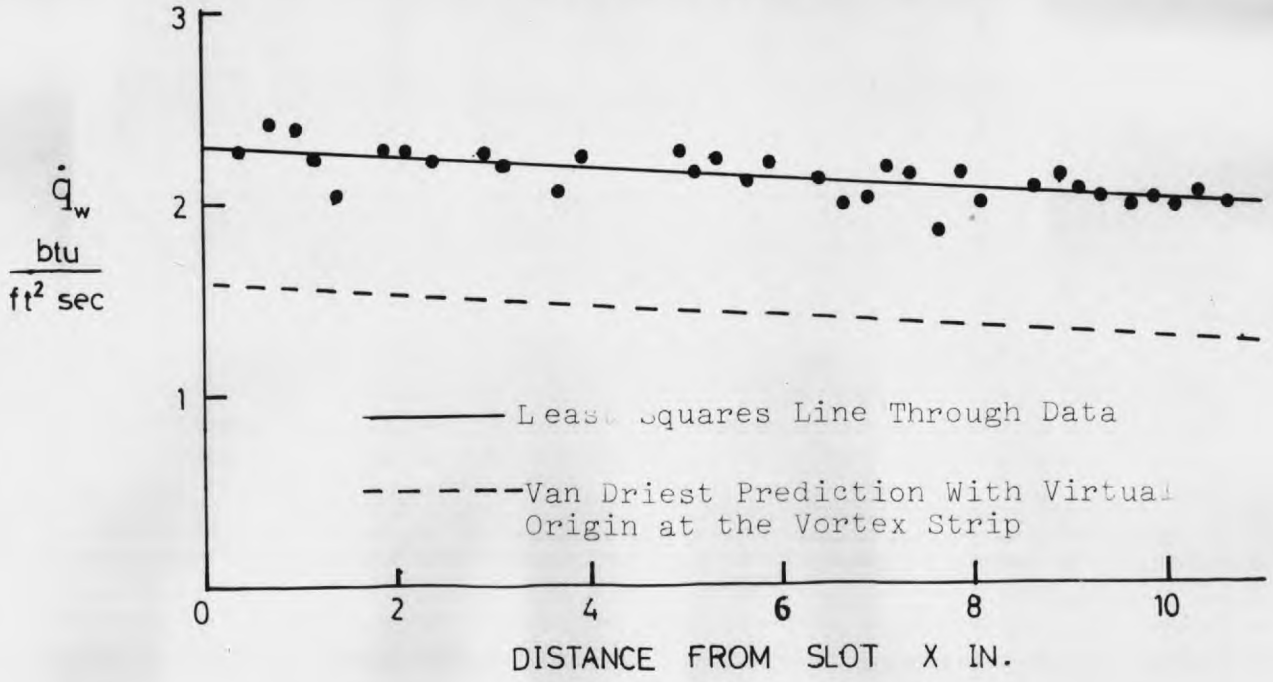

FIG. 14 Heat Transfer Turbulent Flow No Injection No Slot $M_\infty = 8.2$

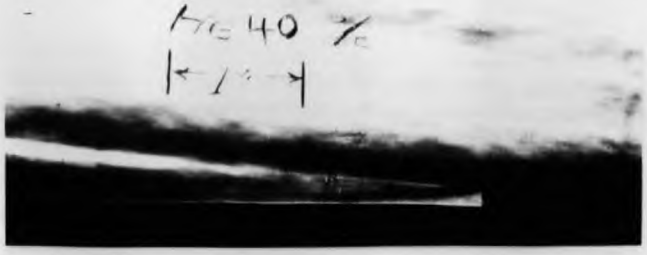

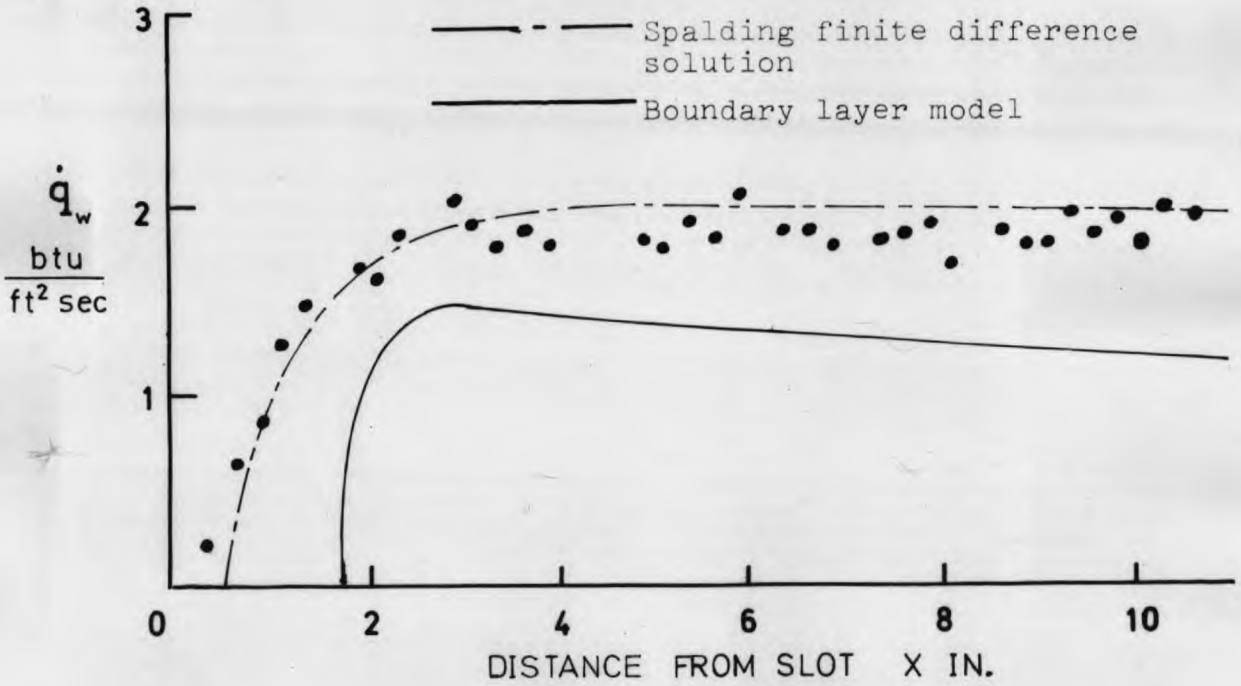

FIG. 15 Heat Transfer Turbulent Film Cooling
Helium Injection $\dot{m}_c = .02925$ lb/min

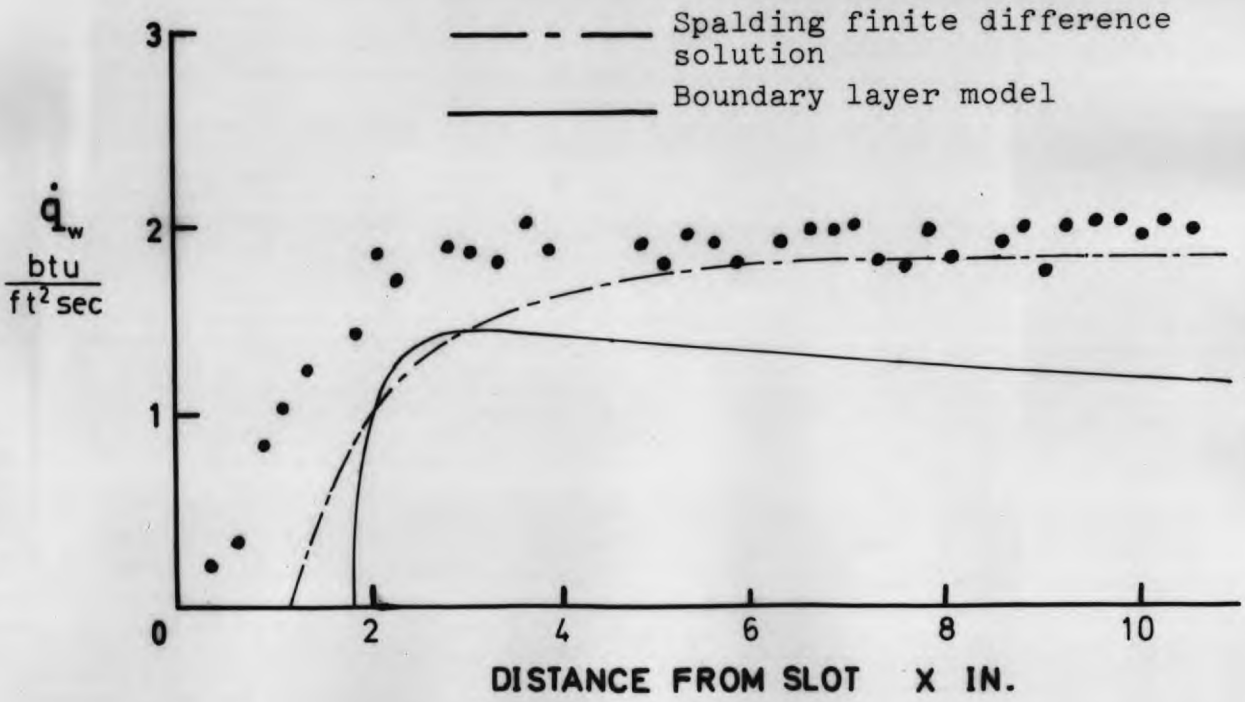

FIG. 16 Heat Trasfer Turbulent Film Cooling
Helium Injection $\dot{m}_c$ = .04275 lb/min

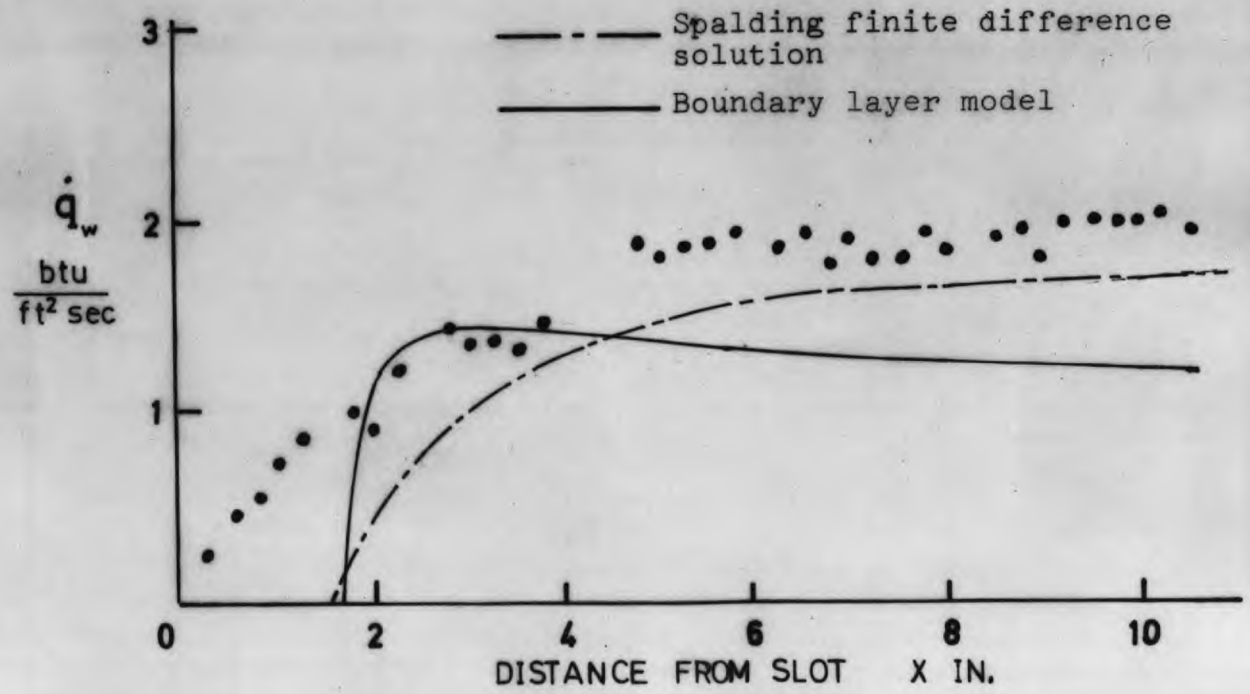

FIG. 17 Heat Transfer Turbulent Film Cooling
Helium Injection $\dot{m}_c$=.0515 lb/min

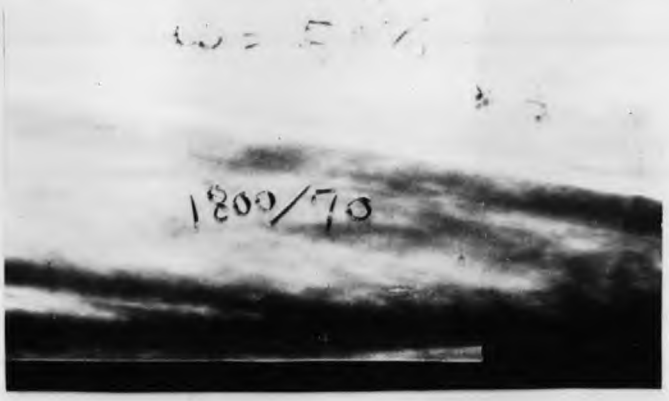

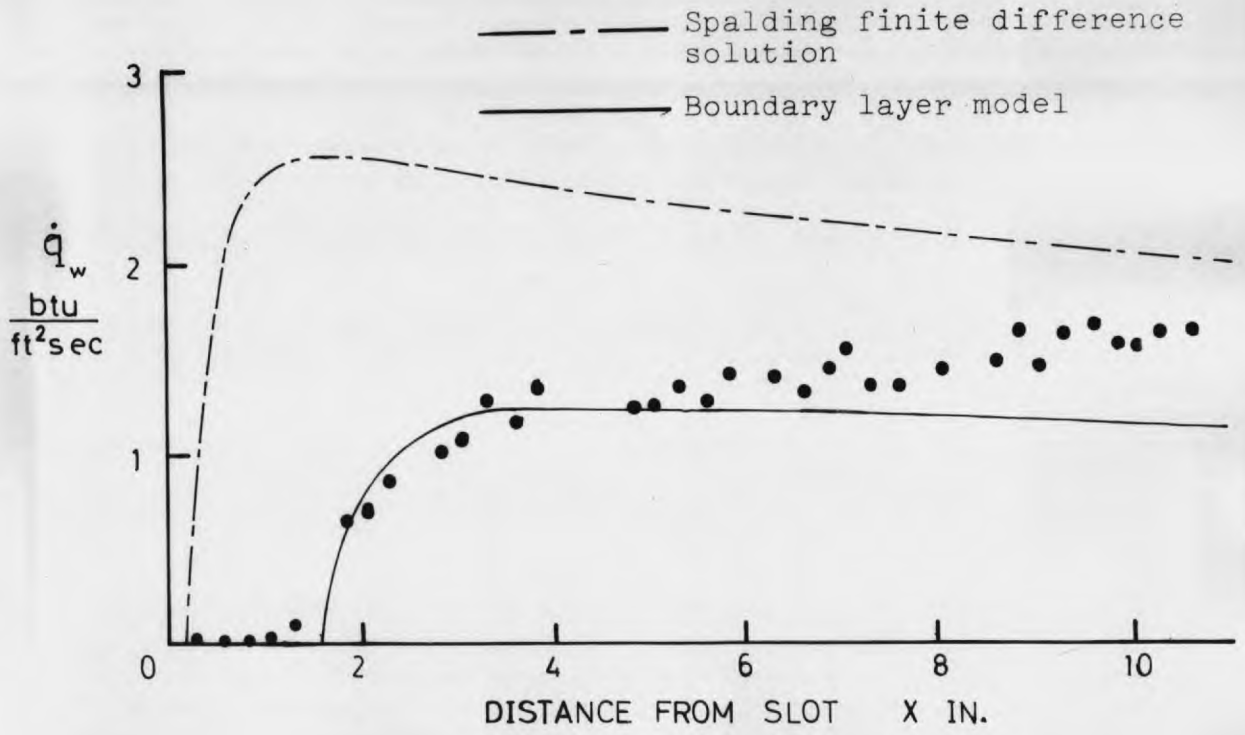

FIG.18 Heat Transfer Turbulent Film Cooling
Air Injection $\dot{m}_c$=.0655 lb/min

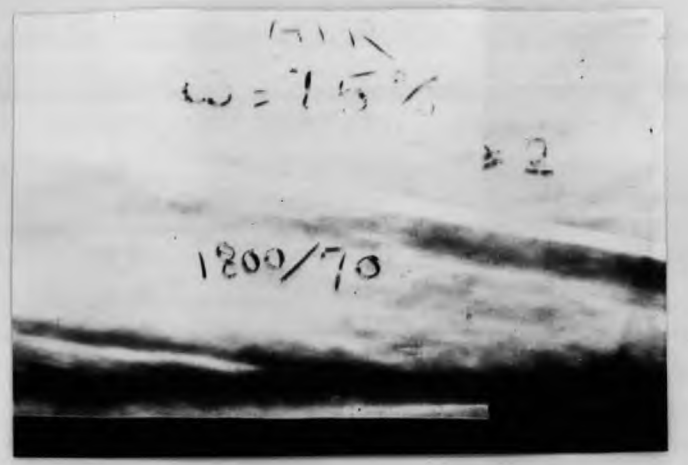

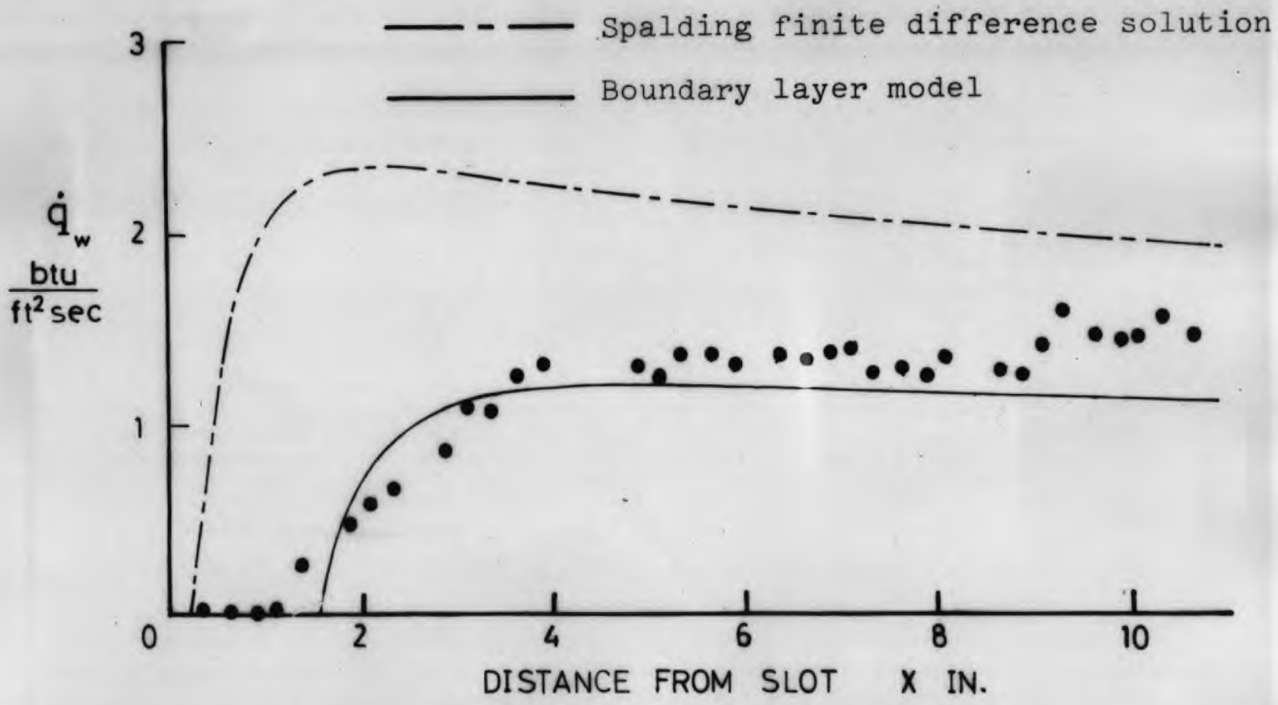

FIG. 19 Heat Transfer Turbulent Film Cooling
Air Injection $\dot{m}_c$=.0955 lb/min

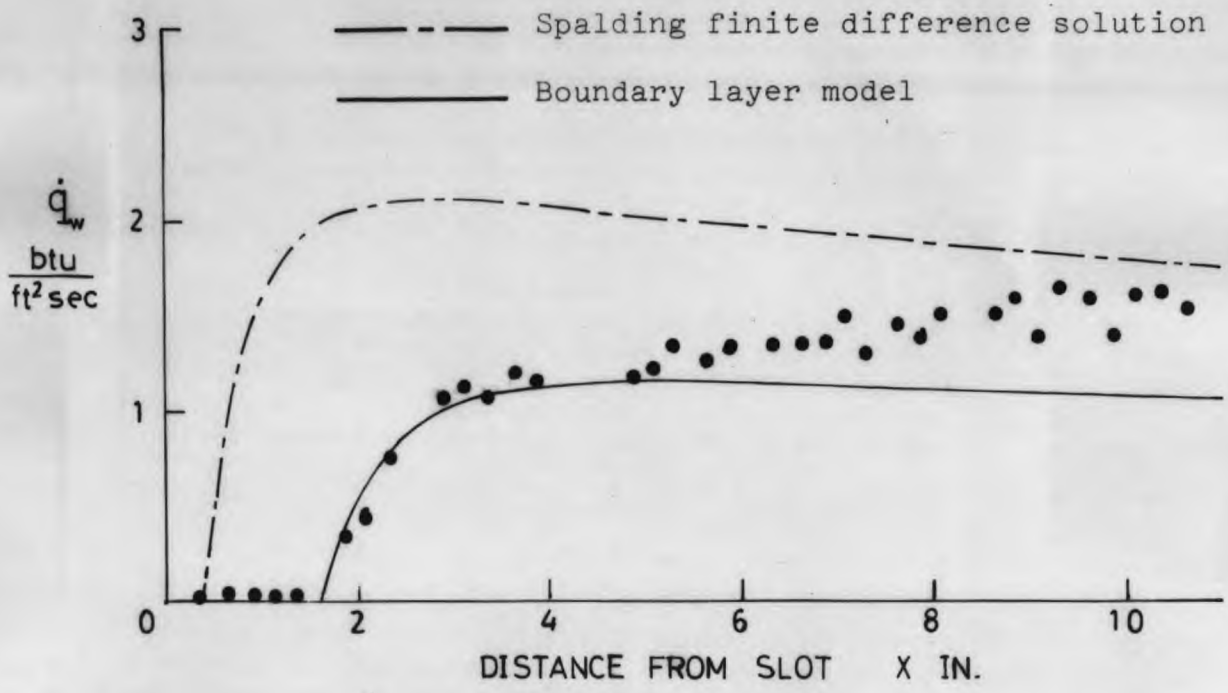

FIG 20 Heat Transfer Turbulent Film Cooling
Air Injection $\dot{m}_t$ = .121 lb/min

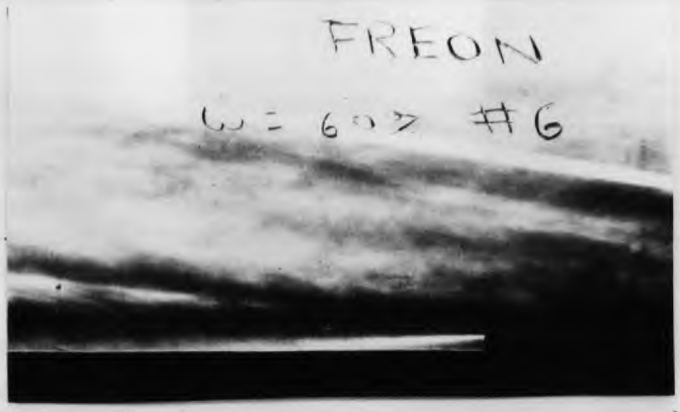

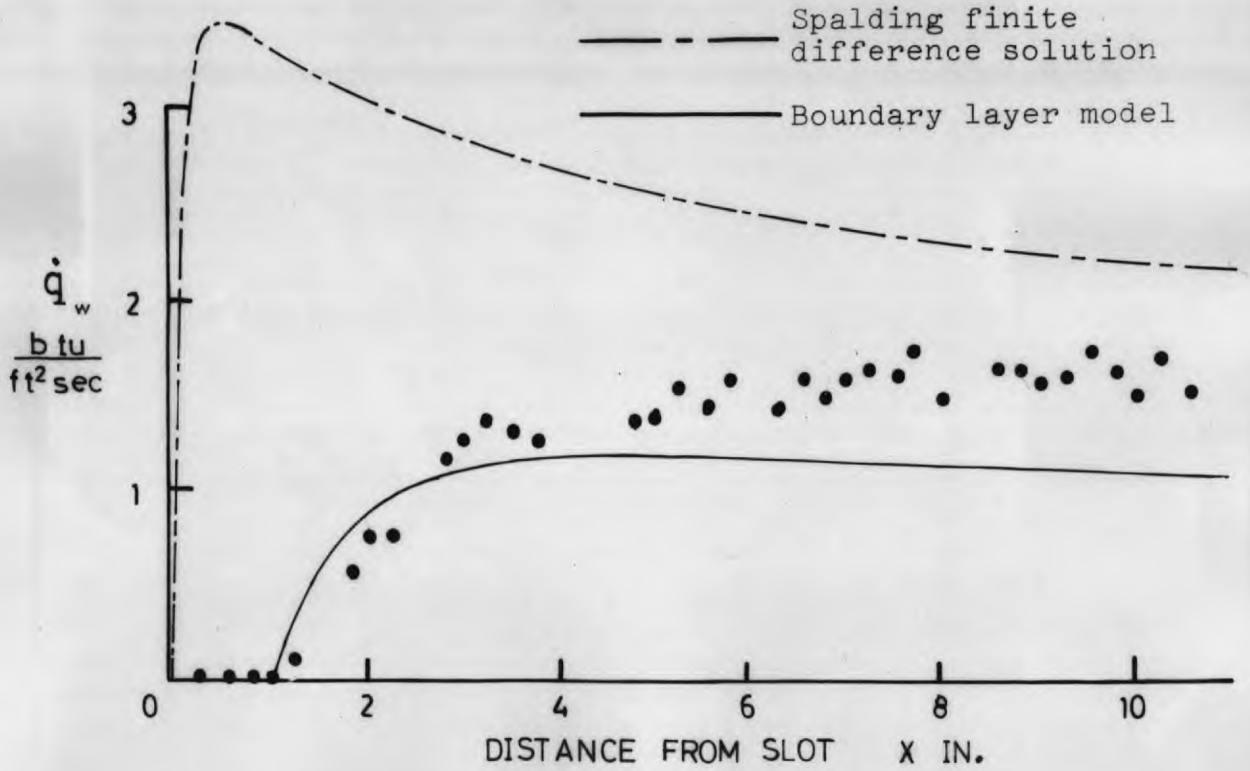

FIG. 21 Heat Transfer Turbulent Film Cooling
Freon Injection $\dot{m}_c$=.0785 lb/min

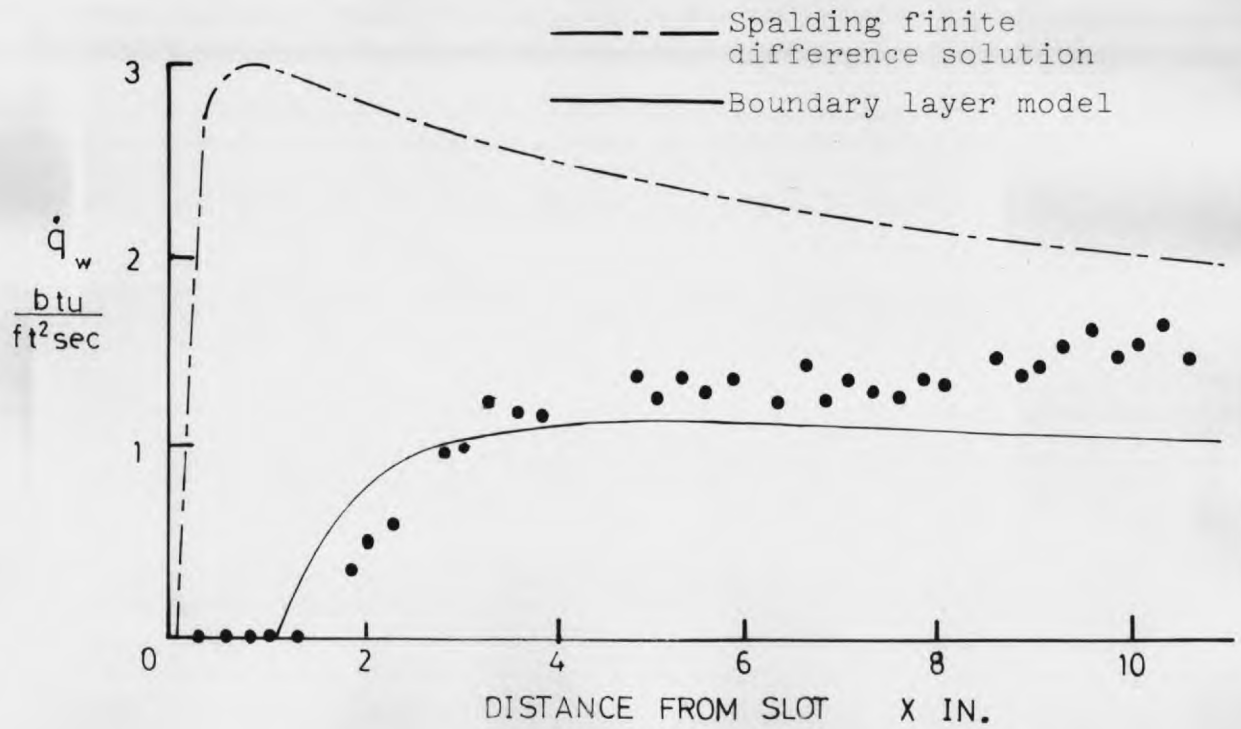

FIG. 22 Heat Transfer Turbulent Film Cooling
Freon Injection $\dot{m}_c$=.101 lb/min

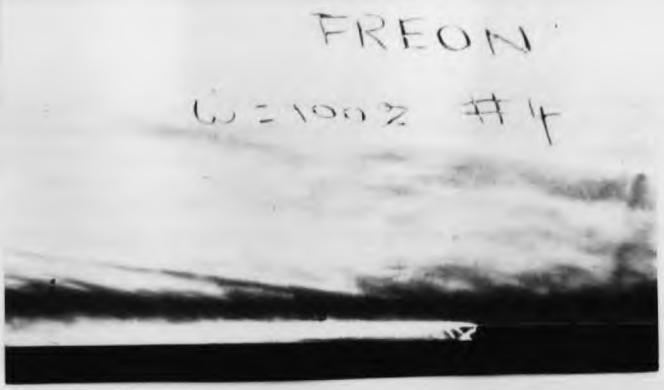

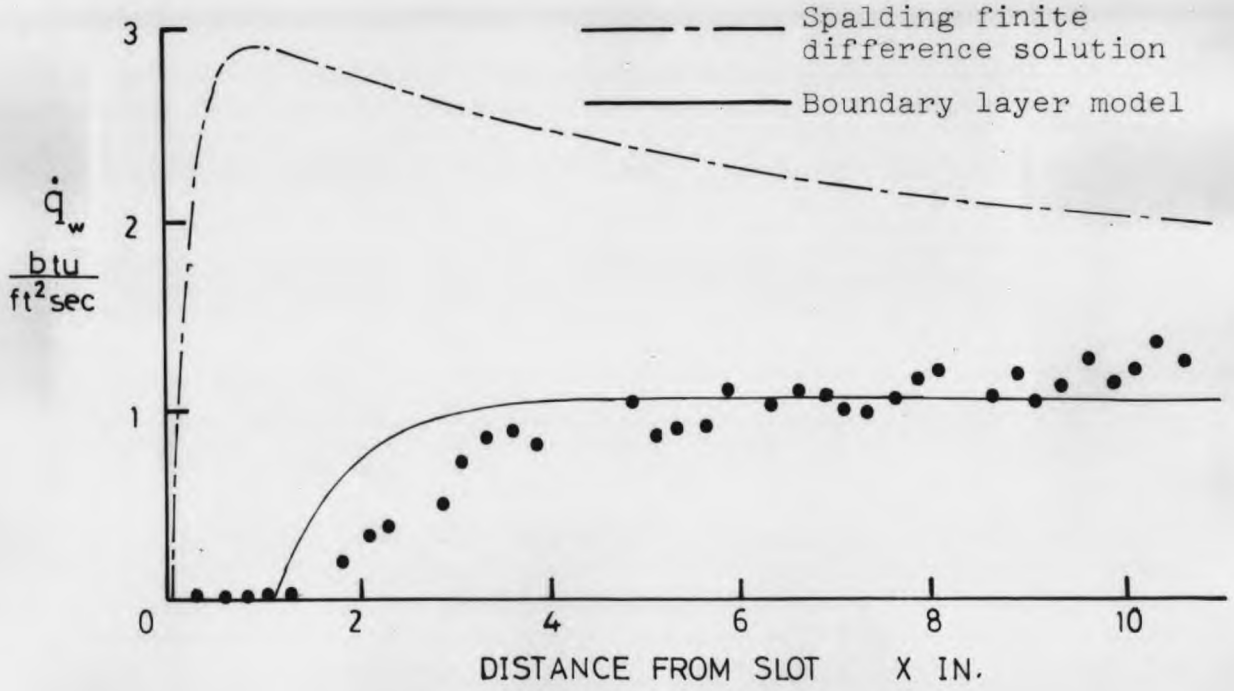

FIG. 23 Heat Transfer Turbulent Film Cooling
Freon Injection $\dot{m}_c$ = .124 lb/min

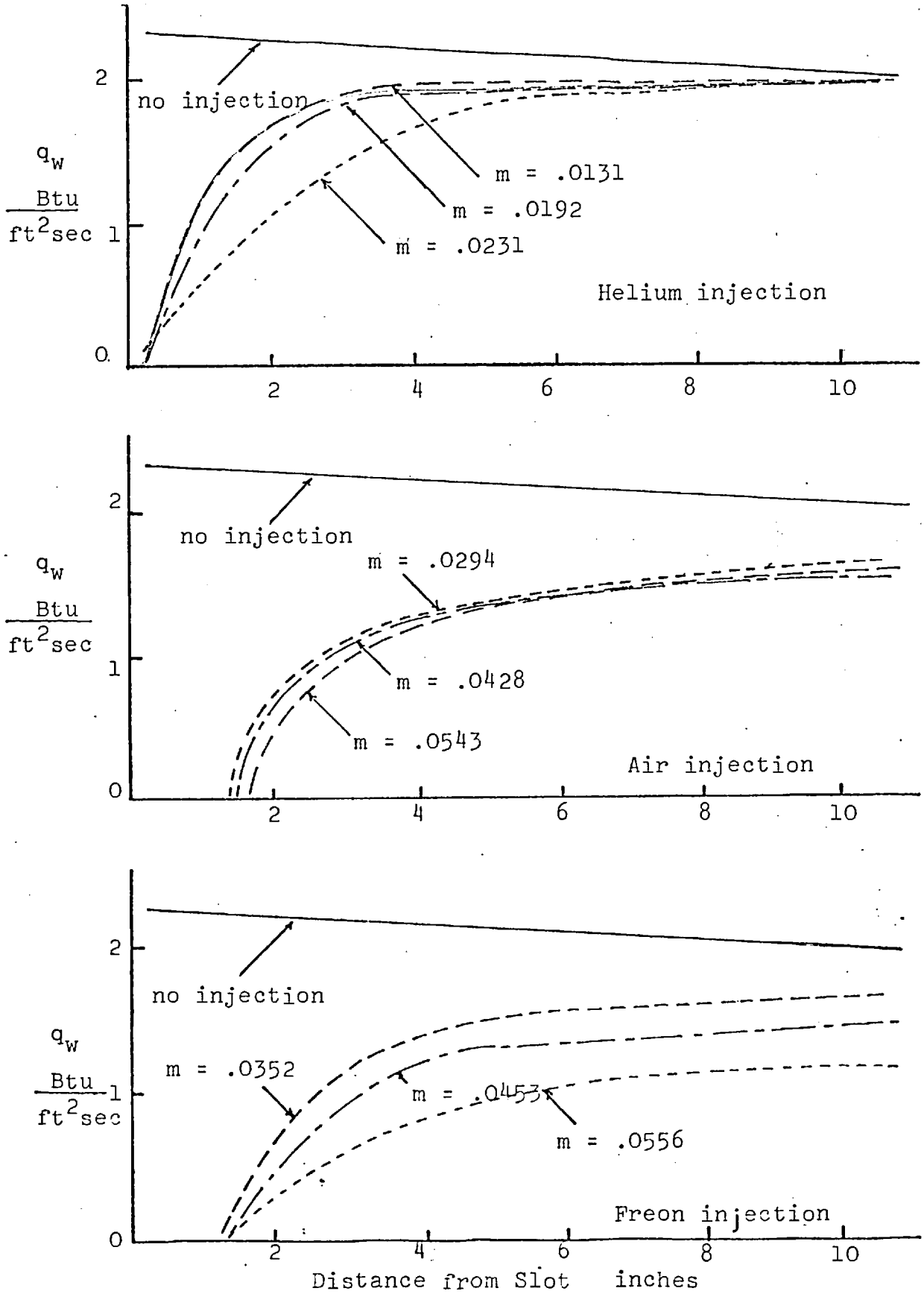

Fig. 24 MEAN LINES THROUGH MEASURED VALUES - TURBULENT FILM COOLING

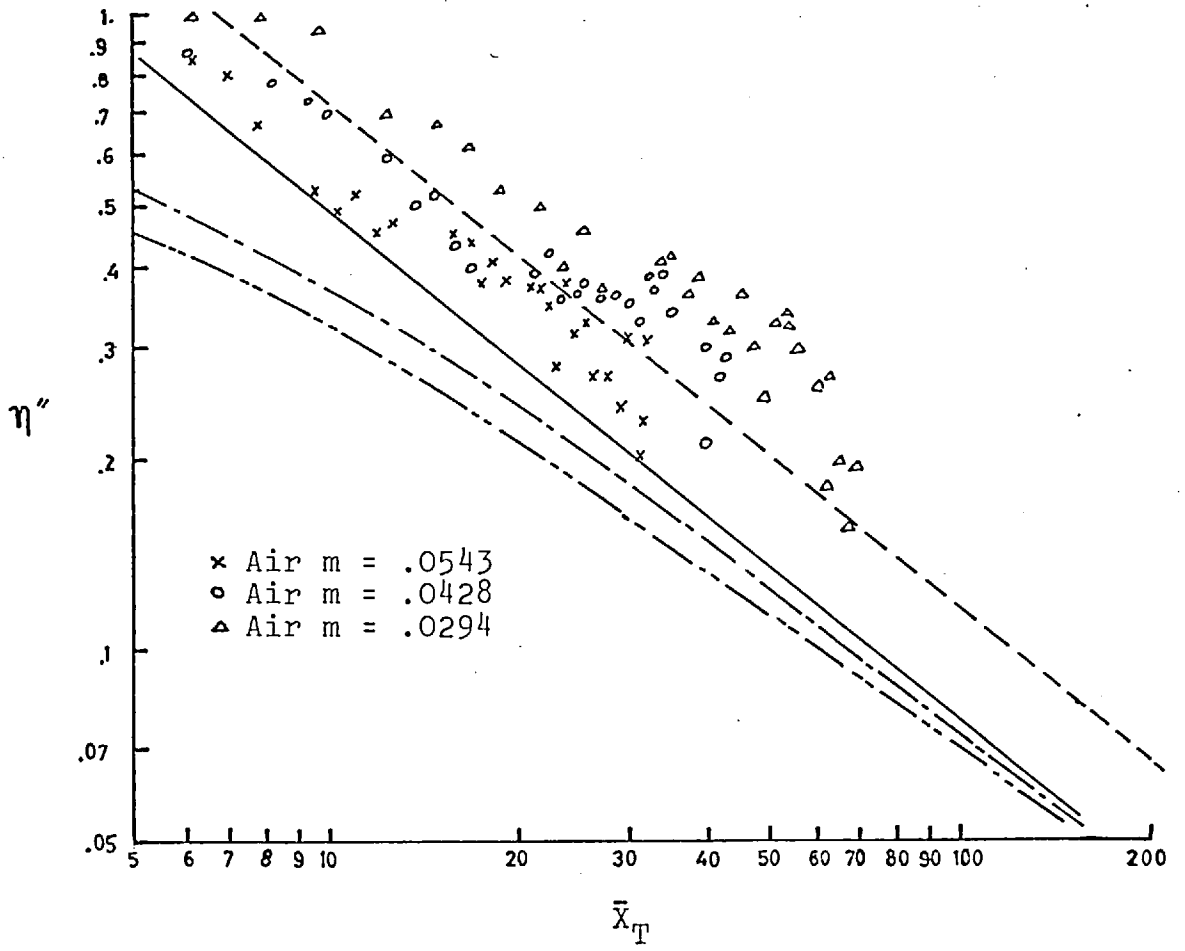

——— STOLLERY & EL-EHWANY (1965)
- - - - TRIBUS & KLEIN (1953)
—·— KUTATELADZE & LEONT'EV (1963)
—··— LIBRIZZI & CRESCI (1964)

Fig. 25. LOW SPEED THEORETICAL FILM COOLING EFFECTIVENESS PREDICTIONS COMPARED WITH AIR INJECTION DATA ADJUSTED BY GOLDSTEIN'S ρ^*/ρ_∞

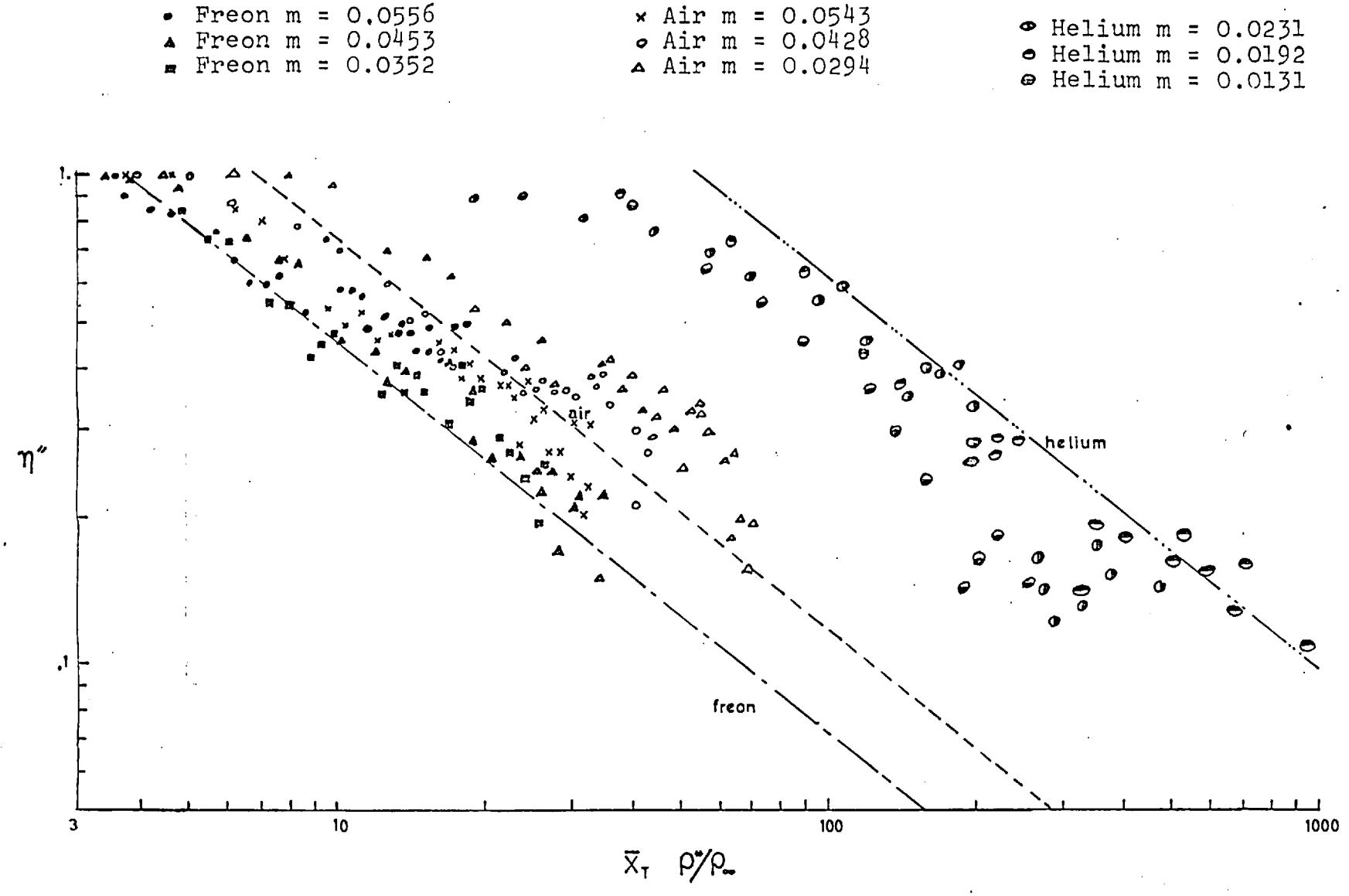

Fig. 26 TRIBUS AND KLEIN LOW SPEED THEORY FOR THREE GASES WITH DATA MODIFICATION ACCORDING TO GOLDSTEIN

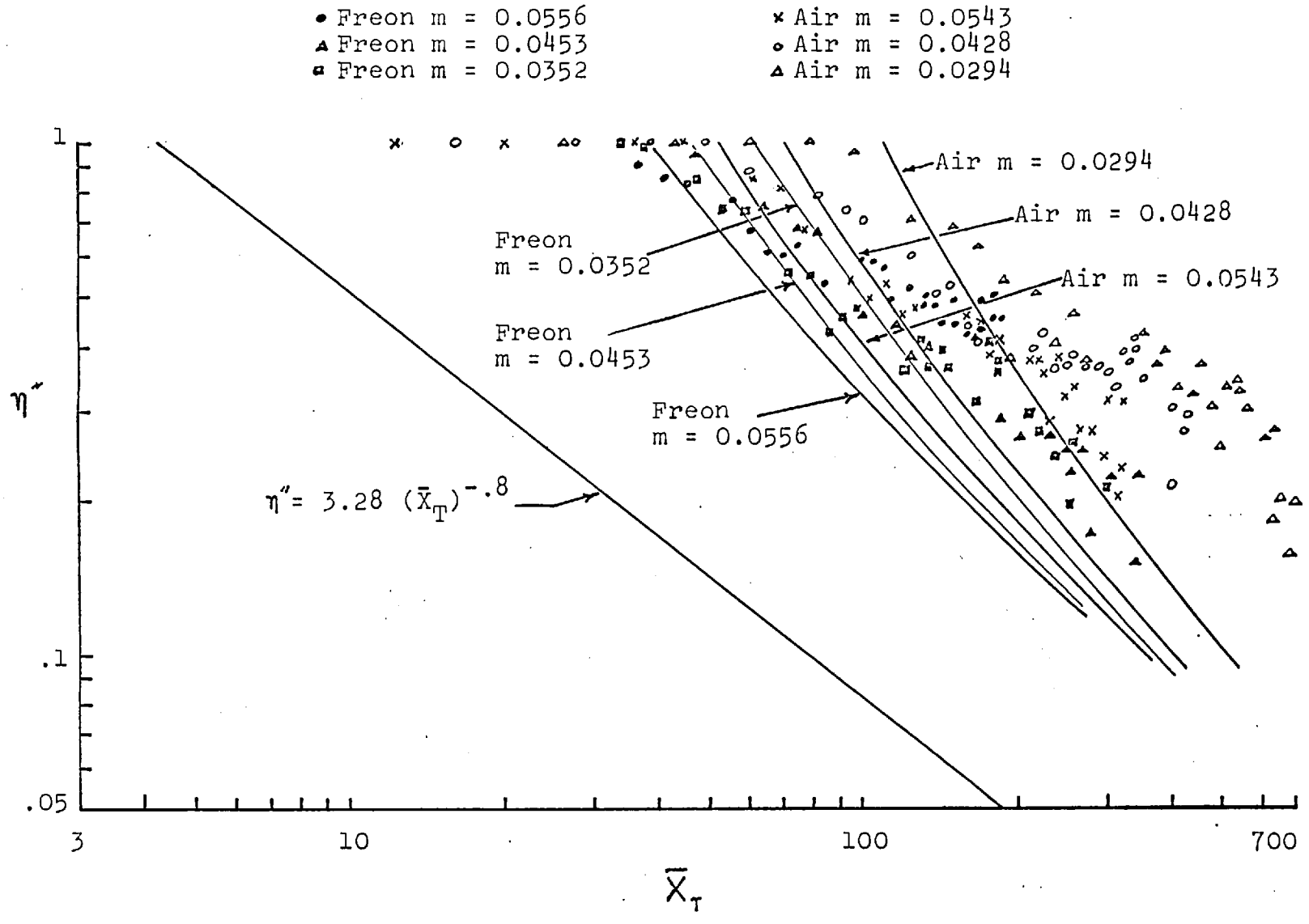

Fig. 27. DELAYED MIXING MODEL FILM COOLING EFFECTIVENESS PREDICTIONS COMPARED WITH MEASURED DATA FOR FREON AND AIR INJECTION.

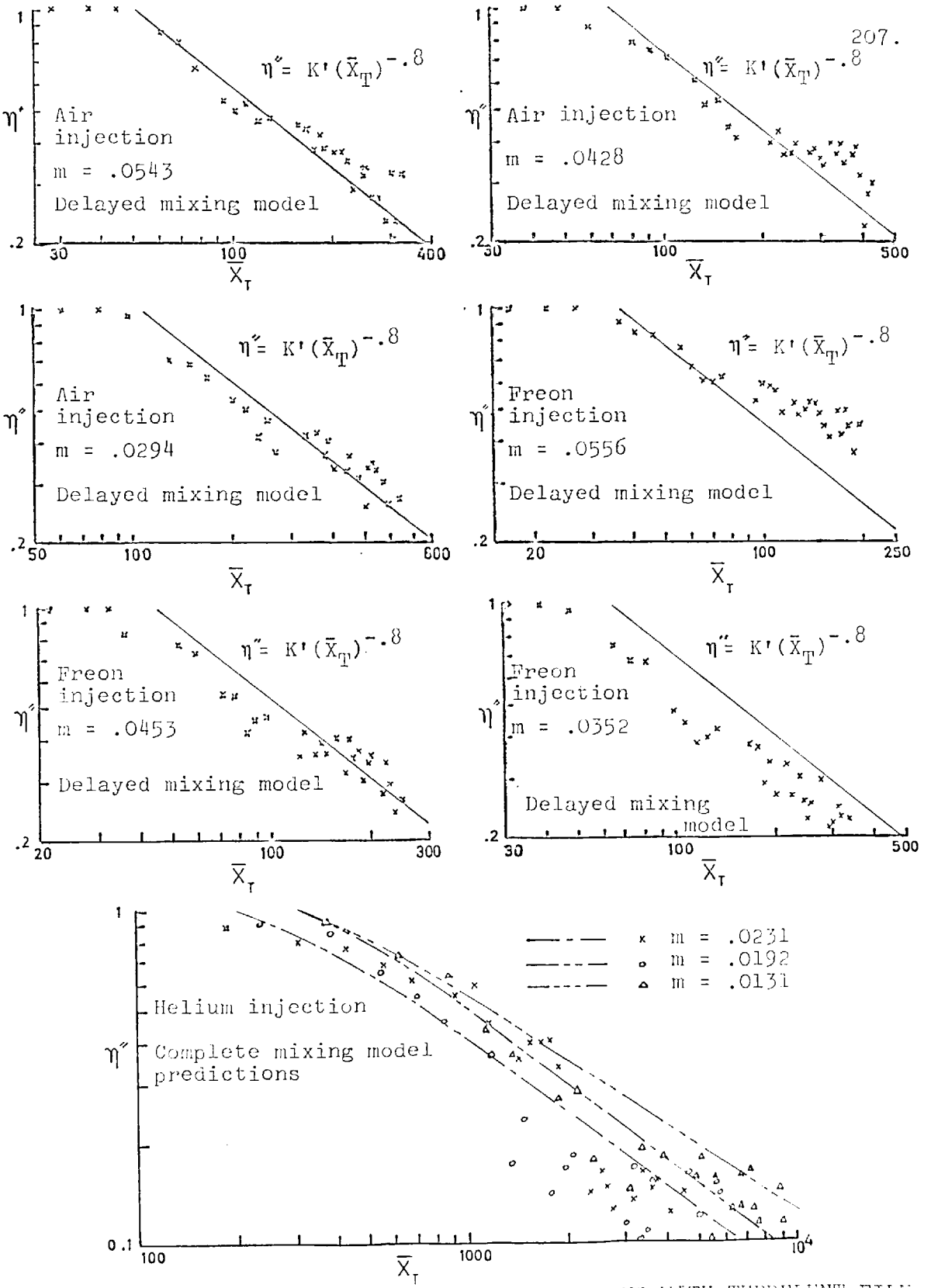

Fig.28. MODIFIED ρu PROFILE PREDICTIONS WITH TURBULENT FILM COOLING

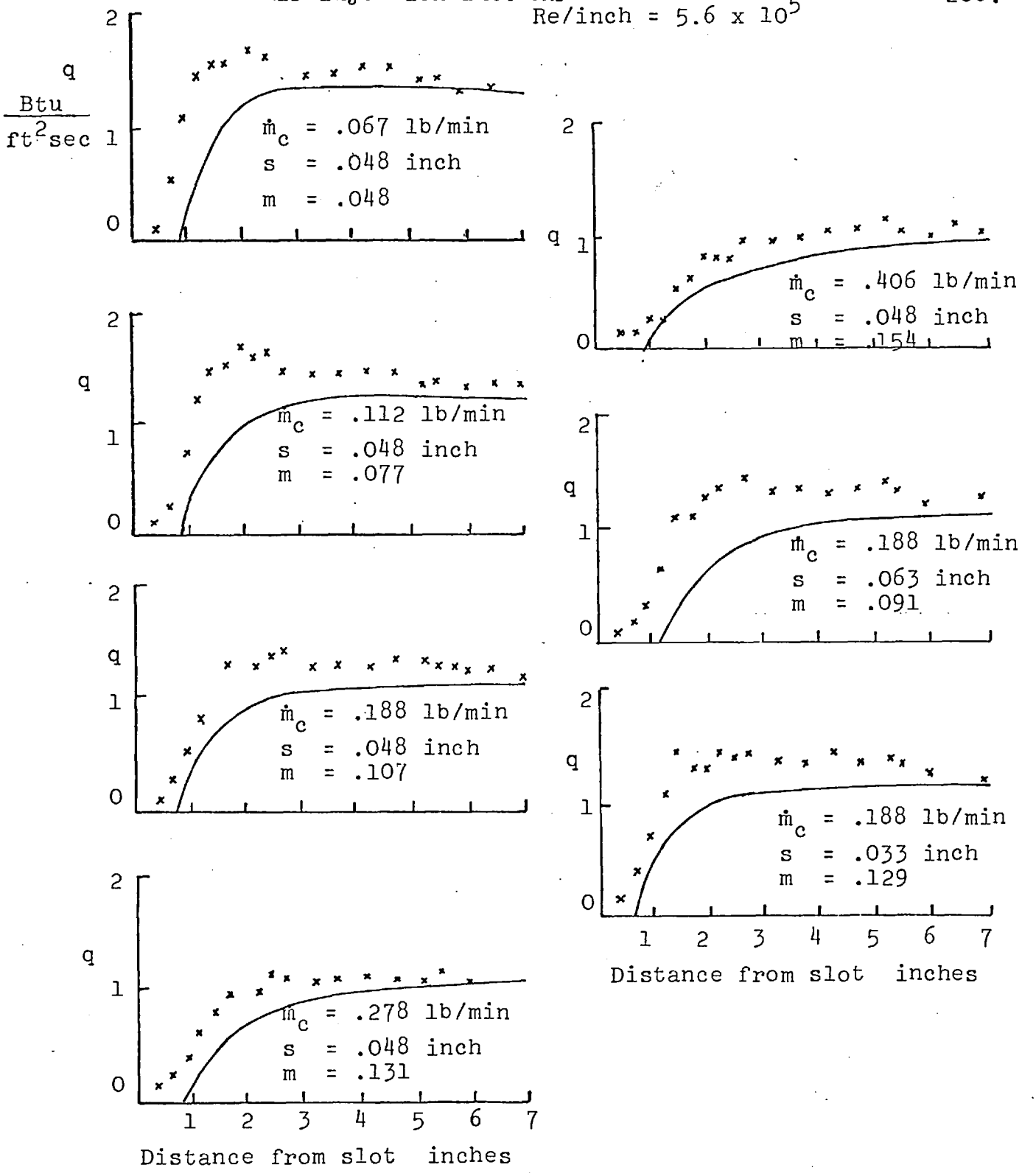

Fig. 29. RICHARDS (1968) DATA TURBULENT FILM COOLING COMPARED WITH BOUNDARY LAYER MODEL HEAT TRANSFER PREDICTIONS.

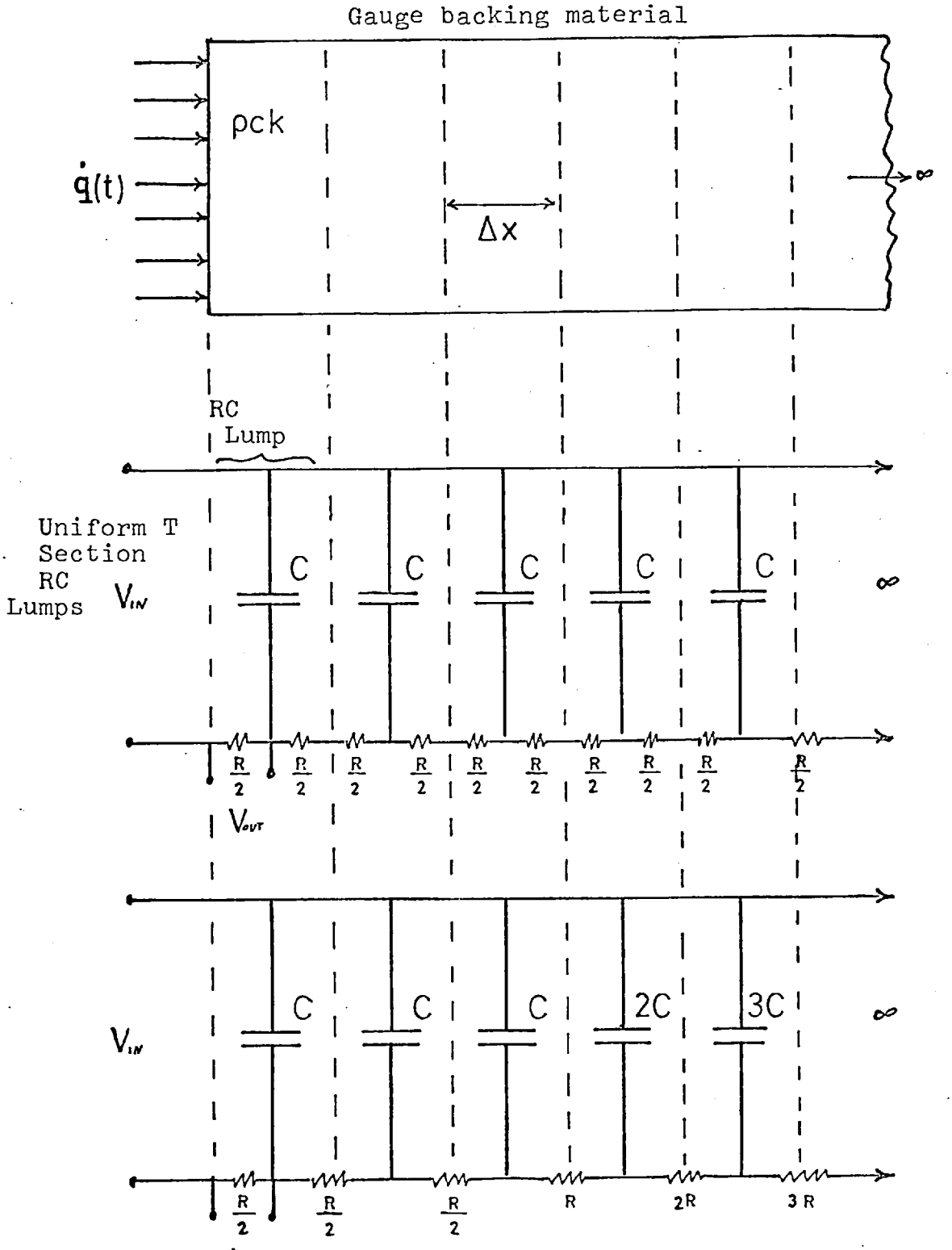

Fig.30. T - SECTION ANALOGUE NETWORK

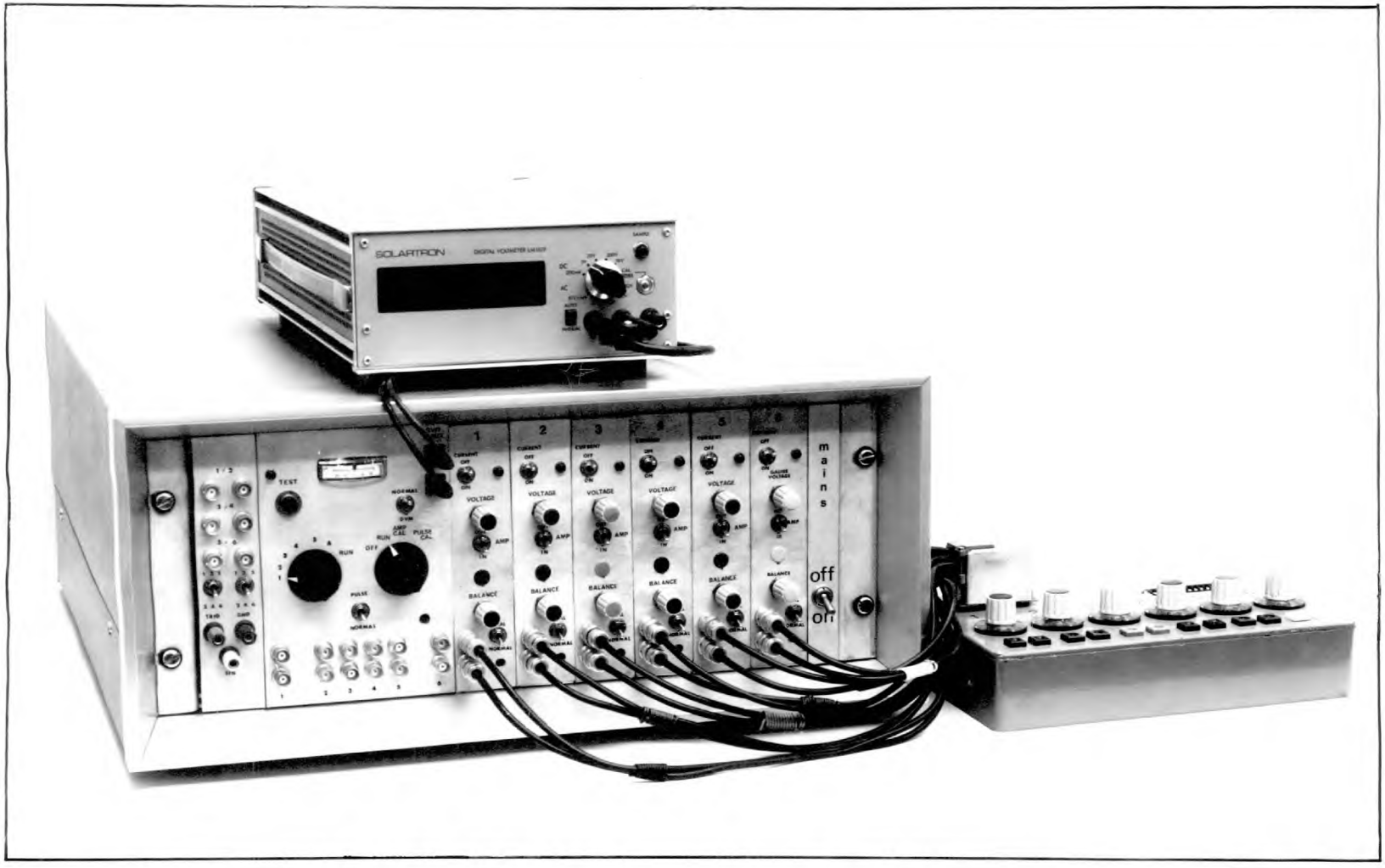

Fig 31. - COMPLETE HEAT TRANSFER EQUIPMENT

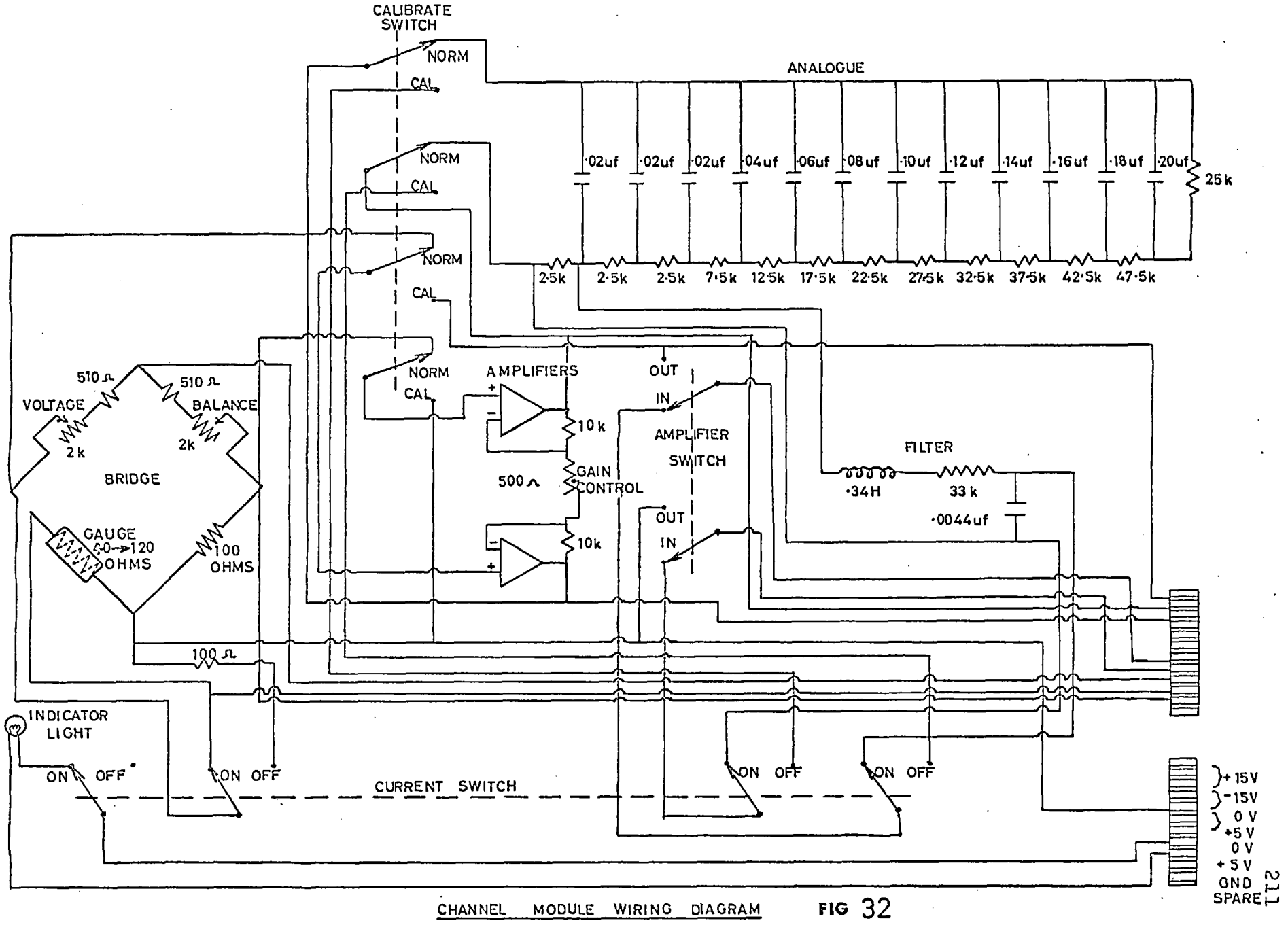

CHANNEL MODULE WIRING DIAGRAM FIG 32

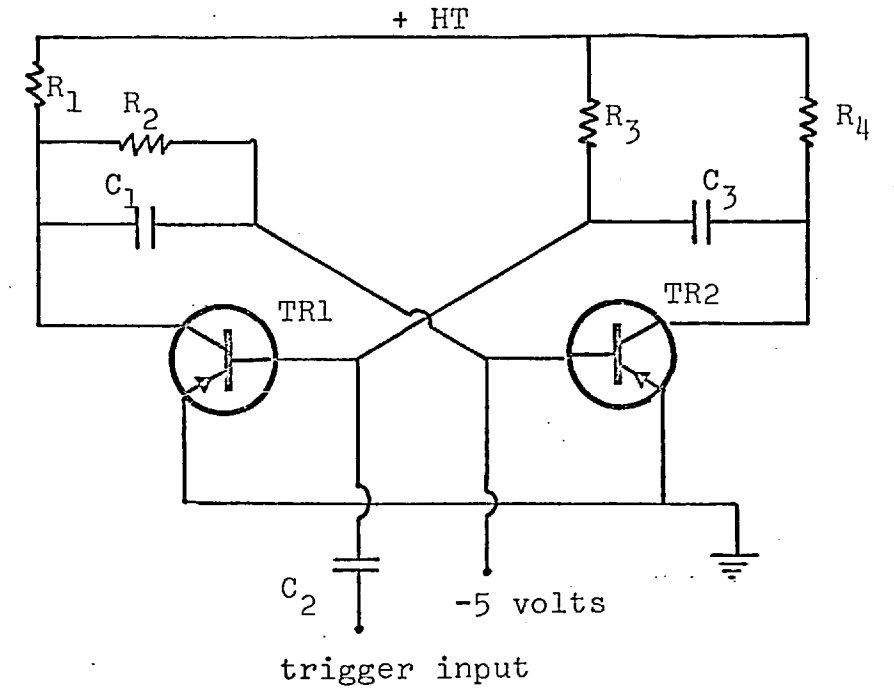

Fig. 33a. BASIC FLIP-FLOP CIRCUIT

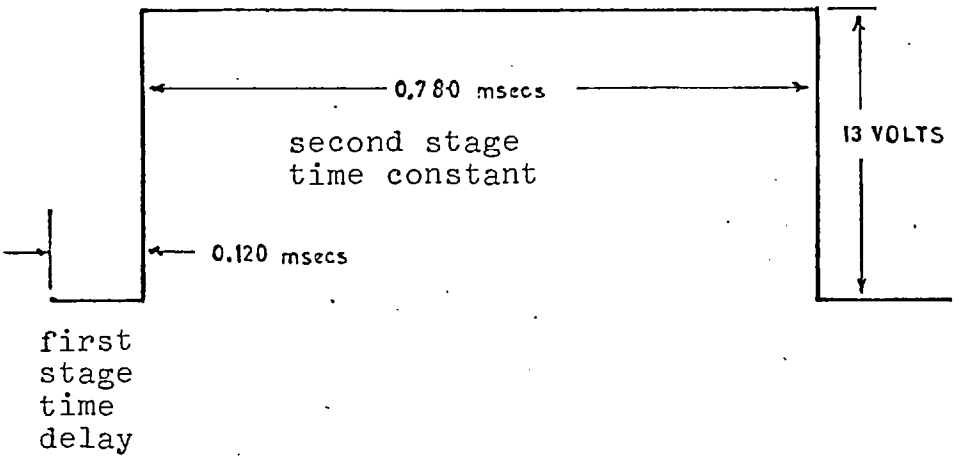

Fig.33b. PULSE CALIBRATOR OUTPUT VOLTAGE APPLIED TO CALIBRATION BRIDGE

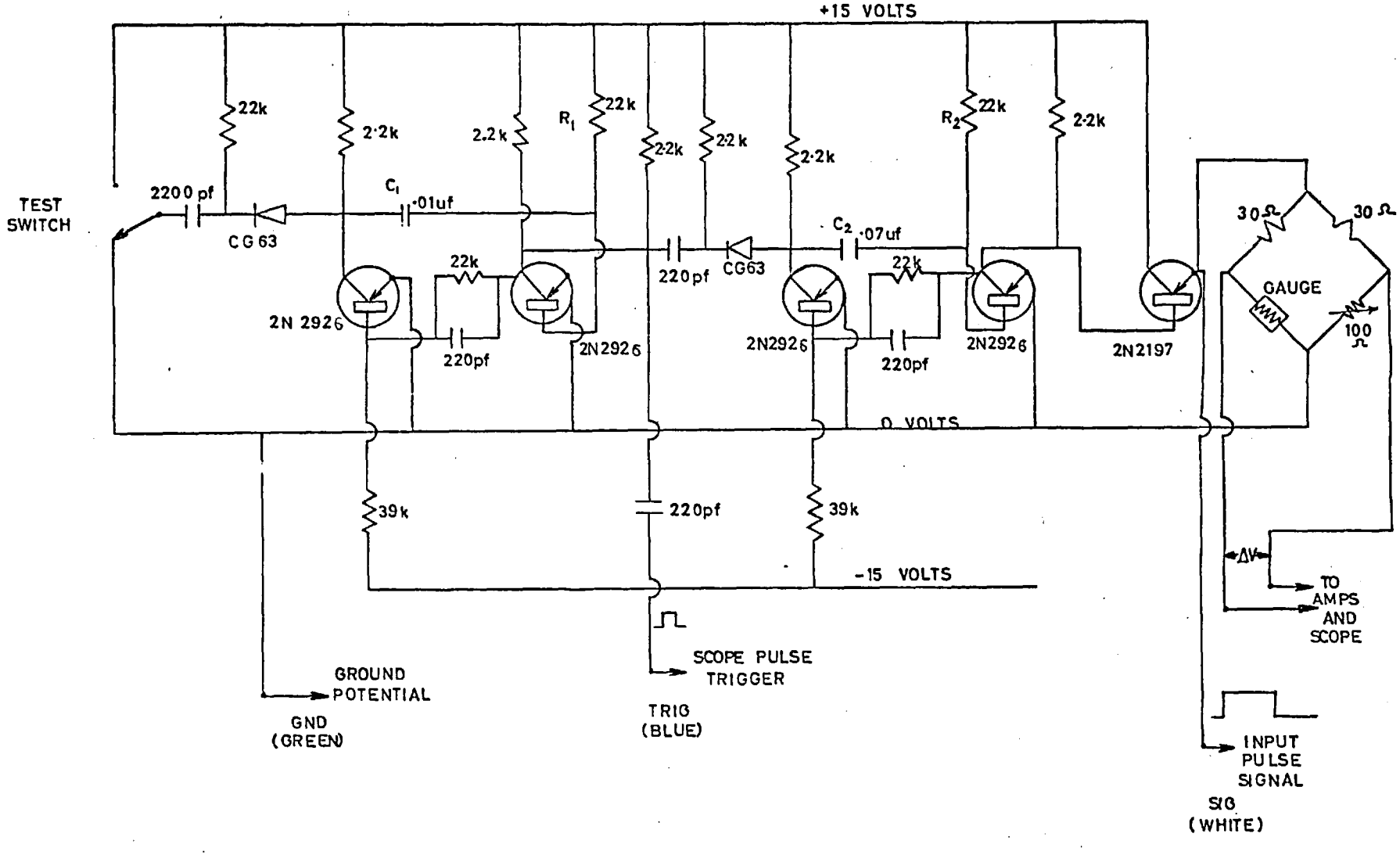

PULSE GENERATOR CIRCUIT

FIG 34

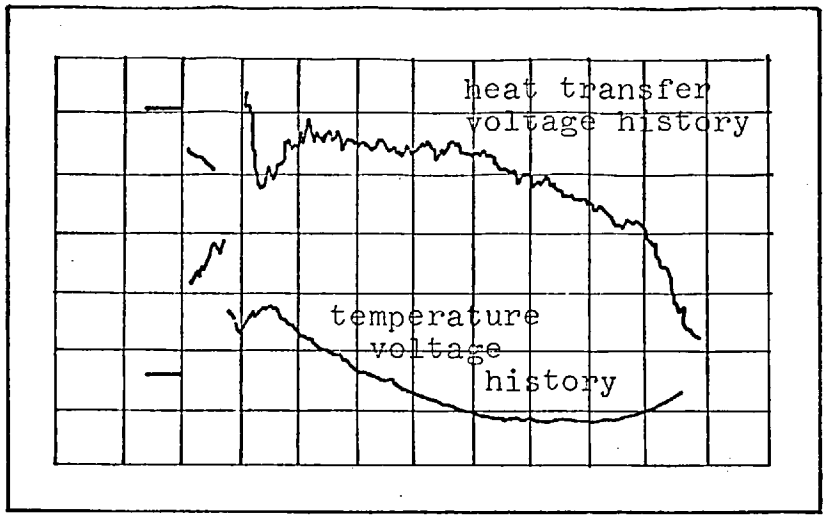

Fig.35a. ANALOGUE INPUT AND OUTPUT VOLTAGE HISTORIES

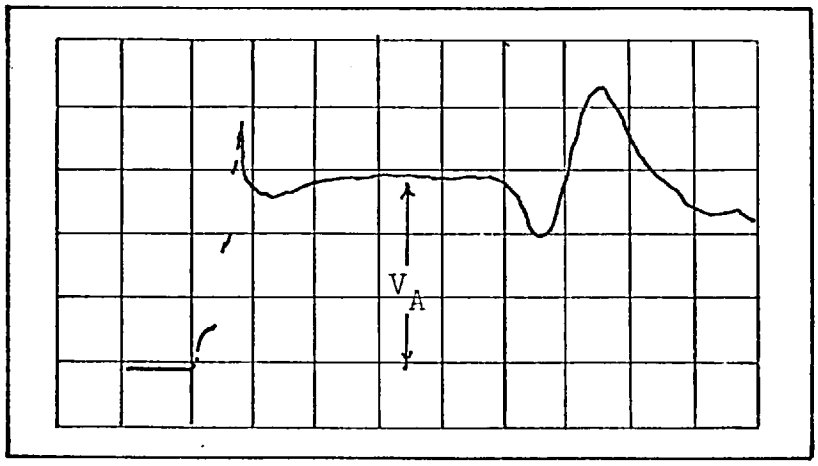

Fig. 35b. TYPICAL HEAT TRANSFER RECORDING

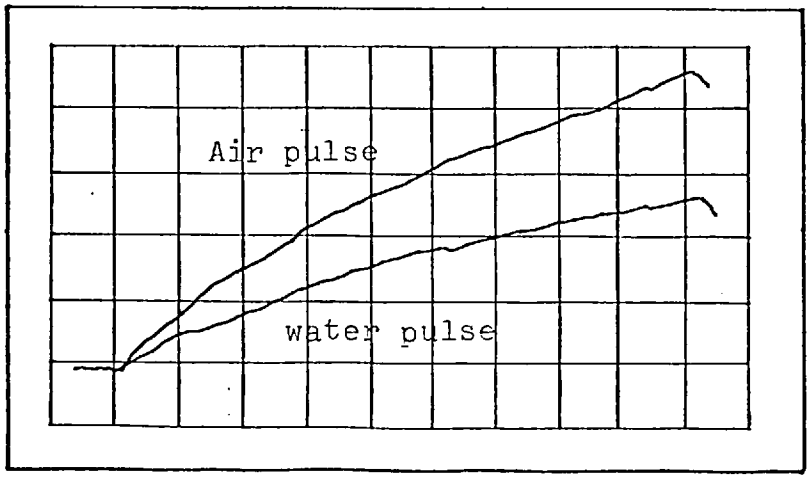

Fig.35c. VOLTAGE HISTORIES WITH GAUGE PULSED IN AIR AND WATER

Fig. 36. - COMPARISON OF ANALOGUE OUTPUT WITH COMPUTER CALCULATED HEAT TRANSFER

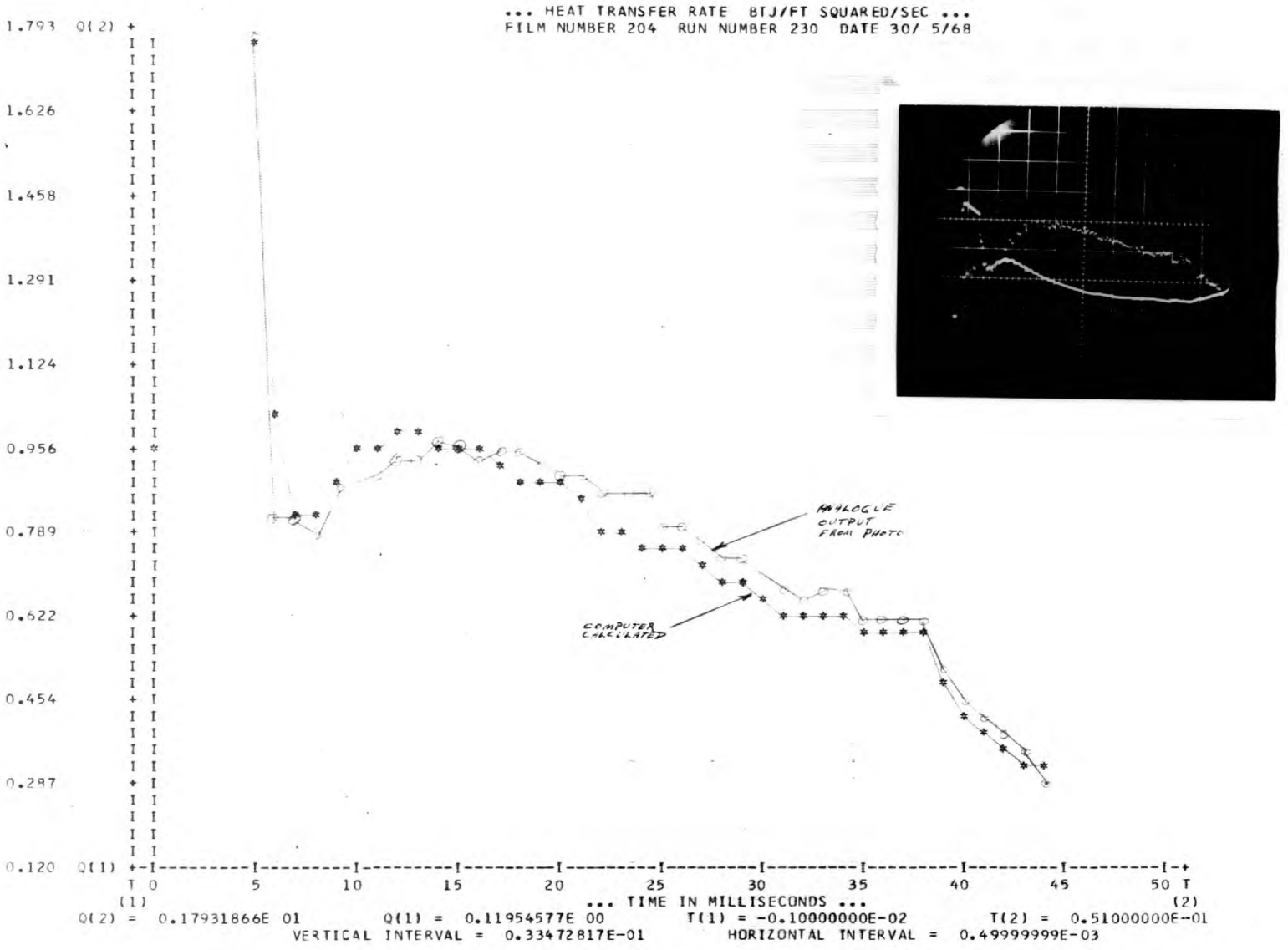

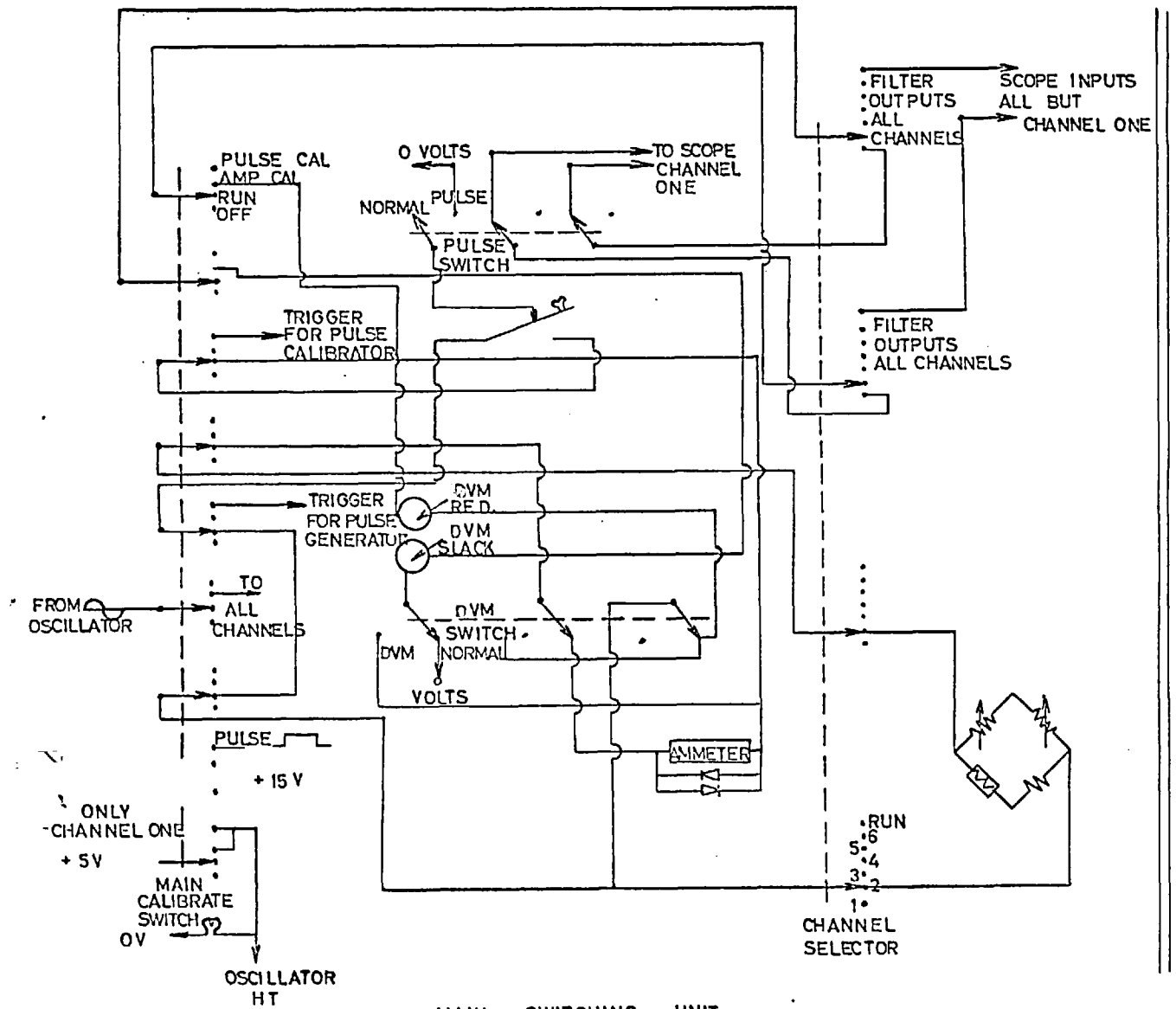

MAIN SWITCHING UNIT

FIG 37

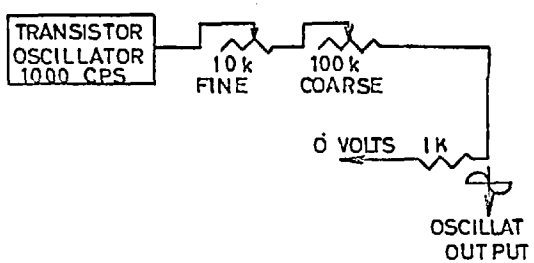

OSCILLATOR GAIN CONTROLS